



**International Doctorate School in Information and
Communication Technologies**

DIT - University of Trento

**MICRO ELECTROCHEMICAL SENSORS AND PCR SYSTEMS:
CELLULAR AND MOLECULAR TOOLS FOR WINE YEAST
ANALYSIS**

Cristina Ress

Advisor:

Dr. Leandro Lorenzelli

Fondazione Bruno Kessler, Trento

Abstract

Nowadays, exciting bioanalytical microsystems are currently receiving increasing attention in biology since they can comply with the considerable demand for reliable, sensitive and low-cost analysis tools. Small reagents volumes, low power consumption, portability, fast analysis, high throughput and systems integration are the key aspects that make these systems more and more appealing within both the academic and industrial communities. In the last years, many microdevices were developed for a wide range of biological applications, particularly dedicated to cellular or molecular analysis. Many efforts were devoted to the realization of Cell-Based Biosensors (CBBs) to monitor the dynamic behaviour of cell cultures for pharmacological screening and basic research. Other researchers focused their interests in the development of so-called Lab-on-a-Chip (LOC) systems for DNA analysis mostly applied to clinical diagnosis.

This thesis deals with the investigation of two miniaturized devices – *a cell-based biosensor and a DNA amplification system* – for the *cellular and molecular* analysis of wine yeasts, respectively.

The first device consists of integrated electrochemical sensors – Ion-Sensitive Field-Effect Transistor (ISFET), impedimetric and temperature sensors – for the real time evaluation of pH and cell settling of yeasts under batch culture conditions. The assessment of yeast performance and robustness has been focused on ethanol tolerance, as it is one of the main stress factors acting in wine, and thus, one of the major causes of stuck fermentations. A good agreement between extracellular acidification and cell growth trends at different ethanol concentration has been demonstrated, significantly reducing the time of the traditional assays. Moreover, resistivity measurements have shown the possibility to follow progressive settling of the cell suspension.

Concerning the second system, a Polymerase Chain Reaction (PCR) microdevice has been biologically validated by successfully amplifying yeast genomic DNA fragments. Additionally, the outcome of PCR has been positively assessed with diluted samples and boiled yeast cultures, demonstrating the possibility to skip the time-consuming purification process for potential lab-on-chip applications with very little or no pre-PCR sample manipulations.

The encouraging results from both microsystems have demonstrated their suitability for wine yeast analysis, aimed at quality improvements of the winemaking process.

Keywords

Electrochemical sensors, Cell-based biosensors, PCR microsystems, DNA amplification, wine yeasts analysis

Contents

CHAPTER 1	1
1 INTRODUCTION	1
1.1 THE CONTEXT	1
1.2 THESIS CONTENT AND INNOVATIVE ASPECTS	2
1.2.1 <i>Micro electrochemical sensors for yeast cell analysis</i>	2
1.2.2 <i>PCR microdevice for molecular analysis of yeast</i>	3
1.3 STRUCTURE OF THE THESIS	4
CHAPTER 2	7
2 STATE OF THE ART	7
2.1 INTRODUCTION	7
2.1.1 <i>Yeast: a powerful microorganism in biotechnology and food industries</i>	7
2.1.2 <i>The alcoholic fermentation and the effects of ethanol on cells</i>	9
2.1.3 <i>Survey of different methods for assessing yeast tolerance to fermentative stress factors</i>	12
2.2 CELL-BASED BIOSENSORS (CBBS)	14
2.2.1 <i>ISFETs sensors</i>	15
2.2.2 <i>Impedance sensors</i>	17
2.2.3 <i>Multiparametric microdevices for cell analysis</i>	19
2.3 DNA AMPLIFICATION ON PCR MICRODEVICES	19
2.3.1 <i>The PCR process and the benefits of miniaturization</i>	20
2.3.2 <i>PCR microdevices: State of the Art</i>	21
CHAPTER 3	27
3 MICRO ELECTROCHEMICAL SENSORS FOR WINE YEAST ANALYSIS	27
3.1 MATERIALS & METHODS	27
3.1.1 <i>Microfabrication of the electrochemical sensors</i>	27
3.1.2 <i>Packaging of the microfabricated device</i>	29
3.2 SENSORS CHARACTERIZATION	30
3.2.1 <i>ISFET</i>	30
3.2.2 <i>Impedance sensor</i>	33
3.2.3 <i>Diode</i>	34
3.3 EXPERIMENTAL RESULTS	36
3.3.1 <i>Yeast cell growth and extracellular acidification</i>	36
3.3.2 <i>Extracellular acidification of yeasts at different ethanol concentrations</i>	40
3.3.3 <i>On-line pH and impedance measurements</i>	44
3.3.3.1 <i>Classical assay for testing ethanol tolerance of wine yeast strains</i>	45
3.3.3.2 <i>Extracellular acidification of different wine strains</i>	47
3.3.3.3 <i>On-line impedance measurements</i>	49
3.4 DISCUSSIONS	52
CHAPTER 4	55
4 A PCR MICRODEVICE FOR YEAST DNA AMPLIFICATION	55
4.1 MATERIALS & METHODS	55
4.1.1 <i>Microdevice design</i>	55
4.1.2 <i>Microfabrication process</i>	57
4.1.3 <i>Electronic board</i>	59
4.2 EXPERIMENTAL RESULTS	61
4.2.1 <i>Yeast genomic DNA extraction and purification</i>	61
4.2.2 <i>Target gene selection</i>	63
4.2.3 <i>PCR master mix set-up</i>	64
4.2.4 <i>PCR-program set-up on the microdevice</i>	66
4.2.5 <i>1st validation test: PCR with gDNA</i>	69
4.2.6 <i>2nd validation test: PCR with gDNA from different <i>S. cerevisiae</i> strains</i>	70
4.2.7 <i>3rd validation test: comparison of PCR efficiency and reproducibility with gDNA</i>	71

4.2.8	<i>4th validation test: comparison of PCR efficiency and reproducibility with gDNA concentrations.....</i>	73
4.2.9	<i>5th validation test: Colony-PCR.....</i>	74
4.3	DISCUSSIONS	75
CHAPTER 5	79
5	CONCLUSIONS AND FUTURE OUTLOOK.....	79
	ACKNOWLEDGMENTS.....	83
	BIBLIOGRAPHY	85
	APPENDIX A: GENERAL PRINCIPLES OF ION-SENSITIVE FIELD EFFECT TRANSISTORS (ISFETS)	115
	APPENDIX B: THERMAL IMPROVEMENTS OF THE PCR MICRODEVICE	127
	APPENDIX C: LIST OF RELATED PUBLICATIONS	131
	APPENDIX D: OTHER RELEVANT PUBLICATIONS	133

Chapter 1

1 Introduction

1.1 The Context

Throughout history, yeast has proved to be of undisputed relevance to mankind since it has always been involved in baking, brewing, distiller's fermentations, and wine making.

Nowadays, yeast is one of the most commonly used model organisms in modern cell biology because it combines the advantages of the eukaryotic expression system with those of fast-growing prokaryotes. The large number of scientific publications and the wide range of biotechnological applications (e.g. production of insulin, vaccines, antioxidants, vitamins, flavours, fuel ethanol, etc.) demonstrate the great academic and industrial interests towards this powerful and versatile microorganism.

In particular, intensive research is currently focusing onto the role of yeast in winemaking in an attempt to improve the selection of high-yielding strains aimed at the development of atypical flavor profiles or at the improvement of microbial tolerance to alcohol and to other stress factors in wines. For the last issues, *cell cultural procedures and molecular methods* are among the main current tools that support microbiologists in quality assessment and yeast ecology of wine strains.

The former are generally performed by cell growth monitoring in Petri dishes, direct microscopic counts, dry weight or by measuring the optical density of a cell suspension; the latter typically involve molecular assays based on nucleic acids amplification.

Most of standard methods are time-consuming, labour-intensive, endpoint tests, and they are often carried out by benchtop instruments that are difficult to integrate in industrial processes and lack of fast response due to the large employed volumes.

Therefore, the incorporation of new technologies for large-scale and low cost analysis is rapidly becoming of emerging interest and microsystems are grown to be a hot topic in today's scientific research by representing an exciting multidisciplinary field in which sensors, actuators, biological and chemical tools are converging. Indeed, the implementation of miniaturized, portable, automated and even multifunctional systems entails true synergized expertise to satisfy the pressing demand of fast, reliable and cost-effective biological

analysis. As it is well known, moving from the “macro” to the “micro” world does not simply mean the downscale of conventional and well-established bioanalytical instrumentations (which is, indeed, itself a challenge), but involves the integration of several components towards multiple and robust analysis systems. Furthermore, most microdevices must be user-friendly since they are often developed for on-field applications and they might be managed by untrained operators.

The high level of systems integration and the low cost manufacturing of MEMS (Micro Electro Mechanical Systems) technologies have encouraged the development of many microdevices for a wide range of biological applications, particularly devoted to cellular or molecular analysis.

In future, exciting prospects for the expansion of novel cell-based biosensors (CBBs) and lab-on-a-chip (LOC) are expected. In the years to come, these integrated analysis platforms will lead to a breakthrough in biology providing handheld and disposable systems able to fulfill a wide number of daily and routine laboratory practices.

1.2 Thesis content and innovative aspects

The goal of this thesis concerns the investigation of two miniaturized devices – *a cell-based biosensor and a DNA amplification system* – for the *cellular and molecular* analysis of wine yeasts, respectively.

1.2.1 Micro electrochemical sensors for yeast cell analysis

The proposed cell-based biosensor consists of integrated electrochemical sensors – Ion-Sensitive Field-Effect Transistor (ISFET), impedimetric and temperature sensors – dedicated to the measurements of pH and settling of a yeast cell culture.

The microsensors were investigated for wine yeast quality assessment by evaluating cell tolerance to ethanol, one of the main microbial growth inhibitors acting in wine, and thus one of the major causes of suboptimal fermentations. Ethanol tolerance is considered an important indicator of yeast industrial performance and robustness, and thereby, it represents a parameter of significant economic value for the wine industry.

To demonstrate the feasibility of the multiparametric system for wine yeast analysis, off-line and on-line measurements were carried out by batch cultivation of three different *S. cerevisiae* wine strains in sterile Yeast Peptone Dextrose Broth at different ethanol concentrations [0-20% v/v]. A positive trend correlation between the extracellular acidification and cell growth was demonstrated, allowing the detection of the exponential growth phase within 5 hours after inoculum and significantly reducing the time of the traditional ethanol tolerance assays (i.e. 5 hours against 48-72 hours with agar plates).

Impedimetric sensors were investigated in function of cell settling over time and preliminary measurements demonstrated to be sensitive to both different particles sizes and cell concentrations at the inoculum level.

Both ISFET and impedimetric sensors were characterized for a completely new application with respect to data reported in literature. Moreover, impedimetric measurements were not focused onto monitoring of cell adhesion or medium conductivity changes, as typically shown in the state of the art of CBBs.

Although at a preliminary level, encouraging results demonstrated its potential suitability for rapid oenological characterization, providing information about the dynamics of ethanol effects and of cell settling throughout a non-invasive and label-free approach.

1.2.2 PCR microdevice for molecular analysis of yeast

The second microsystem is a disposable miniaturized Polymerase Chain Reaction (PCR) module devoted to the DNA amplification of yeasts. PCR is an enzyme catalyzed amplification technique that allows replication of specific fragments of DNA by means of repeated thermal cycles. Since its discovery - by which the biochemist Mullis won the Nobel Prize in 1993 - the PCR technique has become a key tool in modern molecular biology. In particular, the need for improved speed and portability of the PCR systems has encouraged many research groups to move away from benchtop thermocycler and investigate on microchip-based PCR, proposing different possible configurations and candidate materials for the realization of micro scale devices.

In this work, the microchip architecture consists of a hybrid structure made of a silicon substrate with embedded heater and thermometers for the lower portion and a polydimethylsiloxane (PDMS) reactor chamber as disposable element. Silicon was chosen to exploit its thermal characteristics and perform the cycles faster, while polymers were used for the containment of the biological mixture since they are biocompatible, transparent and easily

moldable. The contact between the two parts was assured by a mechanical clamping, which in turn, prevented as a cap the PCR mix from evaporation during thermal cycles. Inlet and outlet of the polymeric chamber were optimized in such a way to avoid bubbles formation, facilitate fluidic handling and recovery of the sample. Then, the device was thermally characterized and validated by successfully amplifying genomic DNA targets of the three analyzed *S. cerevisiae* wine yeast strains in 10 μ l of PCR mixture. Moreover, microdevice-PCR was also positively carried out on progressive diluted sample and even on boiled yeasts, demonstrating the possibility to skip the time-consuming purification process towards the considerable demand for fast, practical, automated analytical systems. The experimental session performed on the microdevice showed its capability to amplify DNA in different working conditions and without any static or dynamic passivation, in contrast to data reported in literature. This means that evaporation phenomena were prevented through efficient inlet and outlet sealing and that a very good biocompatibility inside the microchamber was achieved.

1.3 Structure of the thesis

This thesis begins with the description of the main achievements in the development of cell-based biosensors and PCR microdevices in **Chapter 2 “State of the Art”**. At first, an introduction to yeast and to the most common fermentative stress factors is provided (*Paragraph 2.1*). In particular, the main effects of ethanol on yeast cell membrane and metabolism are briefly summarized (*Section 2.1.2*). Then, conventional methods for yeasts monitoring are surveyed (*Section 2.1.3*), mainly focusing on metabolic measurements (extracellular acidification) and on molecular techniques (DNA amplification). In *Paragraph 2.2*, an overview of the main advances of ISFETs (*Section 2.2.1*), impedance sensors (*Section 2.2.2*) and multiparametric platforms (*Section 2.2.3*) for biological applications is reported. Finally, in *Paragraph 2.3*, after a general description of the amplification process, the state of the art in the development of new promising PCR microdevices is reviewed.

In **Chapter 3 “Micro Electrochemical sensors for wine yeast analysis”**, a cell-based biosensor is investigated for wine yeast quality assessment. Sensors microfabrication, packaging and characterization are described in *Paragraphs 3.1 and 3.2*, while the experimental results are reported in *Paragraph 3.3*. A preliminary correlation study between extracellu-

lar metabolic activity and cell growth is defined in *Section 3.3.1*. Then, extracellular acidification and cell growth are assessed in presence of critical ethanol concentrations (*Section 3.3.2*) and on-line pH and impedance measurements are performed by cultivating yeast cells directly on sensors (*Section 3.3.3*). Finally, the obtained results are summarized and discussed in *Paragraph 3.4*.

Chapter 4 “A PCR microdevice for yeast DNA amplification” describes the development and validation of a hybrid Silicon/PDMS PCR microdevice for yeast molecular analysis. In *Paragraph 4.1*, the main design constraints, microfabrication process and the realization of the electronic board are described. The experimental validation of the microsystems is detailed in *Paragraph 4.2*, which reports the obtained results of the microdevice-PCR performed with genomic DNA of one *S. cerevisiae* strain (*Section 4.2.5*), with genomic DNA of different *S. cerevisiae* strains (*Section 4.2.6*), with diluted sample (*Section 4.2.8*) and from boiled yeast cells (*Section 4.2.9*). Finally, the main achievements are surveyed and discussed in *Paragraph 4.3*.

Chapter 6 “Conclusions and Future Outlook” reports the main results and proposes future perspectives both in terms of improvements and potential applications.

Acknowledgments, Bibliography and Annexes sections (Appendix A “*General principles of Ion-Sensitive Field Effect Transistors (ISFETs)*”, Appendix B “*Thermal improvements of the PCR microdevice*”, Appendix C “*List of related publications*”, Appendix D “*Other relevant publications*”) complete this thesis.

Chapter 2

2 State of the Art

In this chapter, an introduction to yeast and to the most common fermentative stress factors is provided. Then, the main achievements in the development of cell-based biosensors and on PCR microdevices are summarized.

2.1 Introduction

Yeast has been widely recognized as one of the most well studied model organisms and exploited biocatalysts over the years. In this paragraph, the power of yeast and the main inhibitors of the fermentation process are briefly summarized (sections 2.1.1 and 2.1.2). Then, conventional methods for yeasts monitoring are surveyed (section 2.1.3), finally focusing on cell-based measurements (i.e. extracellular acidification) and on molecular techniques (i.e. DNA amplification).

2.1.1 Yeast: a powerful microorganism in biotechnology and food industries

Yeasts are egg-shaped cells and their dimensions range from 5 to 10 μm , with an average volume of 50 μm^3 and an individual weight of $2 \times 10^{-10}\text{g}$. They multiply as single cells that divide by budding (e.g. *Saccharomyces*) or direct division (fission, e.g. *Schizosaccharomyces*), or they may grow as simple irregular filaments (mycelium).

Yeasts are chemoorganotrophs because they use organic compounds as a source of energy and do not require light to grow. The main source of carbon is obtained by hexose sugars such as glucose and fructose, or disaccharides such as sucrose and maltose. Some species can metabolize pentose sugars, alcohols, and organic acids. They grow over a temperature range of 10°-37°C, with optimum temperature in the range of 28°-37°C, depending on the species. Yeasts are typically cultivated as batch cultures: they are inoculated in a sterile medium with all the necessary nutrients without any further supply of other energy sources. Under these physiological conditions, four growth phases are mainly identified: lag phase (yeasts adapt

themselves to the new environment and start to multiply the genetic arrangement for the next cell duplication), log phase (cells double exponentially increasing the overall biomass), stationary phase (all the nutrients are metabolized and cells stop to grow) and death phase (cells exhaust all the energy reserves and undergo to programmable death) (Fig. 2.1).

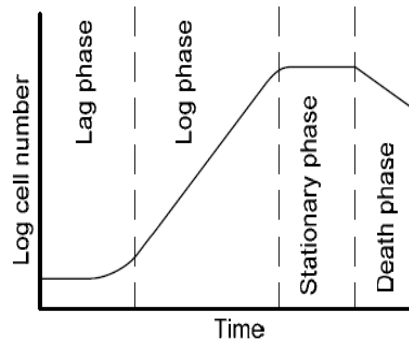


Fig. 2.1 Typical growth curve [Crueger and Crueger, 1990]

The short generation time (typically $\sim 90\div 120$ minutes), the easy and inexpensive cultivation procedures combined with the well studied biochemical and molecular processes have given rise to a considerable exploitation over the years of this powerful eukaryotic organism for the production of several useful products such as vaccines [Garrison and Baker, 1991], insulin [Elliot et al., 1990], and more in general antioxidants, vitamins and flavours [Abbas, 2006; Boekhout and Robert, 2003; Fleet, 2003].

The complete genome sequencing of *Saccharomyces cerevisiae* [Goffeau et al., 1996; Johnston, 1996] has provided significant advances in systems biology through intensive genome-wide analysis [Mewes, 1997; Snyder and Kumar, 2002], proteomics [Gavin et al., 2002; Bond 2006], bioinformatics [Ball 2001; Mewes 2002] to analyze structure-function relationships, and “-omics” level studies, awarding the budding yeast as an excellent model organism for fundamental research, drug discovery [Ishida et al., 2002; Simon and Bedalov, 2004; Parson et al., 2006; Ro et al., 2006] and for unraveling and studying in great detail complex cellular processes.

The power of yeast and its versatility for a wide range of biotechnological applications has attracted the academic community for many decades placing the eukaryotic microorganism at the forefront of scientific research. In particular, the role of yeast in fermentable beverages - especially in wine - it is still today of great interest both for

academy and industry due to its major impact on the quality of the end product [Fleet, 2007, Querol and Fleet, 2006].

Therefore, many studies are focusing on the fermentation process both at cellular and molecular level in order to understand what are the main stress factors that affect yeast survival and investigate the key aspects that are involved in wine yeast performance, as it is briefly surveyed in the next section.

2.1.2 The alcoholic fermentation and the effects of ethanol on cells

Yeast is used in winemaking because it converts the sugars present in grape juice or must into alcohol. The biological process by which sugars such as glucose, fructose, and sucrose, are converted into ethanol and carbon dioxide is called alcohol fermentation and its chemical equation is shown below:



Yeasts metabolize sugar both in aerobic and anaerobic conditions, but depending on the presence or absence of oxygen, they undergo into respiration process (by energy production) or alcohol fermentation (by ethanol production), respectively.

Yeast is normally already present on the surface of grape berries, often visible as a powdery film on their skin. The fermentation can be carried out with this indigenous (wild) population, giving interesting and exclusive organoleptic properties to wine [Heard and Fleet, 1985, Mateo et al., 1991, Schutz and Gafner, 1993]. However, the indigenous microorganisms may give unpredictable results depending on the yeast species that are present on grapes. For this reason, a pure yeast culture is generally added to the must, which rapidly predominates the fermentation as it proceeds. This culture is employed as starter yeast because partially represses wild yeasts and ensures a reliable and predictable fermentation [Querol et al., 1992; Henschke, 1997]. Most added wine yeasts are strains of *Saccharomyces cerevisiae*, with different physiological and fermentative properties but not always suitable for obtaining qualitative alcoholic beverages. Because of the direct impact of the selected yeast strain on the finished product, significant research has been undertaken into the screening of wine yeast strains able to develop different sensory properties

[Lambrechts and Pretorius, 2000], produce atypical flavour profiles [Romano et al., 2003; Swiegers et al., 2005], or increase ethanol concentration in wines.

As regards the latter issue, ethanol is the principal stress factor for yeasts and, therefore, one of the major causes of suboptimal (stuck and sluggish) fermentations [Alexandre and Charpentier, 1998; Ivorra et al., 1999] because it inhibits microbial growth and viability [Thomas and Rose, 1979; Ingram and Buttke, 1984; Piper, 1995; Aguilera et al., 2006] and, as a consequence, adversely affects the fermentation process by stopping further ethanol production.

Therefore, ethanol tolerance is considered an important indicator of yeast industrial performance and robustness [Zuzuarregui and de Olmo, 2004; Schmidt et al., 2006], and thereby, it represents a parameter of considerable economic value for the wine industry [Rose, 1980]. Additionally, each yeast strain imparts different characteristics on wine and at the same time reacts to each stress factor of the fermentation process (e.g. alcohol concentration, temperature, osmotic pressure, starvation) in a different way [Bartowsky et al., 2007].

In the last three decades, many studies were carried out on the effects of ethanol on cells, mainly focusing on cell membrane as one of the principal targets of alcohol [Casey and Ingledew, 1986; D'Amore et al., 1990; Fleet, 2002].

It has been widely demonstrated that ethanol reduces microbial lifespan, cell growth and biomass accumulation [Medawar et al., 2003, Schmidt et al., 2006], principally by inhibiting the glucose transport system [Pascual et al., 1988; Leao and Van Uden, 1982; Salmon et al., 1993] and increasing the rate of proton influx [Leao and Van Uden, 1984; Kilian et al., 1989]. On the other hand, yeast responds to increasingly toxic levels of ethanol in a dose-dependent manner throughout an adaptation mechanism, by changing the lipid composition and fluidity of its membranes [Alexandre et al., 1994; D'Amore et al., 1990], delaying cell cycle [Kubota et al., 2004] and stimulating the ATPase activity [Rosa and Sa-Correia 1991; Rosa and Sa-Correia 1992, Monteiro et al., 1994; Alexandre et al., 1994, Aguilera et al., 2006].

As it is well known, the H⁺ATPase is essential for cell growth, in particular for nutrient uptake and homeostasis regulation [Kotyk, 1994]. Indeed, the plasma membrane H⁺ATPase generates a proton electrochemical gradient which constitutes the driving force for nutrients [Serrano, 1988], whereby an increase of its proton-

pumping activity is supposed to counteract the progressive cytoplasmatic acidification induced by the influx of protons across the membrane (fig. 2.2).

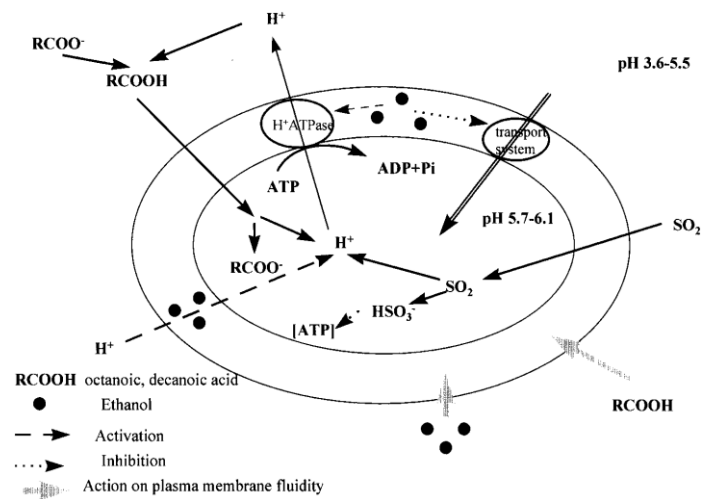


Fig. 2.2 Main effects of wine inhibitors on yeast cell membrane and metabolism [Alexandre and Charpentier, 1998]

These changes depend on the ethanol tolerance of each yeast strain and extensive studies have been carried out on the investigation of the genetic dissection of alcohol tolerance in order to identify which genes are involved in influencing this character and improve the selection of high ethanol yielding strains [Ismail and Ali, 1971; Pretorius and Bauer, 2002; Fujita et al., 2006; Hu et al., 2007; Kumar et al., 2008].

As it is schematically illustrated in figure 2.2 [Alexandre and Charpentier, 1998], ethanol is not the only one toxic by-product of yeast: medium chain fatty acids (MCFAs) such as octanoic or decanoic acids constitute another type of fermentation inhibitors produced during alcoholic fermentation [Viegas et al., 1989; Lafon et al., 1984]. These lipophilic acids act as antimicrobial components [Freese et al., 1973], and as seen for ethanol, lead to the reduction of cytosolic pH [Stevens and Hofemyer, 1993]. In particular, MCFAs act as proton carriers across the yeast plasma membrane, reducing the intracellular pH and disrupting the proton gradient. Among the other acid-stress effects, these events cause the acidification of cytoplasm and, as observed for ethanol, trigger to the stimulation of plasma membrane H⁺-ATPase in order to recover from acid stress and restore the pH homeostasis [Viegas and Sa-Correia 1991, Viegas et al., 1998; Cabral et al., 2001].

Moreover, as Correia pointed out [Correia, 1986], ethanol and these lipophilic acids may act in direct synergy by further slowing down the overall fermentation process.

Apart the high ethanol content and the presence of toxic fatty acids, there are many other factors that lead to stuck fermentation, such as low level of thiamine [Bataillon et al., 1996, Wang et al., 2005] or more in general nitrogen or vitamin deficiencies [Ingledew and Kunkee 1985, Ough et al., 1989], decrease in oxygen availability [Aries and Kirsop, 1978] or exposure to other inhibitory substances as sulphites and acetic acid as reviewed by Alexandre and Charpentier [1998] and by Tanghe et al. [2006].

2.1.3 Survey of different methods for assessing yeast tolerance to fermentative stress factors

As seen in the previous section (2.1.2), yeast strains differ in their ability to tolerate several stress factors present in the must; therefore, yeast quality assessment plays an important role in the prediction of the outcome of fermentation.

Conventionally, yeast cell survival in presence of potential stress factors is evaluated by simple growth assays in Petri dishes, by direct microscopic counts, dry weight or spectrophotometric methods [Ohta et al., 1981; Nwachukwu et al., 2006]. Apart from the commonly known procedures, optimal cell functioning can be assessed in several ways, for example by monitoring the level of important cell constituents [Qain, 1988], lipid composition [Mannazzu et al., 2008], activity of enzymes [Wellhoener and Geiger 2003, Cameron-Clarke et al., 2003], cell capacitance [Asami and Yonezawa, 1995; Noble et al., 1999; Marx and Davey, 1999; Mishima et al., 1991; Mas et al., 2001], intracellular pH [Imai et al., 1994], cumulative acidity [Patino et al., 1993] and throughout the so-called “acidification power (AP) test” [Opekarová and Sigler, 1982; Iserentant et al., 1996].

At a molecular level, the main methodologies are based on genetic dissection of yeast tolerance to ethanol [Hu et al., 2007; Kumar et al., 2008] and more in general involve yeast ecology studies, as it will be briefly discussed below.

- *The AP test to assess the technological quality of microbial cultures*

The cumulative acidity and AP tests measure the ability of cells to regulate homeostasis by actively pumping protons out from the cytosol. A number of authors have proven the correlation between cell growth and extracellular acidification (Roos and

Luckner 1984; Kotyk, 1989; Huth et al., 1990; Sigler and Hofer, 1991) and studies on cell metabolism and net proton production have been proposed over the years [Castrillo and Ugalde, 1994; Castrillo et al., 1995; Vicente et al., 1998; Srinivasan and Mahadevan, 2010].

Nearly thirty years ago, several authors introduced extracellular acidification as a suitable assay to predict the vitality of industrial strains and prevent stuck fermentations.

As widely reported in literature, pH downshift occurs as a result of HCO_3^- production from CO_2 , the action of H^+ -ATPase, H^+/K^+ exchange, secretion of organic acids and consumption of buffering compounds, and all these processes reflect very precisely the metabolic activity of cells [Sigler et al. 1981(a); Sigler et al. 1981(b)].

In particular, the acidification power of a cell is given by the sum of two contributions: the spontaneous protons extrusion (driven by endogenous energy sources) and the substrate-induced protons extrusion (driven by both endogenous and exogenous energy reserves).

The acidification power test was developed as a simple and rapid method for assessing how technological stress factors affect the ability of yeasts to carry out the fermentation process. Therefore, AP test can be defined as a “*sensitive indicator*” of the physiological status of cells and more in general as a significant predictor of the fermentative prowess of a given batch culture [Opekarova and Sigler, 1982; Kara et al., 1988; Malfeito-Ferreira et al. 1990; Riis et al., 1995; Gabriel et al., 2008].

- *Molecular studies for typing of wine yeast strains*

Cultural procedures represent basic techniques for the analysis of yeast tolerance to fermentative stress factors. However, yeast characterization based on physiological properties could give ambiguous results [Tornai-Lehoczki and Dlauchy, 1996].

By contrast, molecular methods are making the study of yeast ecology more and more attractive and offer an important tool in solving industrial problems [Fleet 2007; Beh et al., 2006; Fernandez-Espinar et al., 2006; Josepa et al., 2000].

In winemaking, many ecological studies are focused on typing of wine yeast strains to study and discriminate the authenticity of commercial yeasts [Schuller et al., 2004]. As reported by Vaudano [Vaudano and Garcia-Moruno, 2008], molecular studies can be performed to follow strain dynamics during fermentation, check the do-

minance of inoculated strains over wild strains, control yeast quality and detect fraud. Among the molecular methodologies, polymerase chain reaction (PCR) profile analysis has a good discriminating power for analyzing yeast strains [Ness et al., 1993] and therefore represents one of the most used techniques for wine yeast ecology.

Traditional systems are time-consuming, labour intensive or prone to errors, thus limiting parallelization and high throughput selection of the desirable yeast strains. Moreover, most of them are endpoint tests, and therefore, they seldom provide information about the dynamics and mechanisms of action of the chemicals on cells. The development of silicon technologies has contributed to the creation of alternative methods that could overcome the drawbacks of the conventional systems, as discussed in the next section.

2.2 Cell-based biosensors (CBBs)

In the last three decades, many studies have been focused on microbial metabolism due to the proven correlation between cell growth and either extracellular acidification or ionic conductivity change/biomass detection (section 2.1.3), enabling the development of micro-electronic sensors for culture monitoring, especially based on Ion-sensitive field-effect transistors (ISFETs) sensors, Light-Addressable Potentiometric Sensor (LAPS) [Yoshinobu et al., 2003] and impedance-based microdevices. Furthermore, more recently multiparametric chips have been proposed to carry out comprehensive studies about physiological state and dynamic behavior of cell cultures for pharmacological screening, basic research in systems biology and lab-scale fermentation tests. The main advantage is that they allow online measurements during short and long periods without damaging and labelling cells. The status of living cells can be monitored continuously before, during, and after exposure, providing information on the kinetics of the cell response to chemicals and on the cellular metabolic pathways. In this section, the main advances of ISFETs (2.2.1), impedance sensors (2.2.2) and multiparametric platforms (2.2.3) for biological applications are reviewed.

2.2.1 ISFETs sensors

ISFET is a special member of the family of potentiometric chemical sensors and was proposed for the first time by Bergveld [1970; 1972] (the operational principle is briefly described in appendix A). Since its discovery, it has been soon recognized as a powerful sensing element, as demonstrated by the intensive research and copious amount of published works that have quickly followed with excitement.

After the first patent on ISFET - granted in 1977 by the University of Utah [Johnson et al., 1977] - many other patents were applied over the years and over the world, and later on, ISFETs became commercially available from several companies [Bergveld, 2003; Jimenez et al., 2006; Bratov et al., 2010].

Nowadays, many commercial suppliers furnish ISFETs for agrofood applications as good candidates to replace traditional bulky glass electrodes. However, ISFETs are not directly expected to substitute the conventional glass pH meter since the last one still plays a key role in every day pH measurements thanks to its excellent electrode performances, internal reference system and long-term stability [Vonau and Guth, 2006]. Indeed, pH-sensitive FETs are rather meant for experimental conditions where glass electrodes could not be applied, such as measuring in particularly small sample volumes and with an extremely fast response. ISFETs have other benefits such as they can be dry stored, virtually unbreakable, non-invasive, good for dynamic and on-line measurements, eliminating the need for continuously sampling of the analyzed species [Yuqing et al., 2003]. They can cover both wide pH (typically from 2 to 12) and temperature (-45°C to 120°C) ranges [Schäpper et al., 2009]. Moreover, one of the main advantages of a silicon pH-meter concerns its realization process, which benefits from miniaturization with current planar IC technology and on-chip integration of sensor arrays.

Miniaturization and systems integration have driven many research groups towards the development of benchtop, portable or pocket instrumentations aimed at the measurement of *in vivo* physiological parameters [Bergveld 1985] or for food processing in wine industry [Artigas et al., 2003].

FET-based potentiometric sensors were studied for many biological applications ranging from affinity and enzyme biosensors such as EnFETs (enzyme-linked FETs) to whole cell-based sensors as Cell-FETs hybrids [Shiono et al., 1992; Pohanka and Skladal 2008; Poghosian et al., 2009].

The former consists of enzyme-entrapping membranes on top of the ISFET-gate and can be employed for the detection of glucose [Dzyadevich et al., 1999; Park et al, 2002; Luo et al., 2004], penicillin [Poghossian et al., 2001], urea [Senillou et al., 1990; de Melo et al., 2003] and other analytes as surveyed by Schöning and Poghossian [2006] and Khanna [2007]. The latter belongs to the wide family of cell-based biosensors (CBBs), that have been largely employed for extracellular potential measurements [Offenhäuser et al., 1997; Vassanelli and Fromherz, 1998; Martinoia and Massobrio, 2004; Imfeld et al., 2008] or for the detection of changes in the rate of proton extrusion caused by different external stimuli (i.e. by addition of drugs, toxic compounds or pollutants to the medium) [Offenhäuser and Knoll, 2001; Schöning and Poghossian, 2006; Guth et al., 2009].

The extracellular acidification can be influenced by several mechanisms that occur in the cytoplasm and at the membrane level. As it is well known, glycolysis is one of the main metabolic pathways from which cells take their energy supply and it ends aerobically with acetyl-CoA and CO_2 while anaerobically with lactic acid. As CO_2 goes out the cytosol, it is hydrated to form H^+ and HCO_3^- . Apart from glucose metabolism, other mechanisms such as oxygen consumption (i.e. cell respiration), H^+ ATPase, ion exchange (e.g. Na^+/K^+ ATPases) and nutrients uptake are involved in proton release outside the cell. Thus, the metabolism of viable cells lead to the acidification of the extracellular environment and the acidification rate is correlated to the physiological state of a cell.

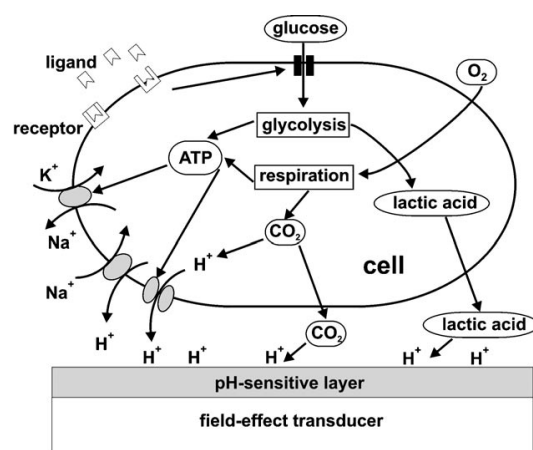


Fig. 2.3 Schematic representation of extracellular acidification process of a cell on an Ion-Sensitive FET [Schöning and Poghossian, 2006]

Over the last two decades, many scientific publications were addressed to the development of ISFET-based sensors for on-line monitoring of *in-vitro* extracellular acidifications [Grattarola et al., 1993; Baumann et al., 1999; Martinoia et al., 2001].

ISFET-arrays were developed to study the microenvironmental pH (pH_M) and the role of glycolysis [Lehmann et al. 2000], distinguish between apical and basolateral acidification of adherent tumor cells [Lehmann and Baumann, 2005] and for *in vitro* toxicity screening applications by cell exposure to toxic agents [Lorenzelli et al., 2003].

The extracellular acidification rate (ECAR) was measured growing cells on sensor's surface [Lehmann et al. 2001; Brischwein et al., 2003], membranes of commercial wells (Transwell®) [Lorenzelli et al., 2003], autoclavable semipermeable barrier [Gerlach et al., 2007], glass plate [Mohri et al., 2006], agarose gel [Bettaieb et al., 2007] or on continuously stirred bacterial suspension [Castellarnau et al., 2008].

2.2.2 Impedance sensors

Impedance spectroscopy is currently receiving increasing attention in microbiology due to its sensitive, high automated and easy-to-use technique. However, "Impedance microbiology" is not a new approach in research field; it is necessary to go back to a meeting of the British Medical Association in 1898 where Stewart presented a paper, later to be published in *The Journal of Experimental Medicine*, entitled "*The changes produced by the growth of bacteria in the molecular concentration and electrical conductivity of culture media*" [Stewart, 1898]. The electrical response curves presented by the researcher followed the putrefaction of blood and serum and they were very similar to those obtained from currently available impedance systems. The significant difference between last century and today is that nowadays impedance can be considered as a rapid microbiological method, whereas Stewart was measuring changes in conductance over thirty days.

Other works followed Stewart's initial studies, but it was not before the mid seventies that the technique began to receive the attention it merited [Ur and Brown, 1975]. This coincided with the introduction of dedicated impedance systems - such as Bactometer [Cady, 1978; Gnan et al., 1982] or Malthus system [Neaves et al., 1988] - and a consequent increase in published works [Firstenberg-Eden and Eden, 1984; Harris and Kell, 1983; Asami and Yonezawa, 1995; Silley and Forsythe, 1996].

Today, impedance-based cell analysis is a well-established technique in biology but the macro-scale implementation suffers from low sensitivity and long assay times due to the employed large sample volumes. Therefore, many researchers tried to overcome these problems by shrinking down the whole impedance sensors dimension with the implementation of silicon microfabrication techniques.

Several impedimetric biosensors were developed over the years [Guan et al., 2004], recording impedance of a cell suspension even in nanoliter-scale volume [Gomez et al., 2002].

In particular, by culturing cells over planar microelectrodes, impedance measurements were investigated as indicators of cell adhesion and spreading [Wegener et al., 2000; Morguet et al., 2007], motility and morphology [Giaever and Keese, 1993; Arndt et al., 2004], and cytotoxicity [Ehret et al., 1997]. In 1997, Ehret and co-workers demonstrated how interdigitated electrodes (IDES) could be used to monitor biologically relevant signals as an alternative method to conventional toxicology tests. Since then, many other studies were carried out on adherent cells, demonstrating the possibility to use microelectrodes as a stable, non-invasive interface for monitoring impedance characteristics of cell populations over extended periods [Xiao and Luong, 2003; Solly et al., 2004; Yeon and Park, 2005; Xiao and Luong, 2005; Guo et al., 2006; Campbell et al., 2007; Ceriotti et al., 2007(b-c)].

If CBBs were widely investigated for adherent cells, few research works were published on microdevices devoted to the monitoring of suspended cells. Microfluidics biosensors were developed for bacterial cells [Gomez et al., 2002; Boehm et al., 2007] and different electrodes configurations were studied for separately monitoring biomass and background medium electrolytes [Krommenhoek et al. 2006; Spiller et al., 2006]. Microbial growth was also monitored by plating yeasts on agar surface in correspondence to the sensitive area (IDES) and measuring conductivity changes of cell medium brought about the metabolic activity [Ress et al., 2009].

For suspended cells, optical density (OD) represents still an alternative to impedance spectroscopy and it is already applied in microbioreactors [Schäpper et al., 2009]. However, air bubbles can interfere with the optical measurements and light-based probes detect even aggregates, cell debris, and other particles that can collect during fermentation.

Moreover, washing steps as well as medium changes can perturb the osmotic potential across the plasmatic membrane, causing instability in the refractive index and therefore in the solution turbidity [Hobson et al., 1996].

2.2.3 Multiparametric microdevices for cell analysis

The measurement of pH or impedance as single parameter was considered too restrictive for getting comprehensive understanding of dynamic cellular behaviour. Many efforts were devoted to the development of multiparametric chips combining several complementary sensors to get inside into the complex metabolic pathway network of cells.

ISFETs offer the potential for on-chip circuit integration and the possibility of multichannel sensing for lab-on-a-cell applications. These silicon-based microsensors typically form the bottom of a cell culture chamber and allow performing parallel measurements of multiple parameters for the interpretation of different effects on living cells.

Therefore, several multisensors chips were realized for the monitoring of different parameters such as extracellular acidification (with ISFETs), dissolved oxygen (with amperometric sensors), cell adhesion or biomass (with impedance sensors), and temperature (with PN-diode or Pt 100) [Wiest et al., 2005; Ceriotti et al., 2007; Krommenhoek et al., 2008; Mohri et al., 2008; van Leeuwen et al., 2010]. Some of these sensors are autoclavable and therefore reusable, others are disposable such as the one-way physio-sensor [Vonau, 2007] that can also detect H₂O₂ through an enzyme covered electrode structure.

Among the state-of-the-art of electrochemical CBBs, a screening system - Bionas[®] 2500 analyzing system (Bionas GmbH, Germany)- is commercially available and it is well-established both for immortalized and primary cells [Ceriotti et al., 2007(a); Thedinga et al., 2007; Mestres and Morguet, 2009]. Moreover, a multiparametric handheld and mobile device - intelligent mobile lab (IMOLA) - was developed for metabolic profiling with a fluidic system, sensor control, data management and software [Wiest et al., 2005]. A further version of the mobile biosensor is the Micro-Lab (μLa) that would deliver, as a Point-of-Care scenario, measurement data via the public cellular network [Schmidhuber et al., 2009].

2.3 DNA amplification on PCR microdevices

In this section, a general description of the amplification process and the main reasons behind miniaturization are presented. Then, the state of the art in the development of new promising micro devices is reviewed.

2.3.1 The PCR process and the benefits of miniaturization

The polymerase chain reaction (PCR) is an enzyme catalyzed amplification technique that allows replication of specific fragments of DNA. Since its discovery [Mullis et al., 1986], by which the biochemist Kary Mullis won the Nobel Prize in 1993, the PCR technique has become a key tool in modern molecular biology. Thanks to its reliability, it is widely used every day in diagnostics, quality analysis of foodstuffs, forensic investigations, paternity testing, environmental monitoring, molecular archeology and in many other general biomedical and biotechnological applications.

DNA amplification is carried out *in vitro* by cycling through three different temperature steps. Each PCR cycle consists of the separation of the double-stranded DNA helix (near 95°C), annealing of the specific primers to their target nucleotide sequence (usually between 55°C and 65°C), and extension of these short molecules to synthesize the complementary strand of the template (about 72°C). This last step is catalyzed by a thermo stable DNA polymerase, called Taq polymerase, that restores the double-stranded nucleic acid by adding free deoxynucleoside triphosphates (dNTPs) to the sequence that must be amplified. Working in this way, the small amount of starting DNA is doubled in each cycle. After 20 cycles, it reaches over one million copies of the original target (fig. 2.4).

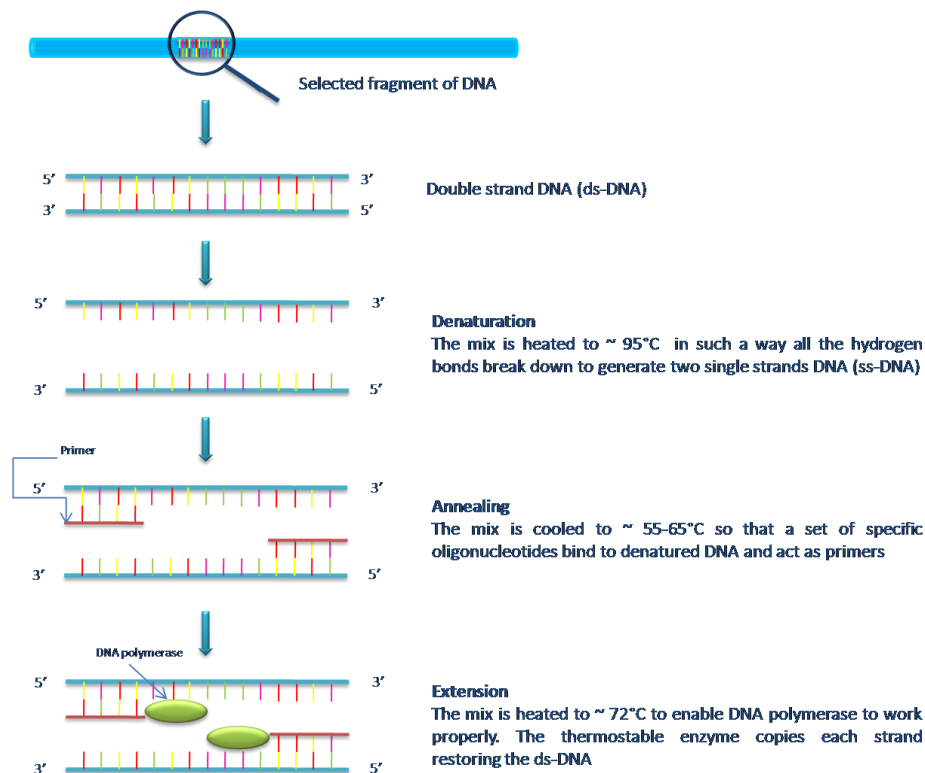


Fig. 2.4. Schematic representation of the polymerase chain reaction (PCR) process

PCR is conventionally performed in benchtop instruments by using programmable thermocycler with large volume sample (~25 μ l) confined in polypropylene tubes, and a complete assay requires a couple of hours or even more. This long reaction time is caused by the high thermal mass of the cyclers and the large reaction volume that entail slow heating and cooling rates.

The lack of fast thermal cycles has given rise to alternative approaches in which MEMS technologies have been successfully employed. Thanks to the strong coupling between life science and technology, several miniaturized PCR chips have been developed in the last decade. By reducing the reaction time (from hours to several minutes), the reagents' volumes (typically in the order of microliters or even nanoliters) and the power consumption levels (in terms of few Watts), miniaturized PCR devices overcome the drawbacks of the conventional laboratory instrumentations. Moreover, by shrinking down the PCR module size, it is possible to achieve a high integration system made up of several analytical components. Indeed, one of the main challenges in miniaturization of PCR is the integration of different functional sections in LOC platform in order to avoid, as far as possible, both manual operation and external macro machine tools. The need for improved speed and portability of the PCR systems has encouraged many research groups to investigate microchip-based PCR, as will be discussed in the next section.

2.3.2 PCR microdevices: State of the Art

Since the 1990s, PCR micro devices have undergone widespread and rapid development [Zhang et al., 2006; Zhang and Xing, 2007]. Currently, PCR microfluidics can be mainly divided into two categories: chamber PCR and continuous flow PCR (CFPCR), (fig. 2.5).

In the first configuration, presented initially by Northrup and co-workers [Northrup et al., 1993], the reaction mix is kept stationary in a single chamber while the temperature is repeatedly cycled among the three different steps. This type of arrangement is the miniaturized version of the traditional PCR instruments, and even though it can provide faster thermal cycling rate by taking advantages of the micro size, it still suffers from the slow overall alternation of rising and fall of the temperature cycles. As in the conventional macro systems, the total time required to carry out each thermal cycle is given by both the hold time (i.e. the time over which the reagent mixture uniformly attains the selected temperature) and the ramping time (i.e. the time that depends on the effective heating and cooling rates). However, this method does not need a complex microfluidics (inlet and outlet of sample) and, as a consequence, it has relatively easy fluid handling.

While the first configuration uses a static approach, the second configuration, CFPCR, can be considered a dynamic system because it is characterized by a continuous flow of the reaction mixture through different thermostatic zones. As the sample flows through thin microchannels, it passes through different zones, each maintained at a constant value. With CFPCR, the temperature transition time is strongly reduced because it actually depends only on the mixture flow rate and the effective time to reach thermal equilibrium by fluids. This kind of micro PCR device was first introduced by Kopp et al. in 1998 [Kopp et al., 1998]. Since then, CFPCR has undergone significant improvement.

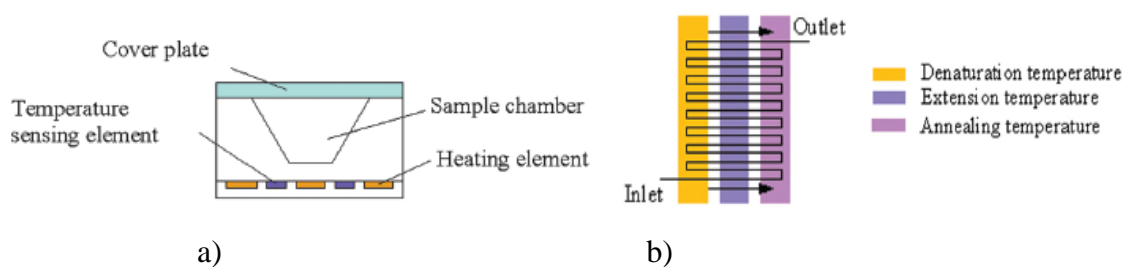


Fig. 2.5. Examples of the two major PCR configurations: microchamber and CFPCR [Zhang et al., 2007]

Although CFPCR seems to be the most advantageous approach when compared to chamber PCR, it has one considerable limitation: CFPCR has a fixed number of cycles due to its channel layout. Thus, CFPCR lacks the flexibility to change some experimental parameters. Chamber PCR, on the other hand, allows adjustments based on the initial amount of DNA. Additionally, CFPCR has other drawbacks that cannot be ignored, such as the generation of gas bubbles and progressive sample dispersion along the microchannels. Both of these problems reduce the efficiency of the biological process. For this reason, they must be carefully considered during the design of the overall microfluidic system.

Lastly, CFPCR typically has a descending series of temperature zones, usually in the following order: denaturation temperature (95°C) - extension temperature (72°C) - annealing temperature (e.g. 55°C). This creates a temperature gradient throughout the device without a forced cooling process during the annealing step. However, this sequence does not match with the correct order of the PCR temperature steps and the single-stranded DNA is very likely to recombine with its complementary portion as it passes through the extension region. In order to circumvent this problem, a circular arrangement has been developed which keeps the right order of PCR steps and avoids the unwanted formation of DNA double strands [Chen, 2006].

The complex microfluidics and fixed cycle number issues with CFPCR can be overcome using an oscillatory-flow PCR that is based on the principle of sample shuttling. The amplifying reaction is carried out inside a straight channel by providing both the quick transition temperature typical of the continuous-flow PCR and the cycling flexibility of the chamber-type device [Frey et al., 2007]. However, even if it is more advantageous with respect to the previous methods, the temperature zones will still have the typical arrangement of the CFPCR instead following the real order of PCR reaction.

Among the micro PCR devices developed in the last few years, there are also other original PCR chips that do not fit within these classifications [Krishnan et al., 2002; Guttenberg et al., 2005; Ottensen et al., 2006]. Most are still far from achieving either high throughput amplifications or high degree of integration.

On the other hand, each specific layout has its own merits and limits affecting the final efficiency of the whole process. Moreover, the success of the reaction depends also on the chosen substrate materials and on the specific fluidic and temperature controls. Therefore, many research groups have tried to use different substrate materials, microfabrication technology and heating/cooling methods to achieve faster and better amplification performance.

Regarding the chip substrates, almost all PCR microdevices are made of silicon [Felbel et al., 2004; Yan et al., 2005; Ke et al., 2007], glass [Gong et al., 2006; Crews et al., 2008] or of both of them [Schneegaß et al., 2001; Erill et al., 2003; Cho et al., 2006].

There are several reasons why silicon and glass are often employed. First of all, the microstructures can be realized by well-established microfabrication technologies, such as the standard photolithography and chemical etching techniques. Further, metal film heaters and temperature sensors can be patterned on their surface providing a high level of integration. Silicon has the advantage of a superior thermal conductivity whereas glass is more biocompatible and allows visual inspection. However, many other promising materials can be used for PCR microfluidics that can also satisfy the needs of biocompatibility, low cost, ease fabrication and optical transparency. These materials are polymers such as polydimethylsiloxane (PDMS) [Prakash et al., 2006; House et al., 2010; Trung et al., 2010], SU-8 [Christensen et al., 2008], polymethylmethacrylate (PMMA) [Yao et al., 2005; Hashimoto et al., 2006], polycarbonate (PC) [Chen, 2006; Wang et al., 2006], cyclic olefin copolymer (COC) [Koh et al., 2003; Münchow et al., 2005] or polyimide (PI) [Giordano et al., 2001]. They can be easily fabricated by replicate moulding or by direct fabrication methods and they can provide a good thermal isolation among the three temperature zones.

Concerning of the issue of biocompatibility, there is often a strong and deleterious interaction between the inner surface of the reaction chamber/channel and the PCR mixture. All the mentioned materials can negatively affect the PCR performance and therefore many research works are focused on various passivation techniques for optimizing the device surface (static passivation) or the composition of the solution (dynamic passivation) [Christensen et al., 2007]. In particular, static passivation involves various coating procedures such as with silanizing agents [Consolandi et al., 2006] or by oxygen plasma activation of the chip surface [Kim et al., 2006] while dynamic passivation consists on the introduction of some additives that are known to improve the final amplification performance by a stabilizing effect. Some of these enhancers are bovine serum albumin (BSA), polyethylene glycol (PEG), polyvinyl pyrrolidone (PVP), Tween-20 [Panaro et al. 2005]. Surfactants are very often employed to limit the critical issue of sample evaporation, especially when small-volume PCRs are performed. Many research groups strongly reduce sample volume from the conventional 25 μ l (typical volume loaded on the polypropylene tubes of the commercial thermal cycler) to 1 μ l [Cho et al., 2006, Neuzil et al., 2006], 40nl [Matsubara et al., 2005] and even to 0.45nl [Marcus et al., 2006]. Although nanoliter or picoliter PCR systems take advantage to the low thermal mass for pursuing high-speed DNA amplification, they may be more exposed to absorption and evaporation phenomena, which can considerable decrease the overall efficiency of the reaction. To prevent evaporation, mineral oil can be used as cover layer [Legendre et al., 2006; Neuzil et al., 2006] since its boiling point is far above the highest cycling temperature of PCR. Other tricks involve solid covers to increment the pressure inside the chamber or special external parylene coating as in the case of the oxygen permeable PDMS [Prakash et al., 2006].

Biocompatible materials play a key role also in the whole fluid handling such as in microvalves and micropumps, which can be in direct contact with the PCR solution. Extensive studies are carried out in the field of fluid switching and driving in attempt to enhance biochemical compatibility, integration, reproducibility, response time and power consumption towards the realization of automated and handheld microfluidic systems. Particularly, microvalves are being deeply investigated in the form of both active and passive microvalves employing mechanical [Münchow et al., 2005], non-mechanical [Liu et al., 2004] moving parts and external systems [Prakash et al., 2006, Anderson et al., 2000]. At the same time, a broad variety of technologies have been exploited for pumping liquids by means of mechanical [Frey et al., 2007, Liu et al., 2004] and non-mechanical [Münchow et al., 2005; Liu et al., 2004] mechanisms. Although the remarkable developments in the in-

tegration of such microfluidic elements, some limits are still raised by the whole thermal management. Indeed, recent efforts aimed at achieving faster and more efficient thermal cycling, are mainly focused into the development of off-chip or on-chip heating systems. The former usually employ external heating sources such as Peltier cell [Liu et al., 2004], infrared radiation [Giordano et al., 2001; Hashimoto et al., 2006] or halogen lamp [Ke et al., 2004], the latter include integrated microfabricated resistive heating element and temperature sensors [Christensen et al., 2008].

However, even with many improvements in performance and integration of current PCR micro devices in terms of fluid handling, heating arrangements and suitable substrates, some shortcomings still exist. In particular, a problem arises when the amplification module has to be coupled on-line with other modules such as the detection system. To date, several integrated genetic analysis microsystems have been realized by involving different downstream sample processes such as microchannel capillary electrophoresis (CE) [Easley et al., 2006] and DNA microarray hybridization [Liu et al., 2004; Anderson et al., 2000], or by monitoring instantaneously the amplification products through a real-time PCR [Cady et al., 2005; Cho et al., 2006; Lee et al., 2006; Frey et al., 2007; Fang et al., 2009; Kim et al., 2009].

Despite of the most recent and exciting accomplishments, the integration of microchip-based PCR and detection system depends still on fluorescence microscopy [Frey et al., 2007; Christensen et al., 2008; Easley et al., 2006] or on the addition of external electrochemically-active indicators [Liu et al., 2004; Lee et al., 2003]. As reported by Lee and co-workers [Lee et al., 2010] more research is needed to improve the reproducibility and sensitivity of these real-time PCR devices and also new directions must be undertaken towards the realization of point of care DNA analyzers with online and label-free detection methods.

Chapter 3

3 Micro Electrochemical sensors for wine yeast analysis

In this work, cell-based electrochemical sensors are investigated, especially focused on yeast quality assessment for wine applications. The device consists of three integrated microsensors - $\text{SiO}_2/\text{Si}_3\text{N}_4$ Ion-Sensitive Field-Effect Transistor (ISFET), Pt impedimetric sensor and a temperature sensor - able to monitor extracellular metabolism, cell settling and temperature, respectively.

The device was developed at Fondazione Bruno Kessler (FBK –Trento, Italy) while the analyzed yeasts were kindly supplied by BioAnalisi Trentina s.r.l. (Rovereto, Italy).

3.1 Materials & Methods

3.1.1 Microfabrication of the electrochemical sensors

The multiparametric sensors were realized with a non-standard fabrication process derived from a $4\mu\text{m}$ Al-gate p-well CMOS (Complementary Metal Oxide Semiconductor) technology [Martinoia et al., 1999] in order to include the realization of double layer $\text{SiO}_2/\text{Si}_3\text{N}_4$ dielectric gate with Pt and Ag electrodes.

Starting from n-type $4''$ silicon wafers, ISFETs were realized on p-well (boron implant and diffusion, final junction depth $4.7\mu\text{m}$) in order to insulate the devices from the n-type substrate (fig. 3.1). Source and drain n+ regions and substrate contacts were realized by diffusion from phosphorus pre-deposition with a final junction depth of 750 nm. Ohmic contacts to p-well were realized with BF_2 implant. The pH sensitive layer - Si_3N_4 - was deposited by Low Pressure Chemical Vapour Deposition (LPCVD).

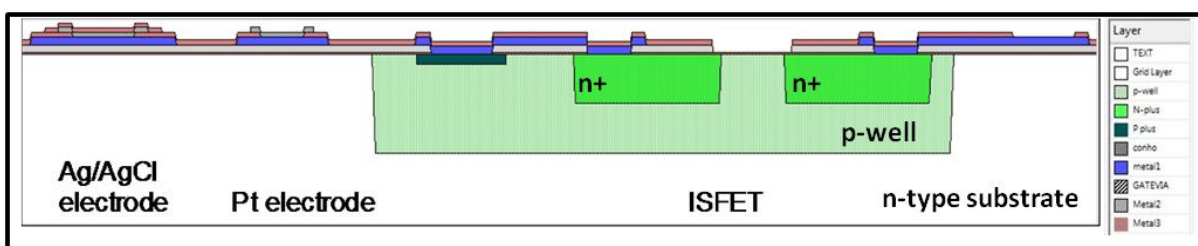


Fig. 3.1 Schematic cross-section of the multiparametric sensor

The choice of the dielectric gate material plays a key role to get sensor performance as close as possible to the Nernst's theoretical sensitivity (59 mV/pH at 300K) and with linear response over the measurement range. Although some materials (e.g. Ta_2O_5) could represent a better choice in terms of sensitivity and linearity (see Appendix A), stoichiometric Si_3N_4 , deposited by LPCVD, allows a good sensitivity and stability with a high compatibility with CMOS technologies and without the need for a dedicated equipment. The ISFET sensor was realized with a W/L ratio of 67 with a meander configuration and long source/drain diffusions for better encapsulation (fig. 3.2 a).

Electrical insulation was provided by a Low Temperature Oxide (LTO) layer with a thickness of 600 nm. Electrical connections were provided with a single-level of multilayer (Al:1%Si/Ti/TiN) metal wiring (660 nm), while the further electrical insulation was implemented with a Plasma-Enhanced Chemical Vapor Deposition (PECVD) Si_3N_4 layer (250 nm).

The technological platform also allows the realization of Pt electrodes (205 nm) exposed to the solution, which can be used for implementing on-chip different electrochemical sensors (e.g. conductivity, voltammetric or chronoamperometric sensors). The conductivity sensor was implemented with a 2-terminals configuration with circular symmetry with a cell constant around 4, which is a trade-off suitable for the selected measurement range (fig. 3.2 b). Electrical contacts to solid-state devices and Pt electrodes were implemented with low resistance Al wires. A Ag/AgCl pseudo-reference electrode was also realized with an evaporated Ag layer (150 nm) and a post-processing galvanic chlorination from KCl 1M solution saturated with Ag (fig. 3.2 d). Diode temperature sensor was obtained with n-diode implant on p-well (fig. 3.2 c). In table 3.3 are reported the cross-section of the device and the main details for a $4\mu\text{m}$ n-MNOS structure.

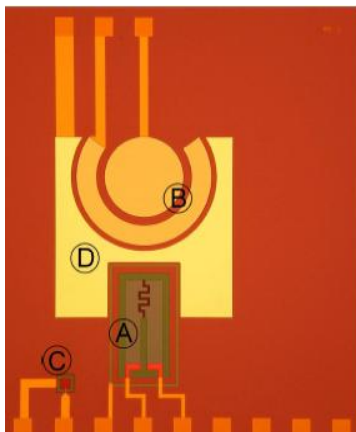


Figure 3.2. (a) Microphotograph of the multiparametric probe, chip size $5 \times 5 \text{ mm}^2$. A) ISFET sensor, B) impedance sensor, C) diode for temperature sensing, D) on-chip Ag/AgCl pseudo-reference electrode.

Table 3.3. Main details of 4 μ m n-MNOS structure

P-well	Junction depth	4.76 μ m
	Sheet resistance	3.5 k Ω /sq.
N-diodes	Junction depth	2.49 μ m
	Sheet resistance	64 Ω /sq.
P-diodes	Sheet resistance	60 Ω /sq.
Dielectric gate	SiO ₂ /Si ₃ N ₄ multilayer	~60nm
Al wires	Sheet resistance	0.08 Ω /sq.
Pt, Ag wires	Typical thickness	200nm

3.1.2 Packaging of the microfabricated device

The encapsulation of ISFET microdevice is a fundamental step that must guarantee the correct functionality of the device and it is often a challenge to sensor technology, as widely reported in literature [Oelßner et al., 2005; Velten et al., 2005]. Therefore, particular attention was devoted to the chip encapsulation. First of all, the sensor chips were bondwired to a printed circuit board (PCB QFP32) and epoxy resin (UHU plus endfest 300) was used for packaging and protection of the bondwires and contact regions (fig. 3.4 left). Polystyrene wells were then glued with the same epoxy resin for the confinement of cell culture and medium solutions (fig. 3.4 right). The encapsulant glue satisfied the following requirements: perfect sealing around the sensors area, good chemical and thermal stability, low absorption for the species to be measured, avoid swelling phenomena and good biocompatibility (no release of toxic chemicals on the growth medium).

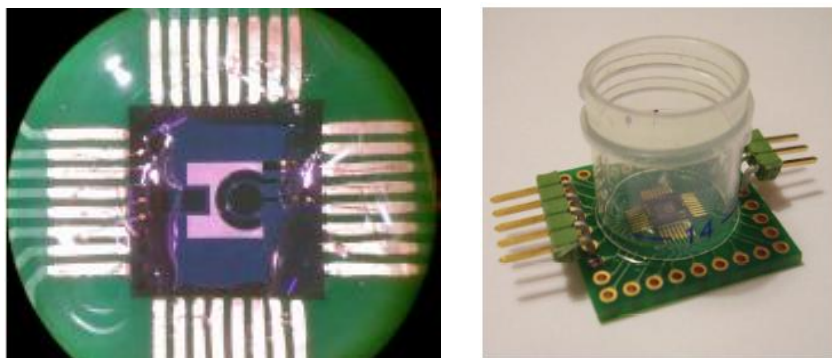


Fig. 3.4 (Left) Encapsulation of the multiparametric probe and (Right) final packaging of the device

3.2 Sensors characterization

3.2.1 ISFET

A preliminary cleaning with 2% HF followed by a conditioning phase of 12 hours with a neutral pH buffer solution were performed in order to respectively remove a thin surface layer of oxide exposed to the atmospheric environment and activate the reactive sites of the sensitive layer.

Then, ISFET sensors were characterized by means of leakage current, input characteristics, pH response and drift measurements.

The leakage current (I_L) was measured to preliminary check the dielectric gate condition and its packaging, thus obtaining useful information about the correct function and electrical insulation of the devices.

The measurements were carried out by applying a linear voltage (typically $-3V \div +3V$) between sensor terminals and a commercial reference Ag/AgCl electrode (InLab 423, Mettler-Toledo GmbH, Giessen, Germany) with a semiconductor parameter analyzer (HP 4156).

The device is considered electrically isolated when the leakage current is lower than $1 \cdot 10^{-9}$ A, as reported in figure 3.5.

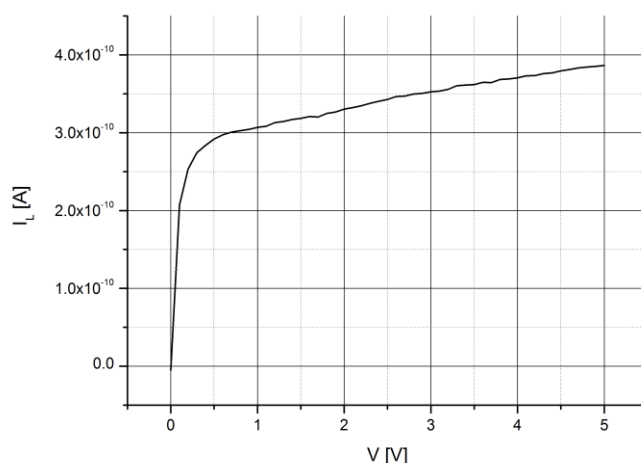


Fig. 3.5. A typical example of leakage current (I_L) measurement

The characterization of Si_3N_4 -gate ISFET sensitivity was performed by measuring the input characteristics ($I_{\text{DS}}/V_{\text{GS}}$) at $0.5\text{V } V_{\text{DS}}$ and with three different (4-7-10) pH buffer solutions (Crison) (fig. 3.6 a).

The threshold voltage V_{th} was then obtained by a graphical method [Tomaszewski et al., 2007] and by plotting V_{th} in function of pH, it was possible to obtain the pH response of the device (Fig. 3.6) and in turn estimate the sensor sensitivity (Table 3.14).

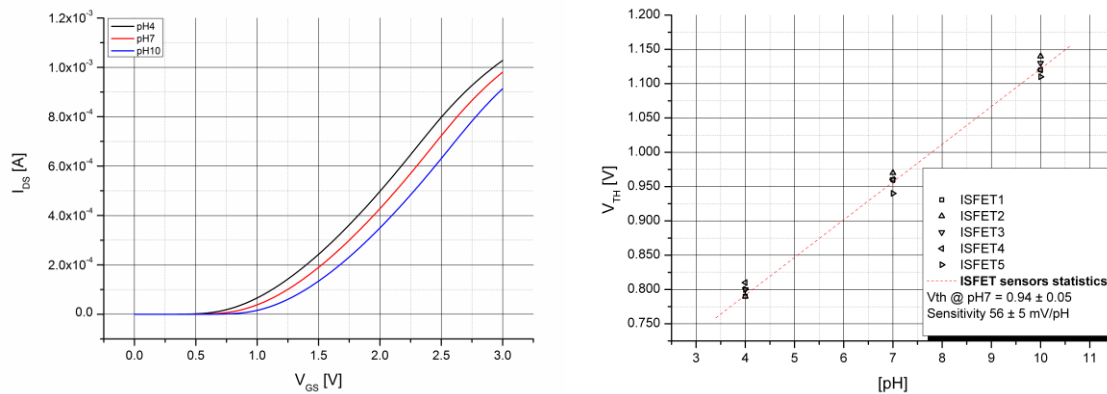


Fig. 3.6. (Left) Input characteristics ($I_{\text{DS}}/V_{\text{GS}}$, $0.5\text{V } V_{\text{DS}}$) in function of different pH buffer solutions; (Right) pH response of the device

Sensitivity of Si_3N_4 ISFET was estimated at 56 mV/pH , a typical value for LPCVD stoichiometric silicon nitride sensitive layer (see Appendix A) and relatively close to the Nernst's theoretical sensitivity (i.e. 59 mV/pH).

Long-term drift measurements were also carried out in such a way to detect the threshold voltage shift of the studied ISFETs. The causes of this phenomenon are still not completely unraveled but there are some models and theories that try to clarify the possible involved chemical and physical mechanisms (see Appendix A).

Drift measurements were performed in a Faraday cage (light-protected) with a buffer solution (pH 7) and a commercial reference Ag/AgCl electrode (InLab 423, Mettler-Toledo GmbH, Giessen, Germany), and by using a DC current source (Keithley 6221), multimeter acquisition system (Keithley 2700) and LabviewTM (National Instruments).

Measurements were carried out for more than 24 hours to avoid the influence of transient events and to obtain a suitable valuation of drift phenomenon (fig. 3.7).

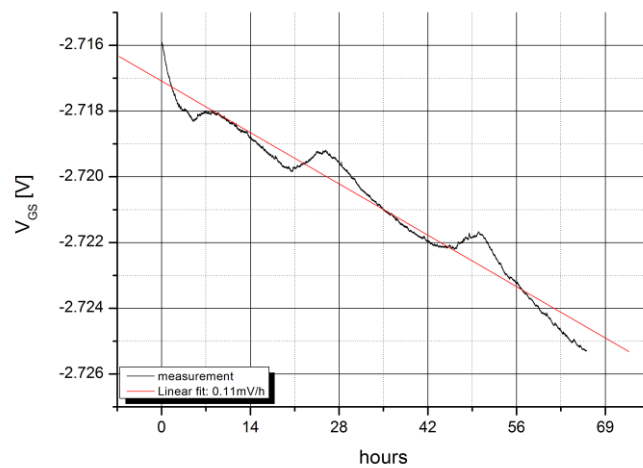


Fig. 3.7. An example of long-term drift measurements

Typical drift values were around 0.3 mV/h (Table 3.14) and considering the average sensitivity of the sensors (56 ± 3 mV/pH), the pH measurement was influenced by a drift of 0.005 pH/h.

The usual way of coping with the effect of drift is to carry out calibrations at regular intervals. The long-term drift rate can be determined prior to any long-term measurements and the obtained experimental data can be compensated for the transient response of the device.

Up to 5 parallel pH measurements were performed by the bias board in such a way to increment measures statistics (fig. 3.8).

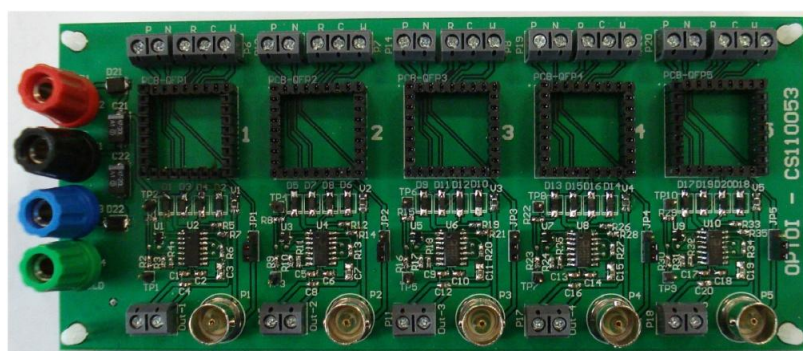


Fig 3.8 Bias board

3.2.2 Impedance sensor

The common calibration procedure involved successive immersions in three conductivity standard solutions: 11.2 mS cm^{-1} [10^{-1} M KCl]; $1413 \text{ } \mu\text{S cm}^{-1}$ [10^{-2} M KCl]; $147 \text{ } \mu\text{S cm}^{-1}$ [10^{-3} M KCl], (Crison).

The impedance measurements were carried out over a frequency range $10^{-2} \div 10^4 \text{ KHz}$ and by applying 0.5V to the two terminals (fig. 3.9) though a HP 4192A impedance analyzer (Hewlett-Packard). Data were acquired through LabviewTM (National Instruments).



Fig. 3.9. Detail of the impedance sensor

In figure 3.10 are shown the typical behaviour of impedance magnitude and phase curves plotted as a function of different standard conductivity solutions.

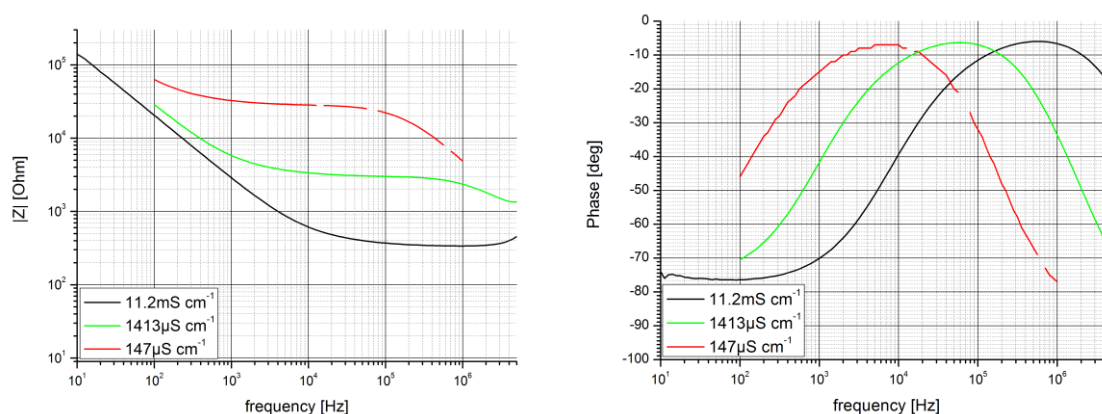


Fig. 3.10. (Left) Impedance and (Right) phase characteristics over $10^{-2} \div 10^4 \text{ KHz}$ as function of different conductivity solutions

From the experimental impedance and phase measurements, a calibration curve of the conductivity sensor was obtained (fig. 3.11).

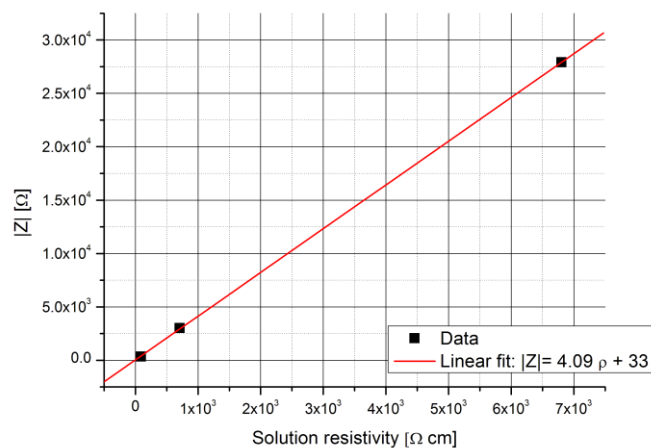


Fig 3.11. Example of impedance sensors calibration

3.2.3 Diode

PN diodes (fig. 3.12) can be used as thermometer as they vary forward voltage with temperature. The diode was characterized by applying forward bias with 10μA of current (fig. 3.13). The estimated sensitivity of the integrated diode was equal to 2.3 mV/°C.

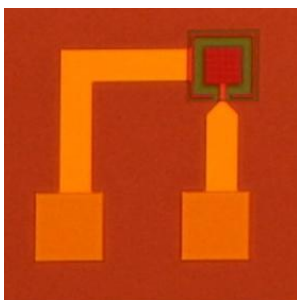


Fig 3.12. Detail of the temperature sensor

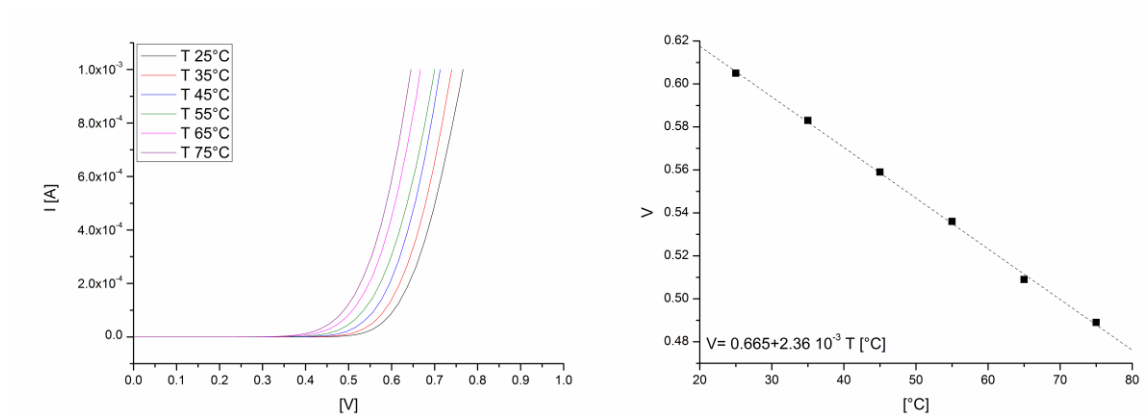


Fig.3.13. (Left) I-V characteristics of forward bias of the PN diode as a function of temperature; (Right) Sensor response with $I_d = 10\mu\text{A}$.

The main characteristics of the three integrated sensors (ISFET, impedance sensor, temperature sensor) are summarized in Table 3.14.

Table 3.14. Main specifications of the integrated sensors

Sensor	Parameter	Value
ISFET	Sensitivity	56 ± 3 mV/pH
	Drift	< 0.3 mV/h
	Threshold Voltage	0.94 ± 0.05 V
Conductivity	Range	$0.2 \cdot 10^{-3} \div 0.1$ S cm^{-1}
	Cell constant	4.3 cm^{-1}
Temperature	Sensitivity	2.3 mV/°C
	Tested range	$25 \div 75$ °C

3.3 Experimental results

3.3.1 Yeast cell growth and extracellular acidification

A preliminary correlation study between extracellular metabolic activity and cell growth was performed in order to individuate the time window of interest during which cells multiply until reaching the stationary phase (chapter 2, section 2.1.1). Cells were cultivated in batch conditions (i.e. without any further addition of nutrients) and their evolution over time was characterized throughout off-line measurements by constantly sampling cell number and pH at regular intervals.

For the investigation of this initial phase, a wine yeast strain of *S. cerevisiae* 300 (kindly provided by BioAnalisi Trentina s.r.l., Rovereto, Italy) - able to survive up to 12% (v/v) of ethanol - was employed (fig. 3.15).

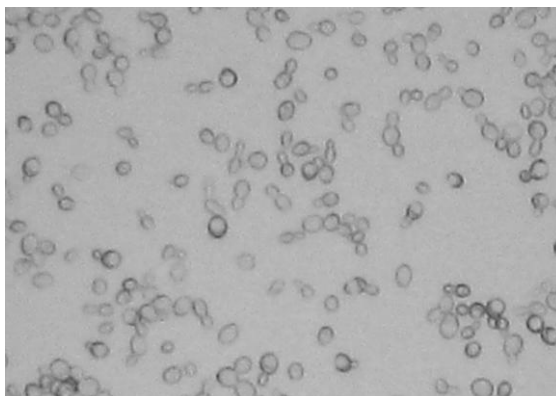


Fig. 3.15. Picture of *S. cerevisiae* 300 (20x, Olympus IX50)

In particular, yeast cells were grown in sterile Yeast Peptone Dextrose (2% Bacteriological peptone, 1% Yeast extract, 2% Glucose, w/v) Broth (Sigma-Aldrich®) and were incubated at 28°C overnight to yield a microbial concentration of about 10^7 cells ml^{-1} . Then, exponentially growing cultures were inoculated in 1 ml of fresh YPD liquid medium at a concentration of about $1 \div 2 \cdot 10^6$ cells ml^{-1} . At regular intervals, cells were harvested by centrifugation (5.6 rpm, 1 min, 25°C), microscopically counted (fig. 3.16, a) and supernatants were employed to monitor the progressive acidification of the culture medium with both a commercial pH-meter (Crison GLP22) and integrated ISFET sensor (fig. 3.16, b).

Viable cells were numbered by using a haemocytometer and methylene blue staining procedure. Living cells and metabolic activity were both monitored for more than 24 hours at a constant temperature of $25 \pm 1^\circ\text{C}$.

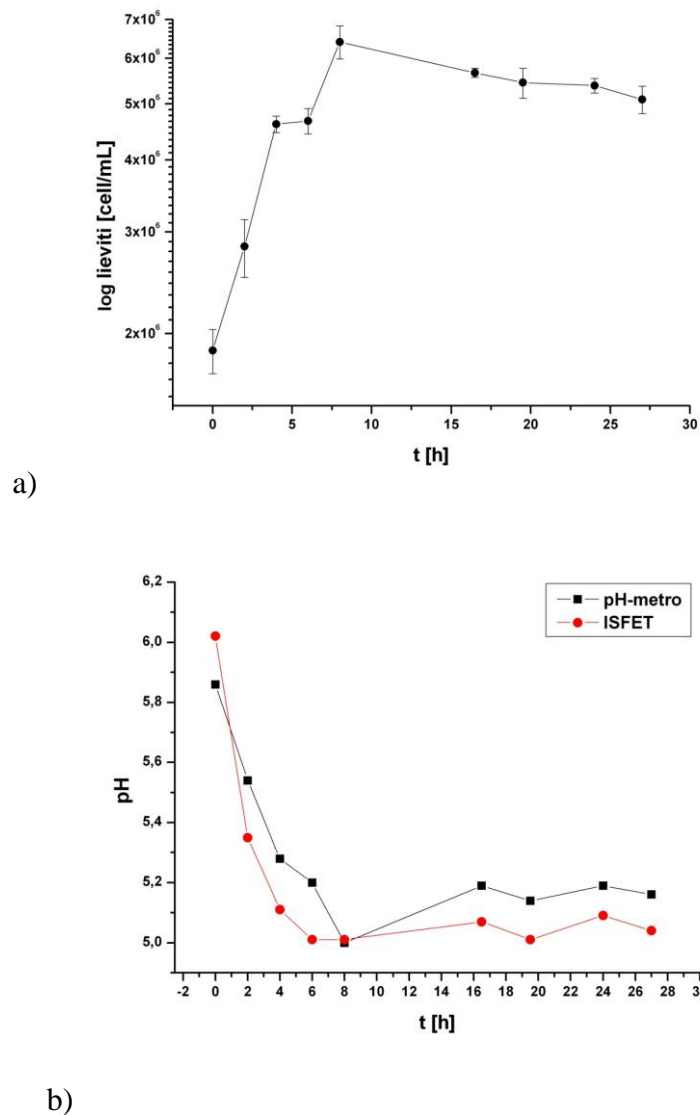


Fig 3.16. (a) Semilogarithmic curve of viable cells over time; (b) pH drop measured by a commercial pH-meter (Crison GLP22) and ISFET.

In figure 3.16 (a) log phase, stationary and death phases can be easily detected. Lag phase is very short because cells were inoculated at exponentially growth phase in medium with the same nutrient composition.

In particular, in the first four hours cells constantly double their biomass and consume sugars and aminoacids provided by the fresh medium. After 4 hours, there is a short stationary phase (about 2 hours) that lends itself to a twofold interpretation: diauxie [Bell, 2009] or sporulation [Kassir and Simchen, 2004].

The former generally occurs when cells preferentially metabolize the sugar on which they can grow faster (typically glucose) and as soon as that sugar is completely exhausted they switch their metabolism to the second. This process is called *diauxic shift* and it is charac-

terized by a lag period in which cells adapt themselves to the new energy sources. Then, after the assembly of the required enzymes, cells start growing again until the total consumption of the second sugar.

The last interpretation, instead, considers full substrate metabolization after four hours and the subsequent growth (6÷8 hours) is attributed to sporulation events that occur in presence of nutrients deficiency or with not fermentable carbohydrates such as ethanol or acetate.

At the same time intervals, the extracellular acidification was measured by both commercial pH meter and integrated Ion-Sensitive FET. The main differences from these two instrumentations were mainly due to the calibration errors of the ISFET. pH quickly decreased from 5.9 to unstable values that ranged from 5.2 to 5. The electrochemical response of the ISFETs were measured using a source and drain follower circuit (fig. 3.17) with a constant drain-source voltage ($V_{DS}=500$ mV) and constant drain current ($I_{DS}=100$ μ A). The isothermal current for the analyzed ISFETs corresponded to a 100 μ A. The operational conditions were chosen at the isothermal point in order to limit the effect of the temperature on the measurement (Appendix A) Up to 5 microdevices were allocated to the bias board (Optoi Microelectronics, Italy) and the instrumentation was connected to the data acquisition board (National Instruments) to capture the signals from up to 5 ISFETs. The whole acquisition process was controlled by a user interface implemented with LAbVIEW (National Instruments).

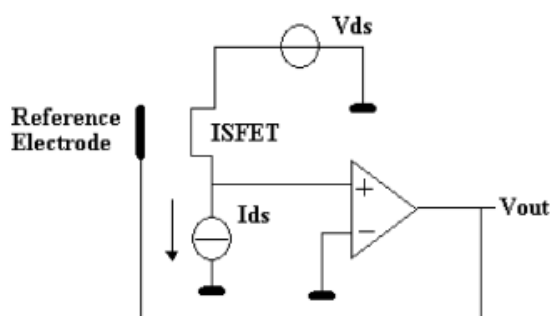


Fig. 3.17. Source and drain follower circuit of an ISFET bias with constant I_{ds}

The trends of growth curve and medium acidification were compared and they both showed a similar behaviour: a sharp variation up to 4÷8 hours, followed by stationary and death phases (fig. 3.18). In particular, taking into account the lag phase between 4÷6 hours (depletion of sugars) and in accordance with the two possible explanation theories mentioned above, the first 5-6 hours were considered the most interesting interval over which focus further measurements.

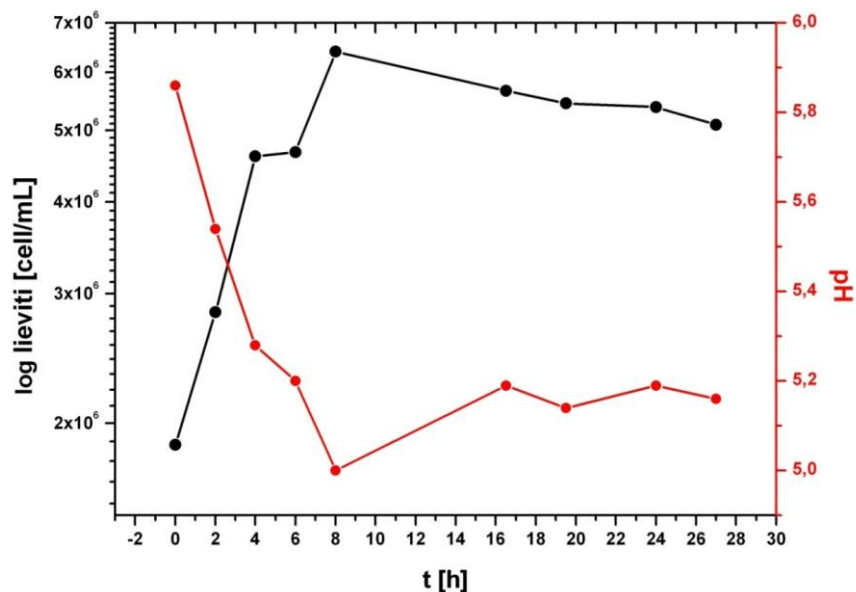


Fig. 3.18. Comparison between extracellular acidification and cell growth over time

To study the influence of sugar uptake in the selected interval, yeasts were inoculated in sterile MilliQ water with 1% and 5% of glucose (w/v) and progressive acidification was monitored with a commercial pH meter (Crison GLP22). As can be seen in fig. 3.19, pH decreases as glucose concentration increases until the complete sugar consumption (within the 5 hours). The considerable measured pH drop (i.e. more than 2 units for 5% of glucose) was attributed to the absence of buffer compounds that are typically present in cellular growth medium.

Indeed, the buffer capacity of the growth medium is not negligible since it influences the rate of pH change [Bousse and Parce, 1994] and the value for YPD broth was experimentally measured to be equal to 3×10^{-3} [mol/l pH].

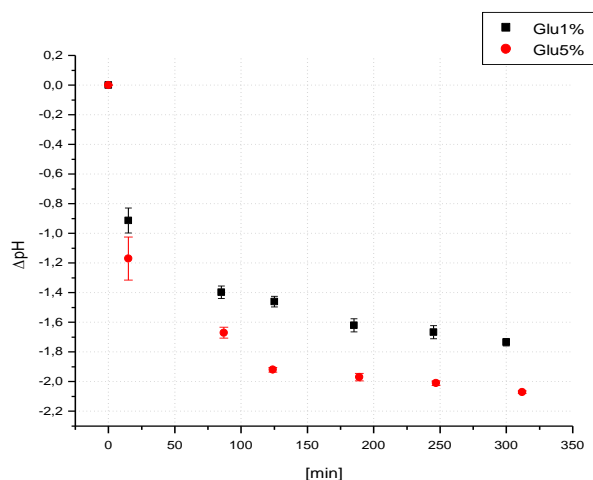


Fig. 3.19. Extracellular acidification in function of different glucose concentrations (1% and 5% w/v)

3.3.2 Extracellular acidification of yeasts at different ethanol concentrations

After a preliminary study of extracellular acidification rate and cell growth, and once individuated a reasonable period for the experimental measurements, ethanol tolerance was monitored in order to detect both changes in yeast proliferation and pH medium in the presence of alcohol.

Therefore, a second series of off-line measurements were performed by adding 12% (v/v) of ethanol, the previously tested (data not shown) critical alcohol concentration for the survival of the analyzed wine yeast.

To perform this assay, the same experimental procedure was carried out by counting cells (fig. 3.20) and monitoring pH (fig. 3.21) every 30 minutes for 6 hours both in presence and in absence of ethanol.

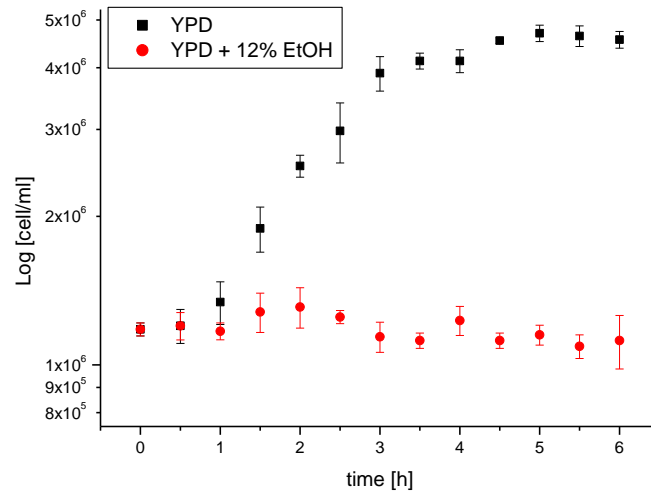


Fig. 3.20. Semilogarithmic cell growth curve in standard conditions (YPD broth) and in presence of ethanol (YPD broth + 12% v/v EtOH)

Initial cell concentration was about $1.2 \cdot 10^6$ cells ml^{-1} and in the first 30 minutes it remained almost constant for both cultures.

Then, after a short common lag phase – estimated of 15 minutes –, yeasts cultivated in standard condition (i.e. in YPD broth without ethanol) went through a logarithmic proliferation while most of cells that grew in 12% of alcohol did not duplicate and tried to adapt themselves and survive to this unfavorable condition. The stationary phase was reached 5-6 hours after inoculation.

The pH curves showed a similar trend from a sharp decrease to a steady value in concomitance with the fast growing culture, while for cells cultivated in presence of ethanol pH initially floated around a constant value and then slowly decreased (fig. 3.21).

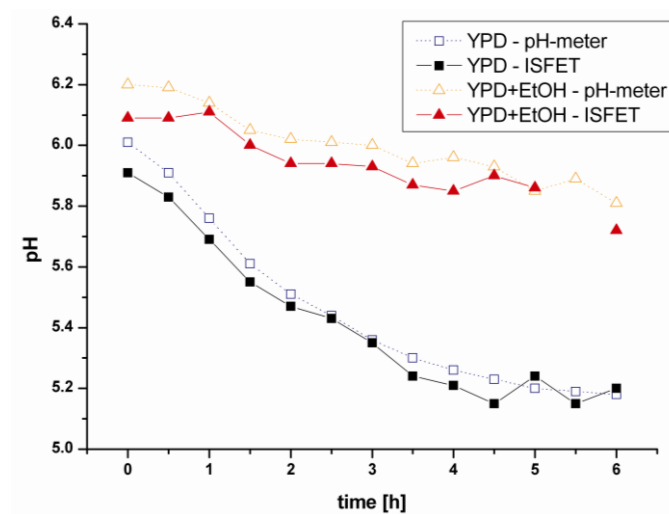


Fig. 3.21. Extracellular acidification in standard conditions (YPD broth) and in presence of ethanol (YPD broth + 12% v/v EtOH) measured with integrated sensor and pH-meter.

In absence of limitation growth factors, cell proton release shows an exponential trend, while in presence of ethanol, proton production has a linear trend (fig. 3.22).

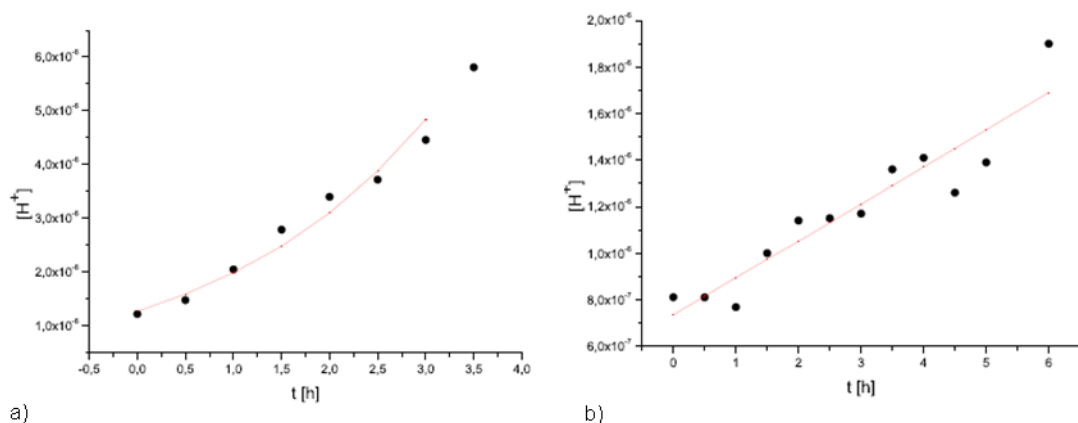


Fig. 3.22. Time course of proton production in absence of growth limitation factors (a) and in presence of 12% v/v ethanol (b).

By comparing the obtained results, the pH variation over time showed a good correlation with the trend of cell proliferation in both presence and absence of ethanol (Fig. 3.23)

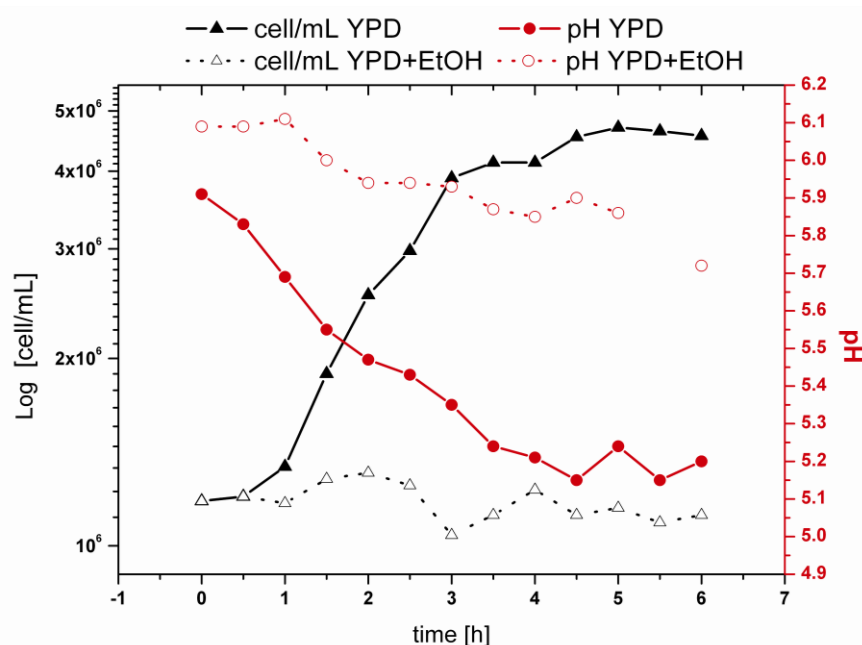


Fig. 3.23. Comparison of pH and cell concentration vs. time at 0% and 12% ethanol concentrations

To deepen the relationship between cell growth and the extracellular acidification, these parameters were investigated on the same wine yeast strain (*S. cerevisiae* 300) at different

ethanol concentrations (0, 10, 12, 16 and 20% v/v). Yeast cell number and pH variations (measured with ISFET sensor) were normalized on the initial cell value in such a way to uniform as much as possible measurements performed in different days and limit the influence of experimental manual errors during the inoculation phases.

As can be seen in figure 3.24, with increasing ethanol content both growth and acidification decrease. At 12% of ethanol yeast stops replication - but it still survives – while at 16 and 20% there is a reduction of viable cells due to the extreme culture conditions.

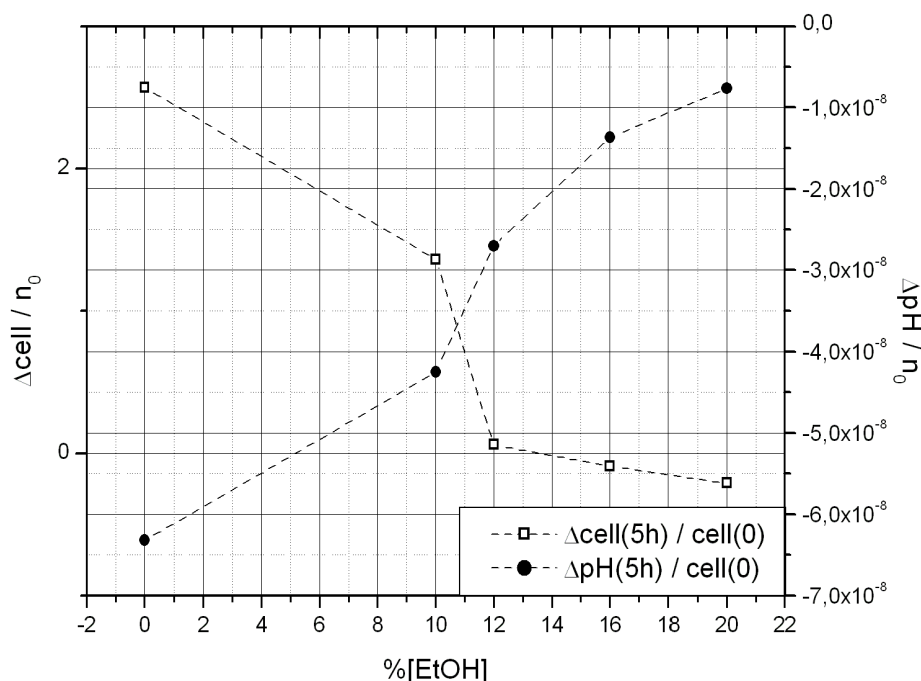


Fig. 3.24. Variation of cell counts and pH both normalized on initial cell number, as a function of ethanol content

Preliminary off-line measurements were required to adjust the experimental parameters (liquid volumes, time window of interest) and study the correlation between cell growth and extracellular acidification in function of different ethanol concentrations.

These measurements demonstrated the suitability of the described method for testing ethanol tolerance in just few hours with respect to the conventional procedures (e.g. cell assays on agar plates) that typically take more than 48 hours (48-72 hours).

3.3.3 On-line pH and impedance measurements

After a preliminary phase of off-line sample collections, a series of on-line measurements were performed by cultivating yeast cells directly on chip surface and by constantly monitoring their metabolic conditions.

To test alcohol tolerance, three different yeast strains (*S. cerevisiae* 303, *S. cerevisiae* 500, *S. cerevisiae* 501, fig. 3.25) with higher ethanol resistance were conventionally characterized and then grown on the electrochemical microdevice.

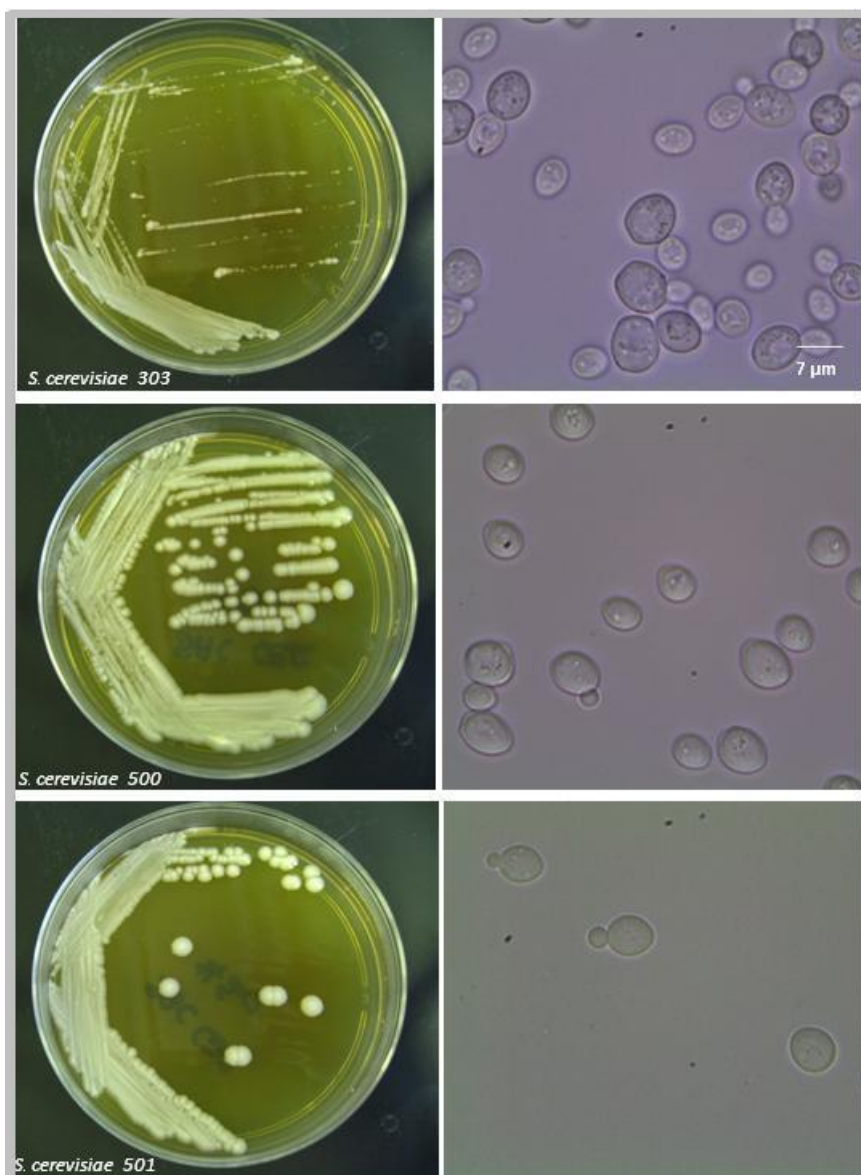


Fig 3.25. (Left) Pictures of *S. cerevisiae* 303, *S. cerevisiae* 500, *S. cerevisiae* 501 grown on YPD agar plates, (Right) cell morphology, (100X Olympus IX 50).

3.3.3.1 Classical assay for testing ethanol tolerance of wine yeast strains

A traditional assay was performed in order to check ethanol tolerance of the different yeast strains.

Three *S. cerevisiae* (303, 500 and 501) wine strains were grown overnight in YPD broth (10^6 CFU/ml), diluted in autoclaved MilliQ water (10^4 CFU/ml) and then plated on sterile 11 YPD Agar Plates (1.0% Yeast extract, 2.0% Bacteriological peptone, 2.0% Glucose, 1.2% Agar, w/v): 1 culture dish was employed as control test and 10 culture dishes were used to attribute ethanol resistance to each yeast strain. These plates contained solid synthetic medium with an increasing concentration of alcohol from 10 to 20% by volume [Vicenzini et al., 2005]. Cells were then cultivated at 28°C and their growth was constantly monitored every 24 hours. After 4 days, cellular resistance to EtOH was verified and the best yeast strain was discriminated among the spots present on each plate (fig. 3.26).

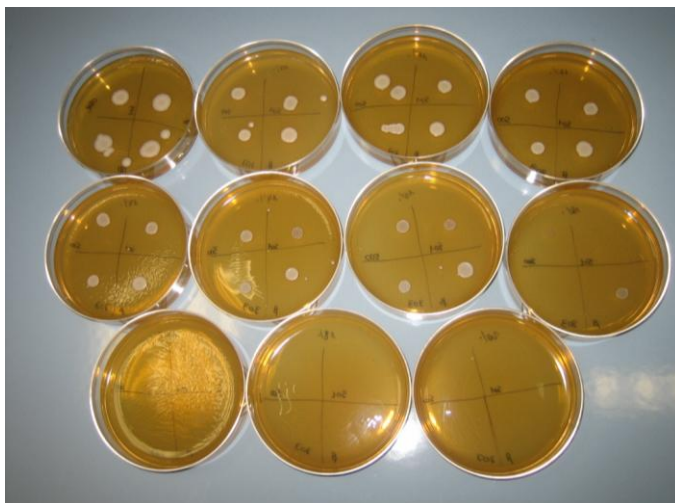


Fig. 3.26. Classical approach for yeast growth monitoring on different ethanol concentrations (0-20% v/v)

As shown in Table 3.27, strains named 303 and 501 had a similar behavior (i.e. they survived up to 14% v/v) while *S. cerevisiae* 500 was the most resistant strains and showed a little grow up to 16% v/v of ethanol.

Table 3.27. Ethanol tolerance of three different strains (*S. cerevisiae* 303, *S. cerevisiae* 500, *S. cerevisiae* 501) at different alcohol concentrations (0-20% v/v). Symbols specify cell growth conditions: (+++) cells grow very well, (++) well, (+) survive and slowly multiply, (+/-) show stunted growth, (-) do not survive.

Ethanol concentration [0-20%v/v]	<i>S. cerevisiae</i> 303	<i>S. cerevisiae</i> 500	<i>S. cerevisiae</i> 501
0	+++	+++	+++
10	+++	+++	+++
11	+++	+++	+++
12	+++	+++	+++
13	++	++	++
14	+	++	+
15	+/-	+	+/-
16	-	+/-	-
17	-	-	-
18	-	-	-
20	-	-	-

Before inoculation, cells were washed thrice by 5-min centrifugation (5,6 rpm at 25°C) with deionized water as reported by the optimized acidification power test [Sigler et al., 2006], with some modifications. Protocols were adapted in terms of reduction of volumes, time of sample centrifugation, time of new growth medium supply.

The washing steps are important because they remove the material adhering to cell surface and causes partial consumption of endogenous sources, increasing the overall AP value [Gabriel et al., 2008].

pH values were measured on 10 ml of cell culture supernatants with a traditional pH meter (Crison GLP22). Experimental measurements were performed on samples at the same cell concentrations ($\sim 10^7$ cells/ml) and results are the average of several trials performed in different days in order to carry out a statistical examination.

As it is shown in figure 3.28, progressive washing steps led to increasing pH values for all yeast strains due to the removal of acids compounds around the membrane surface.

In particular, pH of overnight supernatants were different from each other (with the exception of *S. bayanus* 408 and *S. cerevisiae* 500 that have both a pH of 5), indicating that each strain had its own characteristic metabolic activity. Strain *S. cerevisiae* 303 had the highest pH value while strain *S. cerevisiae* 501 had the most acid waste culture medium.

However, by increasing the number of washing steps these differences among strains decreased and at the third washing step all measures became comparable by reaching a similar value (~ 5.4).

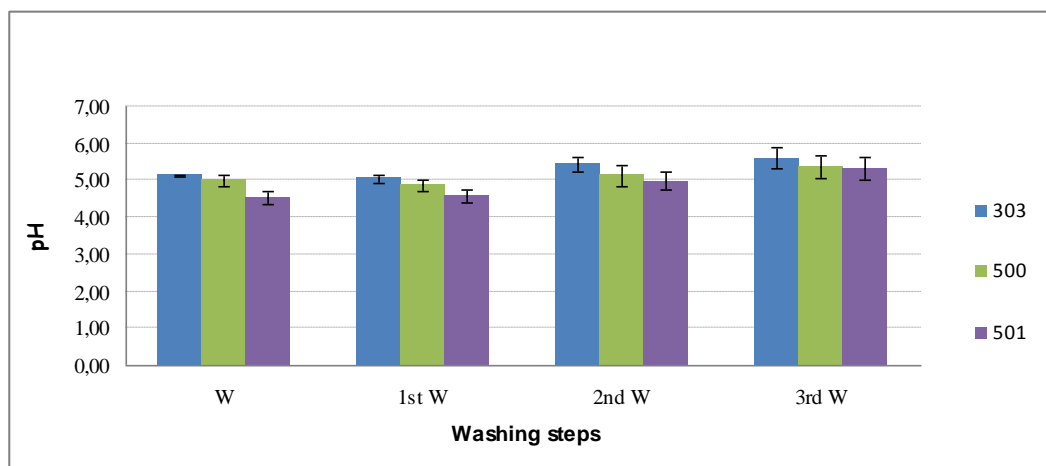


Fig. 3.28. Main pH value and standard deviation of different wine yeast strains in their waste culture medium (W: waste, i.e. before washing steps) and after the first, second and third washing steps.

3.3.3.2 Extracellular acidification of different wine strains

After having characterized yeast strains on agar plates, their alcohol tolerance was assessed by directly cultivating cells on the microsensor. Cell cultures were prepared in accordance with the previously described method and microbial growth was carried out in batch conditions, without further nutrient's additions.

Strain *S. cerevisiae* 500 – able to grow up to 16% of ethanol (Table 3.27) – was cultivated in parallel in four microdevices, each one at different alcohol concentrations (0-12-16-20% v/v). In the fifth position of the bias board was allocated the negative control, i.e. the growth medium without cells. The measurements showed that as ethanol raised up, the pH acidification was progressively reduced. At 16% of ethanol, there was a slight decrease caused by the maintenance of cell survival, according with the data obtained with the traditional agar plates. In presence of 20% of ethanol cells died and no metabolic activity was detected since there was a total overlapping with the curve of the negative control (fig. 3.29). Observing the plot in figure 3.29, it can be noticed that the negative control is not stable and its Δ pH steadily decreases. This behavior was detected also by a resistivity decrease in the impedance measurements (fig. 3.33) and it was assumed that medium proteins could influence both pH and conductivity by progressively settling to the bottom surface of the sensors.

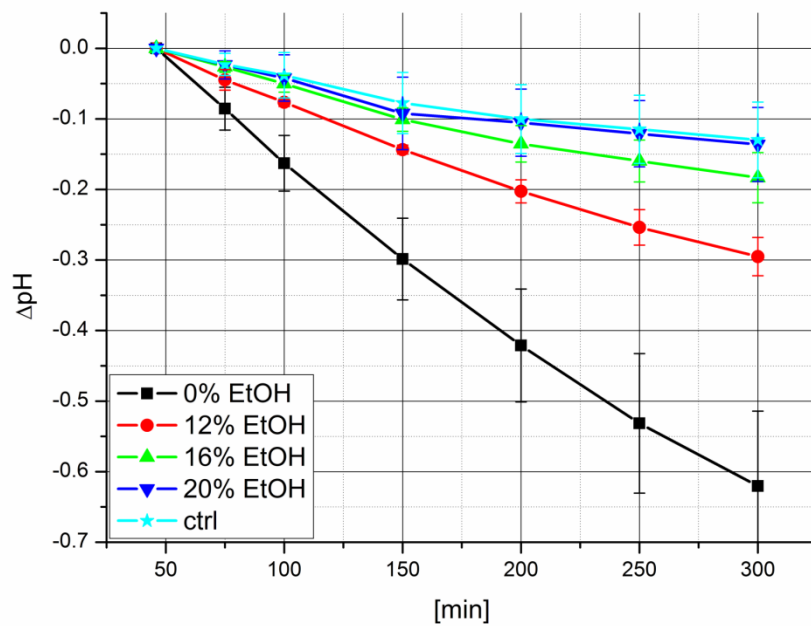


Fig. 3.29. On-line pH measurements of *S. cerevisiae* 500 at different ethanol concentrations (0, 12, 16, 20 % v/v)

Then, a comparison between *S. cerevisiae* 303 and 501 was performed by monitoring the extracellular acidification in standard conditions, with the addition of 5% of glucose and with both 5% of glucose and 14% of ethanol. Ethanol concentration was chosen based on the results obtained by the agar plates and the extracellular acidification at 5 hours was plotted after subtraction of the negative controls (fig. 3.30)

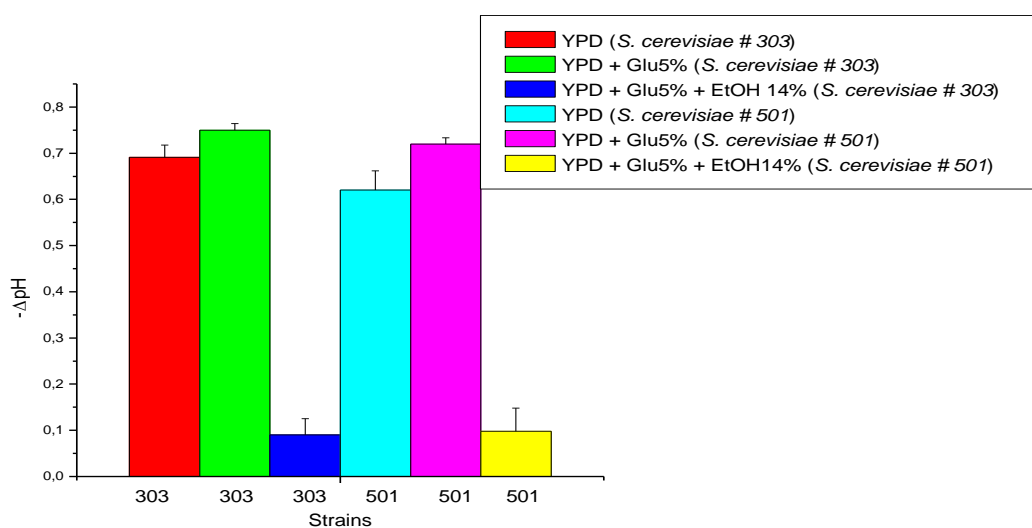


Fig. 3.30. Comparison between *S. cerevisiae* 303 and 501 in standard conditions (YPD), with 5% of glucose (YPD + Glu5%) and with both 5% of glucose and 14% of ethanol (YPD + Glu5% + EtOH14%)

Five hours later cell inoculum, the analyzed strains showed different acidification rates for the standard culture conditions. These differences were strain-specific and reflected the metabolic rates of the two wine yeasts. As expected, in presence of glucose the extracellular acidification of both strains increased due to the sugar's uptake mechanism. When the critical concentration of alcohol was added to cells, both ethanol-stressed yeast cultures showed a similar behaviour with a little pH decrease for maintenance of cell survival, confirming the data obtained with the agar plates.

3.3.3.3 On-line impedance measurements

Impedance sensors were previously studied for online monitoring of yeast growth [Ress et al., 2009]. In particular, cells were plated on solid agar medium in the correspondence to the sensitive area of the microchip. A decrease in conductivity was detected in concomitance with yeast cell growth as a change in chemical composition of the medium brought about by metabolic processes of wine yeast cells. Thus, the microchip was considered to be sensitive to cell proliferation not by monitoring biomass directly, but rather by measuring the alteration in medium composition, and therefore, through an indirect impedimetric assay.

In this work, the impedance sensor was employed for cell settling measurements. As cells were inoculated into the electrochemical platform, they settled down onto the sensor's surface obstructing the current flow.

At first, polystyrene micro particles (Fluka, Sigma Aldrich) of different sizes (5-7-10 μ m) - comparable to those of budding yeasts (~7 μ m, see chapter 2, section 2.1.1) - were used to simulate yeast cells behaviours. Cells (*S. cerevisiae* 303) and microbeads were separately resuspended into YPD growth medium at the same concentration (24x10⁶ beads or cells/ml) and as shown in figure 3.31, two different phases were identified for both cells and microbeads: a settling phase (in which particles settle by gravity to the bottom of the well) and a stationary phase (in which all particles are completely settled on the surface of the impedance sensor). These two phases were influenced by the particles sizes, and as expected, the greater is the volume, the higher are both the rates at which they settle and the measured resistivity.

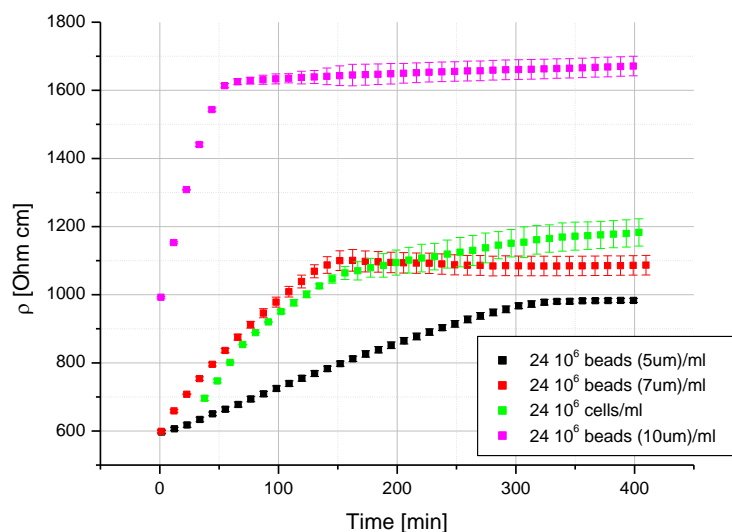


Fig. 3.31. Time course of resistivity of micro particles (5-7-10 μ m) and cells (*S. cerevisiae* 303) at the same concentration (24×10^6 particles/ml).

Cells showed a similar behavior of 7 μ m-beads, in correspondence with the average value of the analyzed yeast strain size. Although they had a parallel settling phase, they diverged in the stabilization phase. These differences could be explained by mainly considering two hypotheses. The former attributes the increasing resistivity of the sample containing yeasts to cell replications (cell-doubling time is estimated to be around 120 minutes, see chapter 2, and section 2.1.1). The latter considers the heterogeneity of cell sizes, and therefore, the different times of their sedimentation. It cannot be excluded that both options can cause together a constant increase of resistivity and other deeper studies will be carried out in order to confirm these preliminary assumptions.

To analyze the repeatability of the measurements during the settling phase, microparticles were inoculated in growth medium and after reaching their stabilization time (specific for each particle size), they were vigorously mixed in order to obtain a homogeneous suspension and repeat again the detection of settling phase. In figure 3.32 is reported an example of mixing with 5 μ m-beads: after 300 minutes, beads were resuspended and the same rate of sedimentation was observed, demonstrating the reproducibility of these dynamic measurements.

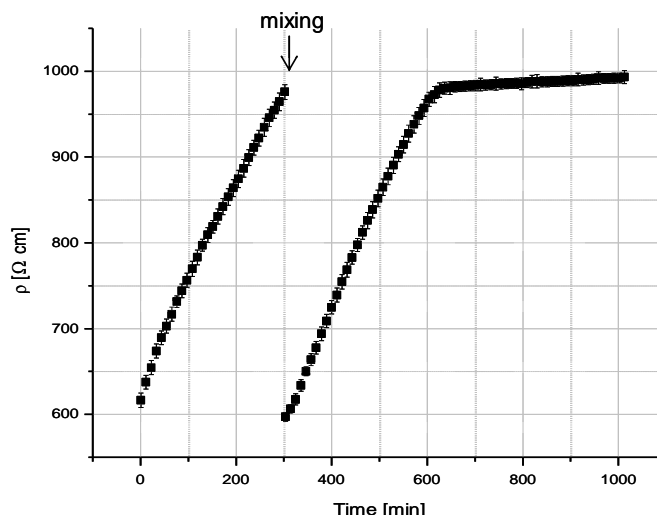


Fig. 3.32. Example of mixing of 5µm-beads (arrow) after 5 hours. i.e. the time required for particles sedimentation. 5 hours later, microbeads reached the stabilization phase with the same rate.

The next impedance measurement was focused on the resistivity changes in function of different yeast cell concentrations ($0 \div 24 \times 10^6$ cell/ml). Resistivity increases with cell concentration (fig. 3.33) and this means that in principle it is possible to obtain useful information about the overall biomass that is inoculated into the microdevice and follow online the dynamic events.

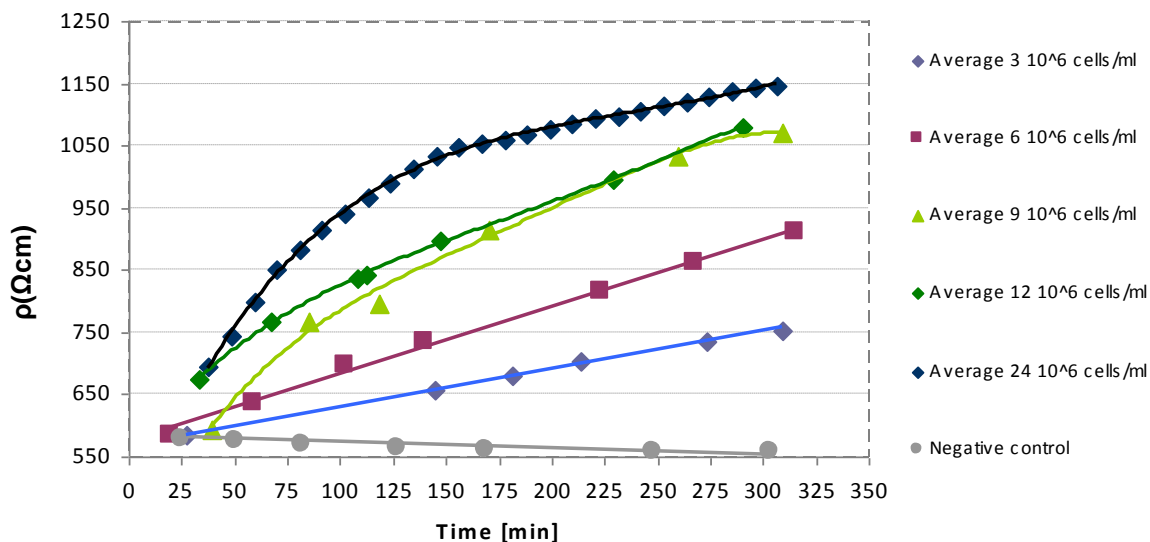


Fig 3.33. Resistivity over time as a function of yeast cell concentrations ($0 \div 24 \times 10^6$ cell/ml).

As reported for ISFET measurements, the negative control was not stable over time and a constant slow decrease of resistivity was detected. It was assumed that this progressive de-

crease was due to the settling of proteins and medium components above the sensors surface.

3.4 Discussions

In this work, a cell-based multisensor device for wine yeast analysis is presented. The investigation and the feasibility study of this microsystem were especially focused on ISFET and Pt impedimetric sensors, for extracellular pH and cell settling detection.

Wine yeast (*S. cerevisiae* 300) was batch cultivated in small YPD volume without any further supply of fresh nutrients. At first, a preliminary trend correlation between growth and metabolism was examined in order to individuate the time interval over which address the experimental measurements.

Medium acidification was periodically measured both with a commercial pH-meter and ISFET sensor and its trend was compared with the obtained cell growth curve. The most interesting interval was identified within the first 5÷6 hours that followed yeast inoculum.

Then, cell growth and pH variation were investigated also in presence of different ethanol concentrations, demonstrating the validity of the approach for assessing alcohol tolerance of wine yeast strains. Afterwards, online measurements were carried out by on-chip cultivation of three *S. cerevisiae* wine strains (303, 500, 501) and by the evaluation of their resistance to ethanol both with ISFET sensor and standard agar plates.

The obtained results showed that ISFET measurements were in good agreement with conventional methods and at the same time provided a strong reduction of time, from 48-72 hours (with agar plates) to just 5 hours.

On the other hand, impedance sensors provided interesting information related to biomass concentration at the inoculum level and to other important parameters such as particles sizes and settling time. However, the microsystem needs some improvements such as the integration of a reference electrode. The presence of an external bulky electrode interfere with the impedance measurements, therefore pH and resistivity were measured separately. Moreover, a controlled temperature will be required during the experimental session in order to increment the reproducibility of the measurements. Thermal changes within the microsystem will be constantly monitored by using the integrated temperature sensor as internal reference.

Nevertheless, the encouraging preliminary results have shown the system suitability for wine yeast analysis. Interestingly, impedance sensor has demonstrated great versatility and

could be employed also for the investigation of flocculation phenomena [Stratford, 1989], extremely interesting for wineries, breweries and more in general for industrial applications [Zhao and Bai, 2009].

Chapter 4

4 A PCR microdevice for yeast DNA amplification

This chapter describes the development and validation of a hybrid Silicon/PDMS PCR microdevice. The device was developed at Fondazione Bruno Kessler (FBK – Trento, Italy) while the biological validation was performed in collaboration with the Microbial Genomics Lab (CIBIO - University of Trento). The analyzed yeasts were kindly supplied by Bio-Analisi Trentina s.r.l. (Rovereto, Italy).

4.1 Materials & Methods

4.1.1 Microdevice design

The amplification device consisted of a chamber-type-stationary chip in which the PCR mix was confined and subjected to the thermal cycling.

A key step in microdevice design was the selection of the building materials. The evaluation of proper substrates considers the main requirements of micro PCR devices such as good thermal conductivity for the temperature zones and good biocompatibility for channels and chambers walls. After an accurate literature research, the microdevice was realized with a hybrid structure, i.e. composed of two different parts and materials: a silicon microchip with embedded heater and thermometers and a polydimethylsiloxane (PDMS) microchamber for containment of the biological mixture (fig. 4.1).

Silicon can guarantee a constant heating region and can be easily patterned with the metal layer. The heating element is made of Platinum, due to its ideal temperature versus resistance relationship, good chemical stability and its easy micromachining. On the other hand, PDMS shows a significant versatility as structural material and can be used as disposable element. Moreover, this soft elastomer can be obtained by inexpensive fabrication techniques and it has a good biocompatibility. It is transparent and presents low autofluorescence under laser irradiation, making this material suitable for the coupling with optical detection.

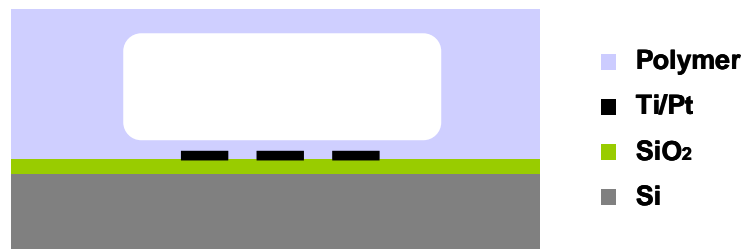


Fig. 4.1. Cross section of the designed microdevice

The microchamber was built with a polygonal shape, as this shape in contrast considered to a circular or a rectangular one, was described to be superior in preventing bubble formation [Cho et al., 2006; Niu et al., 2006]. In particular, this shape facilitates the liquid movement and avoids residuals at the edges.

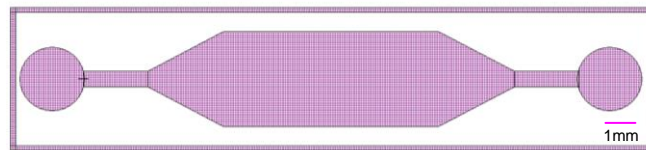


Fig. 4.2. A first design of PCR chamber for stand-alone testing purpose made using commercial CAD software (L-Edit Tanner EDA Tools)

The layout reported in figure 4.2 includes the reaction chamber, two channels and two inlet/outlet ports. The chamber is 7mm long, 3mm wide and 210 μ m deep with a volume capacity of 4.4 μ l.

The total volume of the microchamber, including the inlet and outlet channels is 10 μ l.

This volume is small enough to guarantee rapid thermal cycling and at the same time is sufficient to avoid evaporation of the reaction mix.

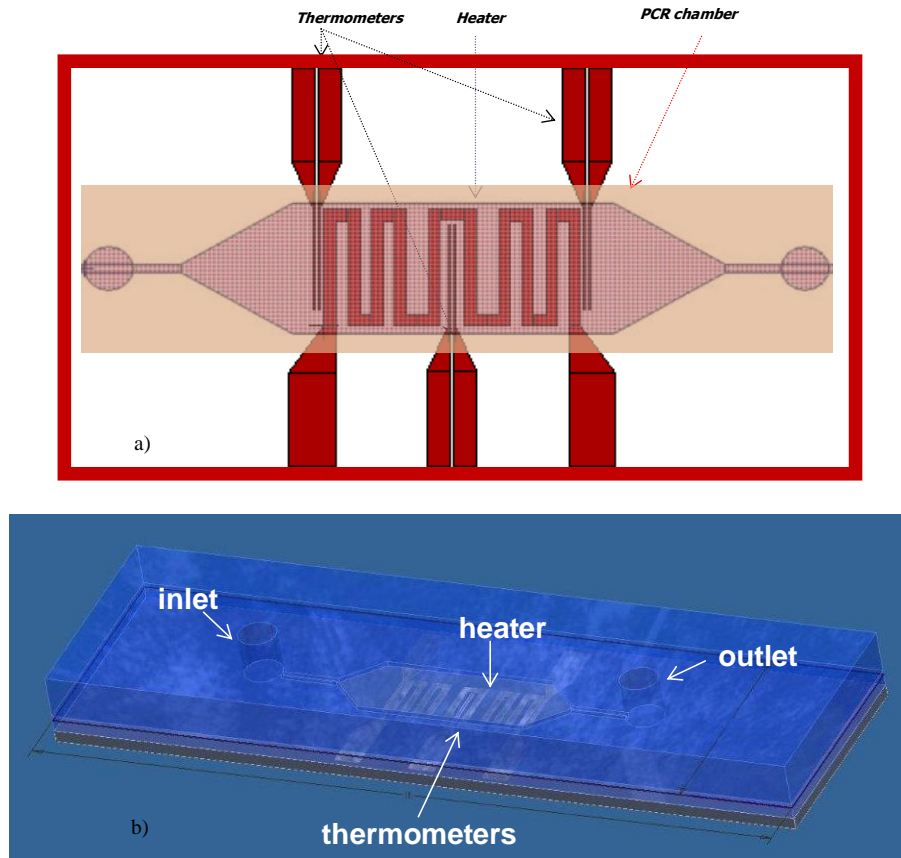


Fig. 4.3. a) Layout and b) 3D schematic sketch of the hybrid PDMS/Silicon PCR microdevice

The platinum heater has a serpentine shape that is larger in the middle in order to make a uniform heat generation. Three thermometers are distributed along the chamber for the measurement of the temperature (fig. 4.3).

4.1.2 Microfabrication process

The fabrication process was divided in two steps: the microchamber was realized using soft-lithography techniques, while heater and thermometers were micromachined through conventional MEMS technologies.

Soft lithography

The master of the microchamber was obtained by spinning and patterning 210 μ m-layer of SU-8 3050 (MicroChem) on a silicon substrate (figures 4.4 and 4.5, right).

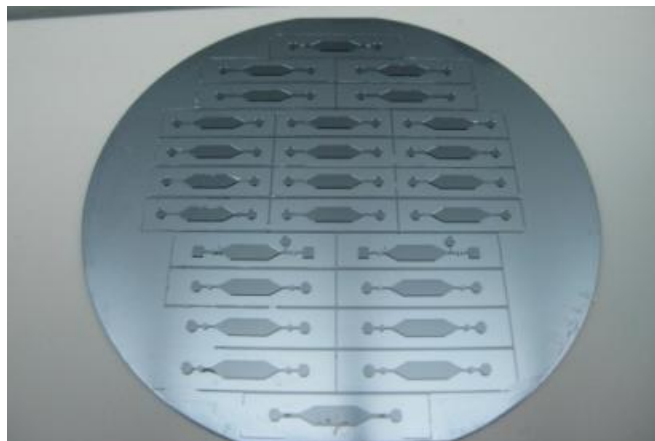


Fig. 4.4. SU-8 master for the microchambers

PDMS, in ratio of 5:1 (5g of pre-polymer and 1g of curing agent), was then poured onto the master, let polymerize for 20 minutes at 80°C and peeled away (Figure 4.5, right). Holes for reagent loading and fluidic connections were punched to obtain inlet and outlet ports with a diameter of 1mm.

In the meantime, a thin membrane (400µm) of PDMS (20:1) was obtained and pre-polymerized 10 minutes at 80°C. The two layers were placed one on top of the other and permanently glued after the complete polymerization of the PDMS.

Silicon-based components

The microchip fabrication started with a 4-inch silicon wafer covered with a dielectric multilayer for a good insulation (300nm of Growth Silicon Dioxide, 100nm of LPCVD, 300nm of TEOS). Negative photoresist (AZ4562, MicroChemicals) was then spun on the wafer and patterned using photolithography technique in order to define the heater and thermometers for the next lift-off step (figure 4.5, left). The wafer was inserted in e-gun evaporator (ULVAC EBX-16C) to obtain a Titanium/Platinum (15/100nm) layer on the surface. The unexposed photoresist was removed using acetone in ultrasonic bath and the Ti/Pt was sintered at 500°C for 1 hour. Finally, 400nm of PECVD SiO₂ was deposited on the wafer in order to passivate the heater and thermometers. The heater resistance is 175Ω, while the thermometers have a resistance of 680Ω at room temperature (table 4.6). The measured TCR for the thermometer is 2320 ppm/°C. The dimensions of the whole PCR device are 9 mm x 4 mm x 3mm. The described device was bonded on a PCB designed for a Plastic Leaded Chip Carrier (PLCC).

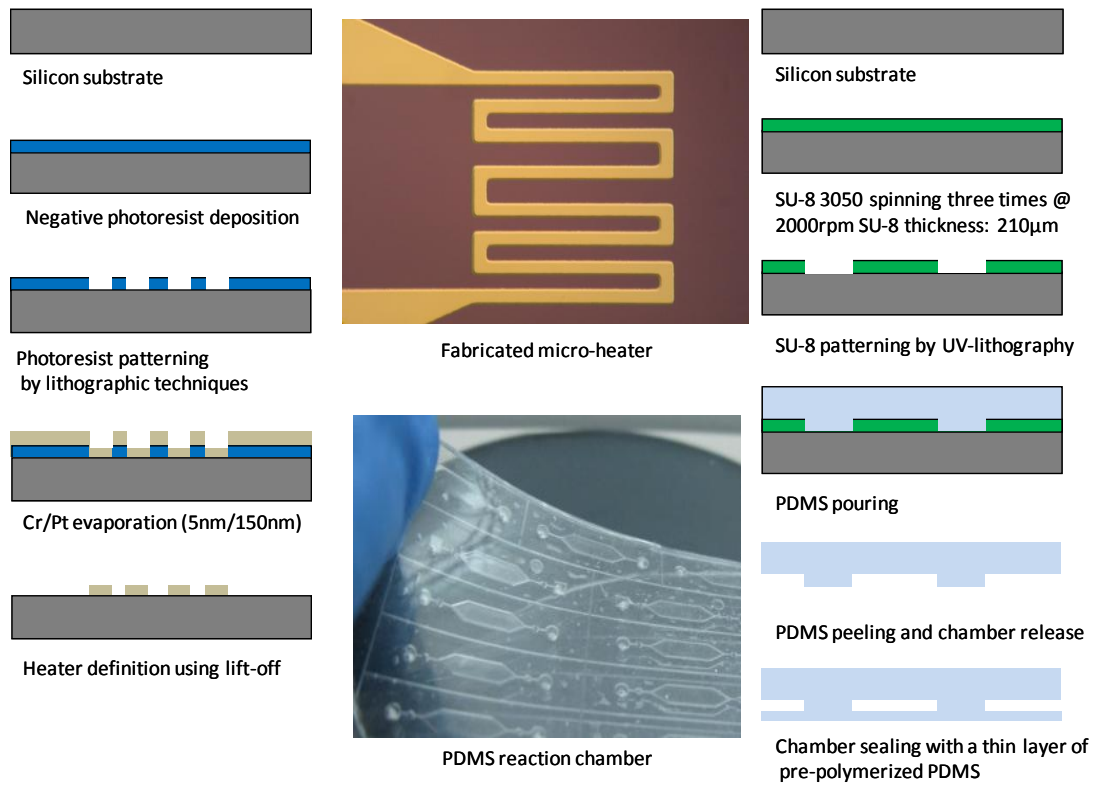


Fig. 4.5. Microdevice fabrication process : (Left) Fabrication of the silicon layer with heater and thermometers; (Middle) Picture of the fabricated heater serpentine (top) and PDMS microchambers (bottom); (Right) fabrication of the PDMS chambers.

Table 4.6 Main values of heater and thermometers

Parameter	Value
Heater Resistance	175 Ω
Power	2.9 W
Applied Voltage	22 V
Thermometer Resistance	680 Ω

4.1.3 Electronic board

A mechanical clamping system was employed to guarantee perfect contact between the microchip and the microchamber and seal inlet and outlet channels, thus avoiding potential evaporation or air bubbles formation within the reaction mix (fig. 4.7).

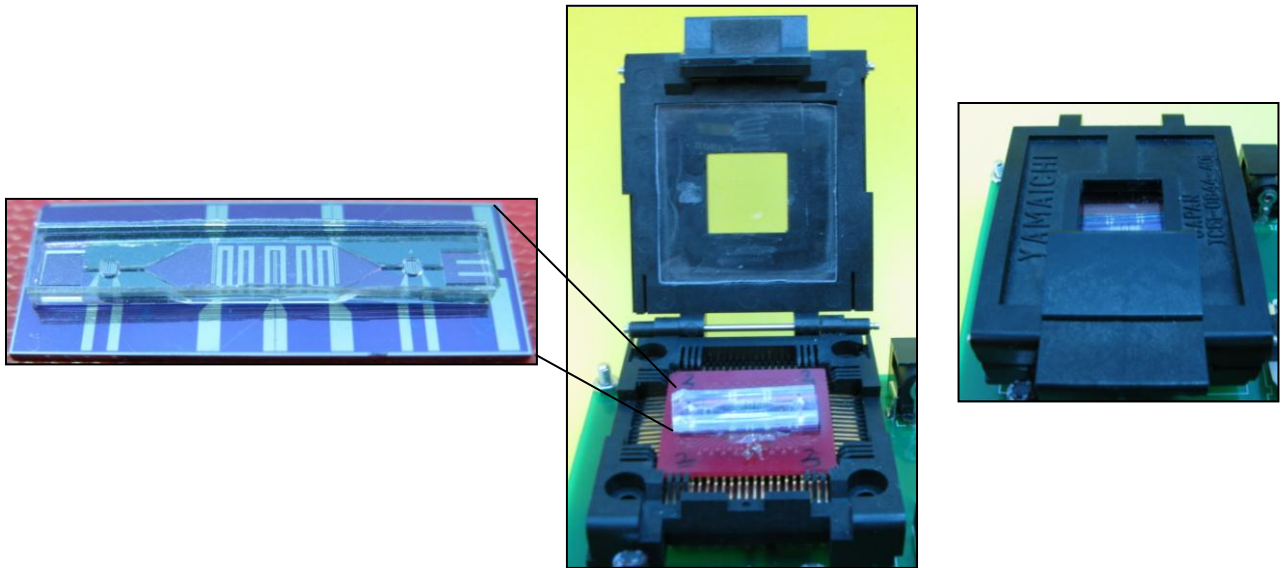


Fig. 4.7 Picture of the assembled PCR device inserted in the Plastic Leaded Chip Carrier (PLCC)

An electronic board was designed and realized to control the embedded heater. The thermal control is based on proportional-integral-derivative (PID) controller coupled to a Pulse Width Modulator (PWM) to regulate the input power. The PID received the actual temperature value from the internal thermometer in a feedback configuration, as represented in figure 4.8.

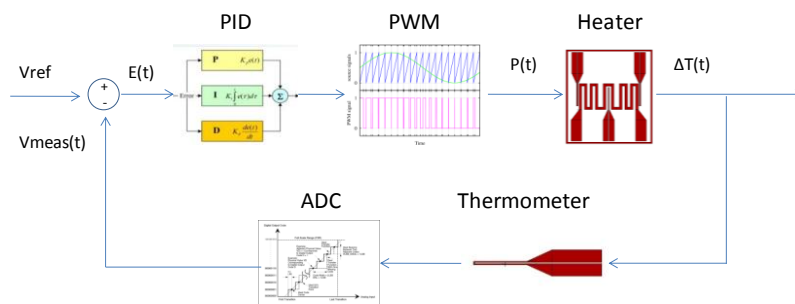


Fig. 4.8 Block diagram of the temperature control loop

A microcontroller (ATMEL atmega16) was used to implement the PID, the PWM and the Analog to Digital Converter (ADC) for data visualization and storing. The electronic board was connected to a computer via a serial-USB interface (FTDI MM232), (fig. 4.9).

Home-built software was used to provide to the microcontroller all the parameters for the PCR settings (i.e. number of cycles, temperature, duration, initial denaturation and final

extension) and visualize in real time the temperature read by the thermometers and the course of the thermal cycles. This set-up was able to control the temperature with a precision of 0.5 °C.

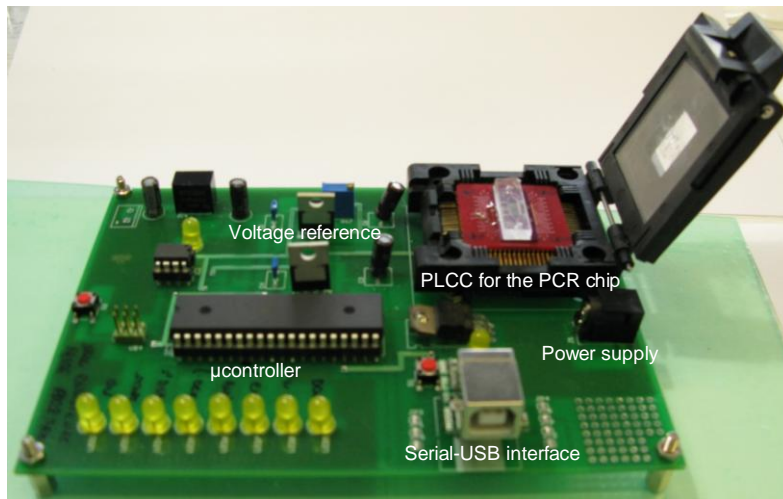


Fig. 4.9 Photograph of the electronic board

4.2 Experimental results

4.2.1 Yeast genomic DNA extraction and purification

Yeasts were inoculated into 5 ml sterile YPD Broth (Yeast Extract, Peptone, Dextrose; Sigma Aldrich) and grown at 30°C, 200 rpm for 18-24 h. Then, cells were harvested by centrifugation (5 min at 1400 x g) and resuspended in 0.5ml 1M sorbital solution. The suspension was transferred to a 1.5 ml microcentrifuge tube with 25 µl lyticase solution (5 mg/ml) (4000 U/mg Sigma) and incubated at 37°C for 30 min. Then, the tube was microcentrifuged for 1 min and the supernatant was discarded.

Cells were well resuspended in 0.5 ml TE buffer (10 mM Tris-HCl, 1 mM EDTA, pH 7.4) and 25 µl of 20% sodium dodecyl sulfate (SDS) were added to the solution.

The samples were mixed by inverting the tube 10 times and where incubated at 65 °C for 20 min. After this thermal incubation, 0.4 ml 5M potassium acetate were added to the solution, and the samples were mixed thoroughly by inverting the tube 10 times and setting on ice for 30 min.

Samples were centrifuged at 5000 rpm for 5 min, then 0.75 ml of the supernatant was transferred to a new microcentrifuge tube and 0.75 ml of isopropanol were added at room temperature. The solution was mixed and incubated for maximum 5 min at room temperature. After removal of the supernatant, the pellet was partially air-dried for 20-30 min.

To obtain purified genomic DNA (gDNA), the pelleted DNA was resuspended in 300 μ l of Tris-EDTA buffer and 30 μ l 3M sodium acetate with 200 μ l isopropanol were added to the solution. The microtube was inverted 5 times to mix the obtained solution and microcentrifuged for 5 min at room temperature. Finally, the supernatant was discarded and the purified pelleted DNA was air-dried for 30-60 min and resuspended in 50 μ l TE buffer.

The gDNA quantity and purity was measured with the Nanodrop ND-1000 Spectrophotometer (NanoDrop Technologies, Inc) by exposure of the samples at 260nm (the absorption wavelength of nucleic acids), as shown in figure 4.10.

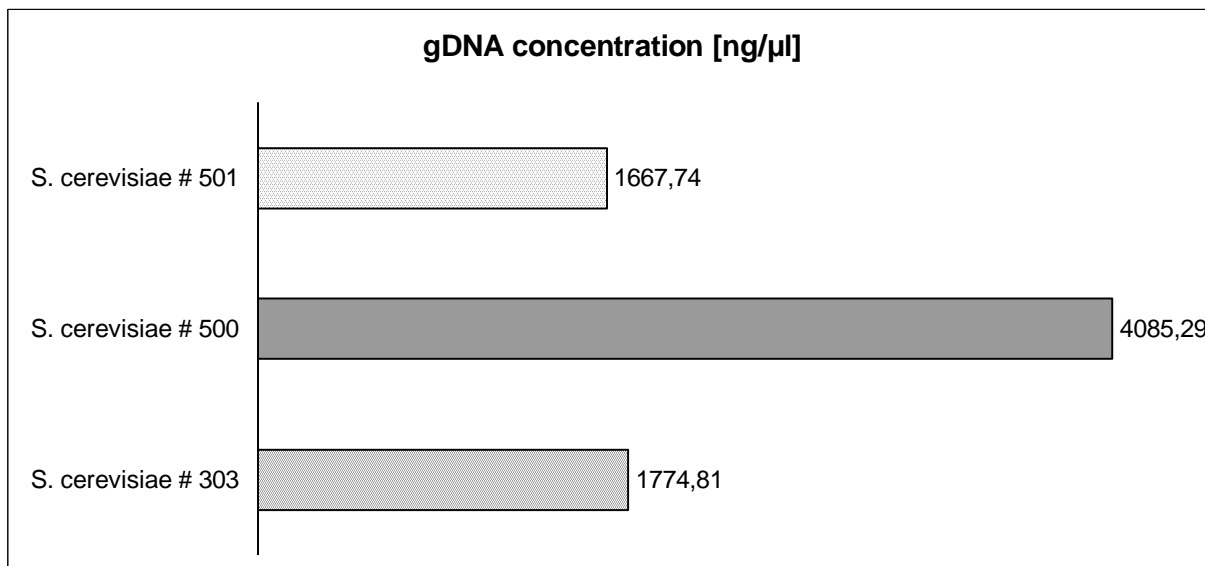


Fig. 4.10 Genomic DNA concentrations [ng/ μ l] of different yeast strains (*S. cerevisiae* 501, 500, 303) as calculated with the Nanodrop ND-100

The degree of purity was also assessed by examining samples at wavelenghts in which proteins ($A_{280\text{nm}}$) and polysaccharides ($A_{230\text{nm}}$) are known to have their maximum absorptions. It is generally accepted that for “pure” DNA, $A_{260/280}$ is ~ 1.8 and $A_{260/230}$ is ~ 2.2 . If the ratio’s values are lower, aminoacids, phenols, sulphidryls or other contaminants could be present in the sample and further purification may be required.

In the examined yeast strains, gDNA showed a good quality with $A_{260/280}$ higher than 1.8 and $A_{260/230}$ close to 2.2 (fig. 4.11).

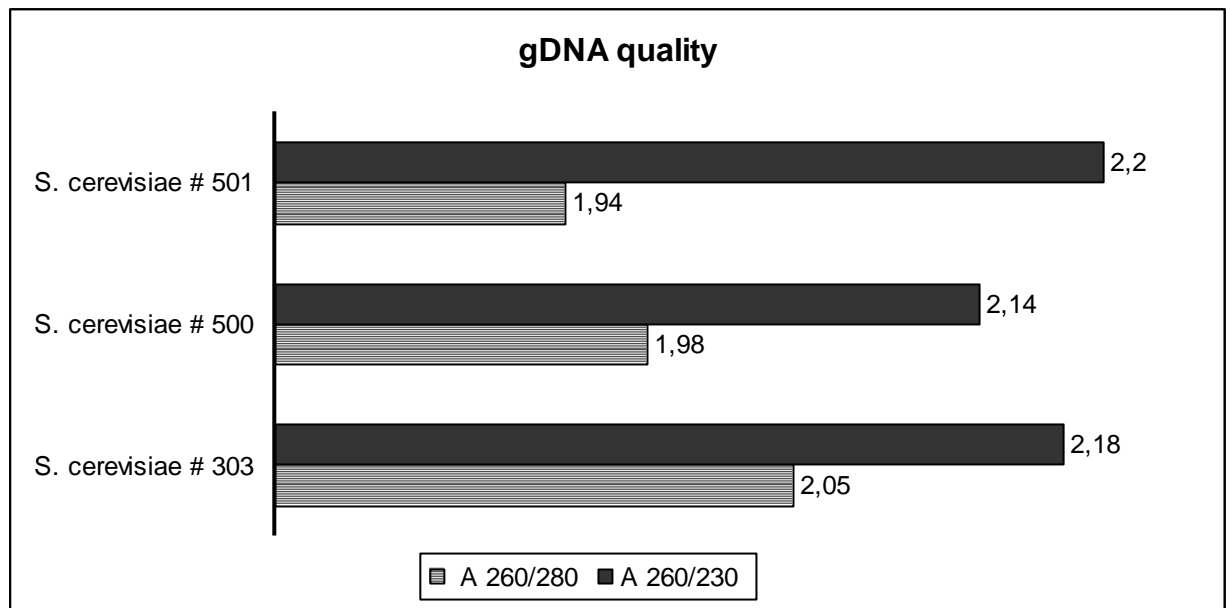
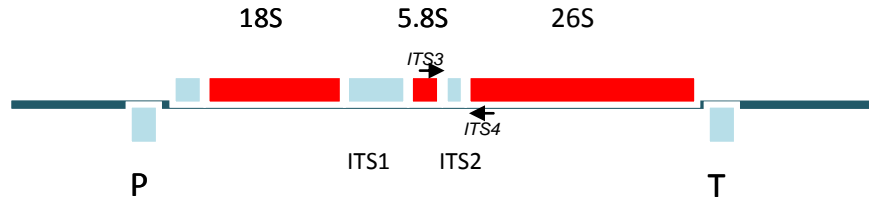


Fig. 4.11 Genomic DNA purity of different yeast strains (*S. cerevisiae* 501, 500, 303)

4.2.2 Target gene selection

The chosen primers amplify a non-coding region called “internal transcribed spacer” (ITS), localized inside the ribosomal DNA (rDNA) repeat unit. In *S. cerevisiae*, rDNA genes are grouped in repeat units and form a single cluster on chromosome XII. The rDNA encoding for 18S, 5.8S and 26S ribosomal subunits are known to display high identity among the species of the *Saccharomyces sensu stricto* group, while ITS regions have a high sequence variability within the group and can be commonly used for detection and differentiation between yeast species [Guillamon et al., 1998]. As shown in figure 4.12, the 18S, 5.8S and 26S rDNA genes are separated from each other by two internal transcribed spacers ITS1 and ITS2. In particular, the chosen primers - ITS3 and ITS4 - amplify a 420 bp DNA fragment located in the ITS2 region.



a)

ITS3_fw	5'-GCATCGATGAAGAACGCAGC-3'
ITS4_rv	5'-TCCTCCGCTTATTGATATGC-3'

b)

Fig. 4.12 a) Sketch of the yeast rDNA repeat unit and its organization; b) Primer pair sequences (White at al., 1990).

4.2.3 PCR master mix set-up

At first, 10µl PCR master mix (Table 4.13) was prepared and tested with the commercial DNA Engine (PTC-200) Peltier Thermal Cycler (Bio-Rad, Life Sciences) in order to set the proper experimental conditions (buffer concentration, Taq polymerase concentration, primer pairs, etc.).

Table 4.13. 10µl-PCR master mix used for the commercial Peltier Thermal Cycler (PTC-200, Bio-Rad) and for the validation of microchip

Component	Volume (µl)
PCR grade water GIBCO	4
5X PCR Buffer solution with 1.5 mM MgCl ₂	2
Primer forward (ITS3) 10µM	1
Primer reverse (ITS4) 10µM	1
dNTPs 10mM	0.5
Template DNA	1
Robust Hot Start Taq Polymerase	0.5

Scaling down to the micro size, the surface-to-volume ratio increases and often causes undesirable adsorption of the biomolecules (especially of the enzyme) on the inner surface of the chamber/channel walls. Moreover, it is worth noting that amplification efficiency is also deeply influenced by magnesium salts, which are very likely to interact with the nega-

tive charged surface of the device by subtracting important cofactors to the enzyme. Therefore, a highly robust and versatile enzyme was chosen in order to avoid an eventual reduction of amplification efficiency. The selected Taq polymerase is called Robust HotStart (KAPA2G™, KAPA Biosystems), as it gets activated only after a 95°C initial step and it has a high performance even in the presence of PCR inhibitors.

In particular, the chosen DNA polymerase could work with three different buffer solutions (A, B and GC), depending on the presence of sample contaminations, template conditions or nucleotides contents. All buffers contain MgCl₂ (1.5mM MgCl₂ at 1X final concentration). Buffer A is recommended for amplicons with GC content higher than 65%, buffer B for samples containing anionic inhibitors or crude samples (e.g. colony PCR), and buffer GC for GC-rich amplicons or for difficult templates with stable secondary structure.

We defined the appropriate working conditions by running in parallel singleplex PCR of all three *S. cerevisiae* wine yeast strains with the three buffer solutions. The selection of hold times was carried out on the basis of the specific extension rate of DNA polymerase (30sec/kb) and on the sequence length of the amplicons (~420bp). The thermal cycling parameters for the Peltier thermal cycler (PTC-200, Bio-Rad) were an initial denaturation at 95°C for 3 min, followed by 30 cycles of denaturation at 95°C for 10 sec, annealing at 58°C for 10 sec, and extension at 72°C for 10 sec, with a final extension at 72°C for 3 min. The PCR outcome was assessed by EtBr-stained agarose gel electrophoresis, loading 2 µl of PCR products and running at 80V (52mA, 4W) for 40 minutes. The amplification reaction was successfully only in the presence of buffer B, as shown in figure 4.14.

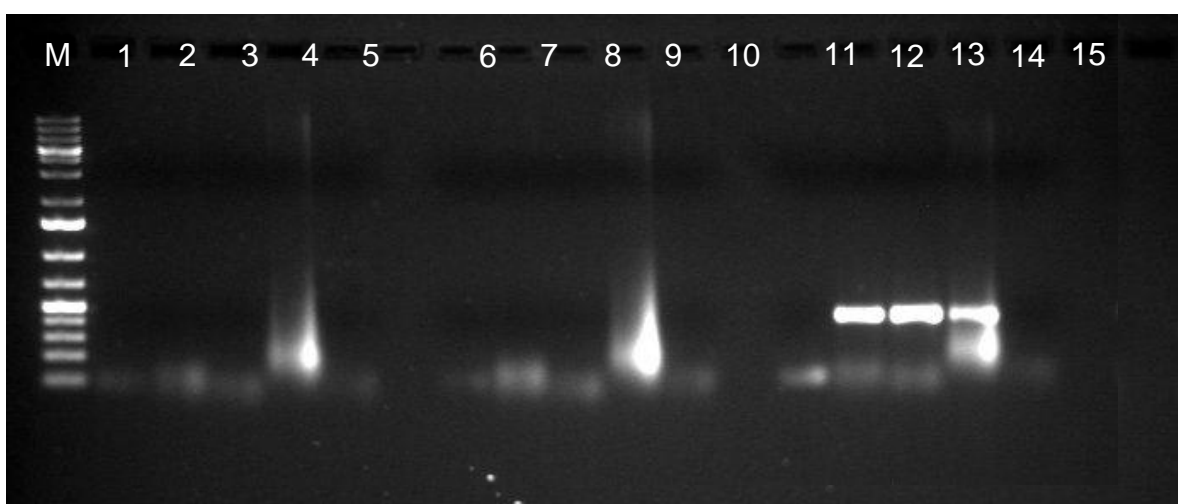


Fig. 4.14 Electrophoretic patterns obtained with 1.2% TAE-agarose-EtBr gel of PTC200-PCR amplified rDNA region. Lane M corresponds to molecular size standards (GeneRuler™ 1kb DNA Ladder Plus, Fermentas Life Sciences) from left to right: 1st negative control (master mix without DNA template), *S.cerevisiae* #303, *S.cerevisiae* #500, *S.cerevisiae* #501 and 2nd negative control (master mix without Taq polymerase). The same order is repeated for A (Lanes 1-2-3-4-5), GC (Lanes 6-7-8-9-10) and B (Lanes 11-12-13-14-15) buffer solutions.

4.2.4 PCR-program set-up on the microdevice

Thermal characterization

The thin layer of PDMS physically separates the chemical reagents from the metal wires but at the same time acts as an insulating material due to its low thermal conductivity. This means that the temperature inside the chamber will be lower respect to that one measured by the silicon-embedded thermometers and the heating program has to be calibrated to achieve the desired temperature at the level of the PCR reaction mix.

For the preliminary thermal calibration, a test PCR protocol was run on the microchip. It included a denaturation step at 95°C for 5 min followed by 30 cycles of denaturation (95°C for 60 sec), annealing (65°C for 60 sec), extension (72°C for 60 sec). At the end, the temperature was kept at 72°C for 5 min. The program was launched from the software by applying voltage amplitude of 22V (2.9W). The temperature values measured by the thermometer and by thermocouple (Type K) were plotted during the cycling against the set point (figure 4.14).

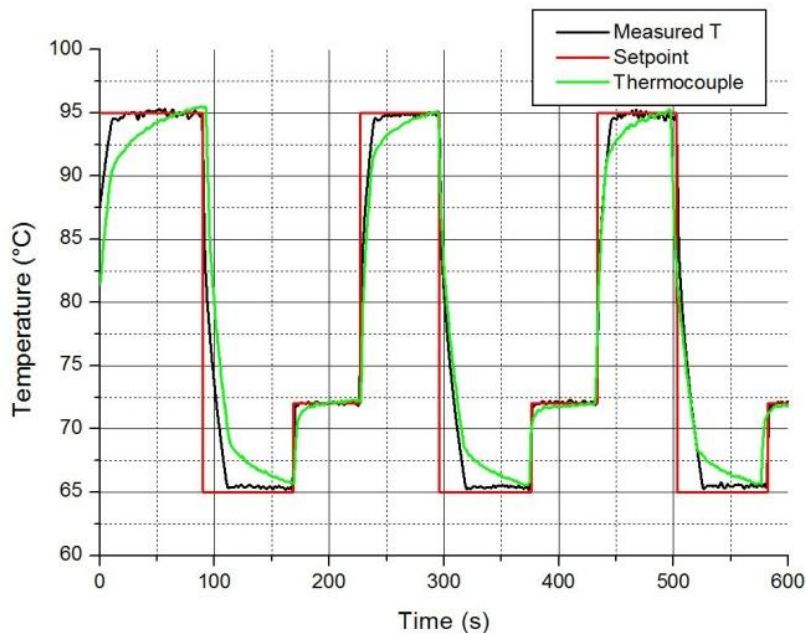


Fig. 4.14. Temperature values with internal thermometer (black) and thermocouple (green) versus set point (red).

As inferred from the graph, our microdevice needs 23 sec to decrease the temperature from 95°C to 65°C (1.3°C/s) and 12 sec to increase the temperature form 72°C to 95°C (1.9°C/s).

After the thermometer thermal characterization, we also measured the effective temperature present inside the microchamber taking into account of the polymeric insulating layer above the silicon surface. Thus, a thermocouple was placed inside the microchamber just above the 400 μ m-PDMS membrane and temperature measured by both the embedded thermometer and the thermocouple was compared (fig. 4.15)

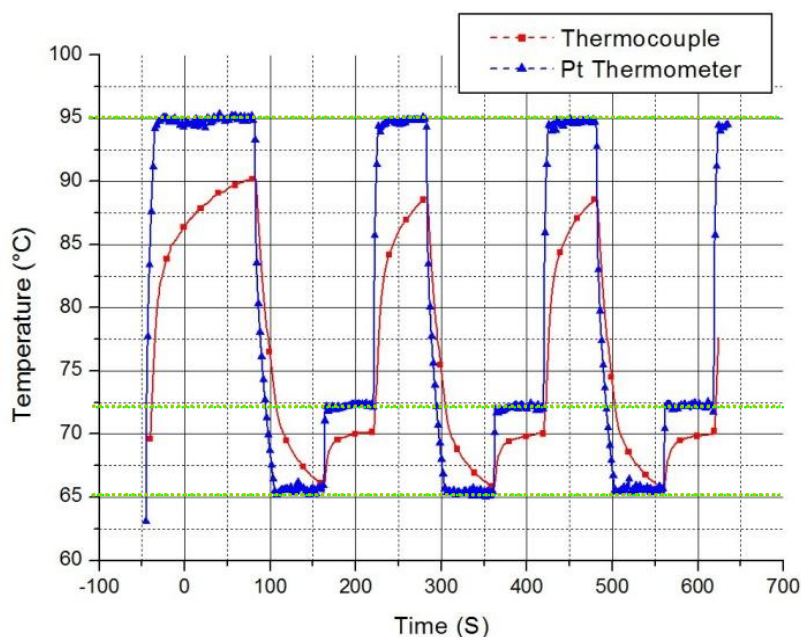


Fig. 4.15. Measured temperature on the top of the 400 μ m-PDMS membrane (blue) compared to the temperature read by the thermometer (red) and the set-point (green dashed lines).

The presence of the PDMS membrane affected considerably the overall thermal profile inside the microchamber. Therefore, we compensated the PCR protocol by measuring the differences in thermal profiles and alter the temperature settings (i.e. heating/cooling temperatures and cycling times), accordingly.

Thermal protocols obtained with the commercial thermal cycler (*section 4.2.3*) were adapted to the microchip as follows: initial denaturation at 98°C for 5 min, followed by 30 cycles of denaturation at 100°C for 30 sec, annealing at 53.5°C for 30 sec, and extension at 74°C for 30 sec, with a final extension at 74°C for 5 min (Table 4.16).

Table 4.16 Real temperature values for the conventional thermocycler and the microdevice. For the microchip, the temperatures were measured with a thermocouple inserted through the polymeric microchamber.

Thermal steps	PTC200-PCR		Microchamber-PCR	
	Temperature (°C)	Time (sec)	Temperature (°C)	Time (sec)
Initial denaturation	95	180	95	180
Denaturation	95	10	95±0.5	10
Annealing	58	10	58 ±0.5	16
Extension	72	10	72 ±0.5	9
Final Extension	72	180	72 ±0.5	300

The temperature profile detected by the thermocouple inside the microchamber is plotted in figure 4.17 and compared with the desired temperature (set in the standard PTC-200 PCR machine) and the temperature detected by the silicon-embedded thermometer.

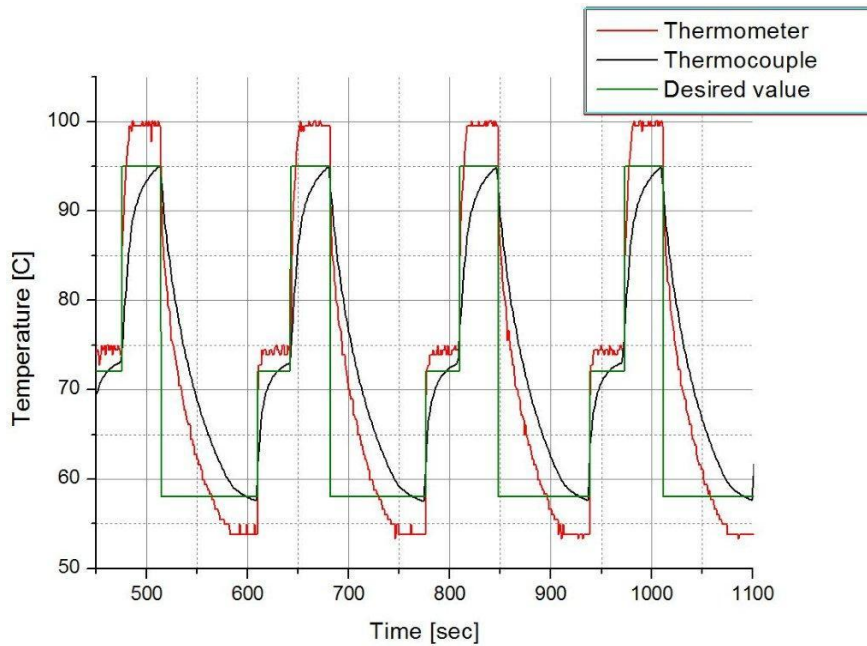


Fig. 4.17 Temperature profiles measured by the silicon-embedded thermometer and by the thermocouple compared with the desired profile as defined in the commercial thermocycler.

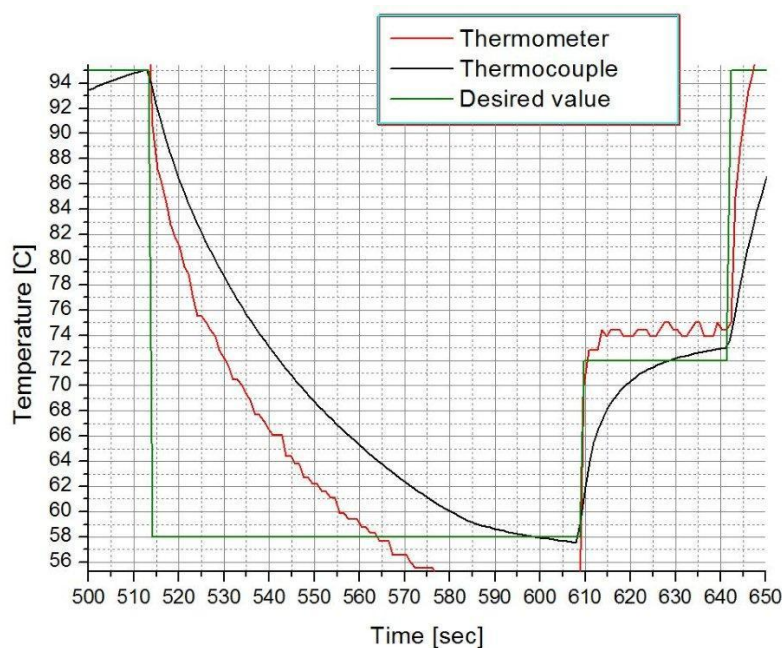


Fig. 4.18 Detail of a thermal cycle

The thermal calibration allowed to reduce the difference between the observed and expected temperature; however, temperature setting would require further optimization, especially for the hold times at each temperature step. In particular, considering a temperature range of 0.5°C around the desired value, the annealing phase takes a longer time while extension is shorter with respect to the desired value. The observed differences may affect the hybridization of the primers and elongation of the amplicons, reducing the overall PCR efficiency.

4.2.5 1st validation test: PCR with gDNA

Once the thermal calibration was performed, the PCR amplification was run on the microdevice introducing into the microchamber $10\mu\text{l}$ -PCR master mix (Table 4.13, buffer B, DNA template of *S. cerevisiae* 303) and applying the thermal protocol reported in Table 4.16. Afterwards, the PCR product was recovered from the microchamber with a micropipette and the volume was measured in order to check if evaporation events were occurred. Volume variation was undetectable and so all the available sample ($8\text{-}9\mu\text{l}$) was loaded on 1.2% TAE-agarose-EtBr gel. As shown in figure 4.19 (a), the target region was successfully amplified, giving an amplicon of $\sim 420\text{bp}$, as in the conventional PCR. The experiment was then repeated starting from the same master mix for standard PTC-200 PCR machine and microdevice and by loading on agarose gel only $2\mu\text{l}$ of amplified DNA. As can be seen in figure 4.19 (b), the loaded volume was sufficient for the detection of the gel bands and it

was set as optimal loading volume for the quantification procedure during the PCR efficiency evaluation.

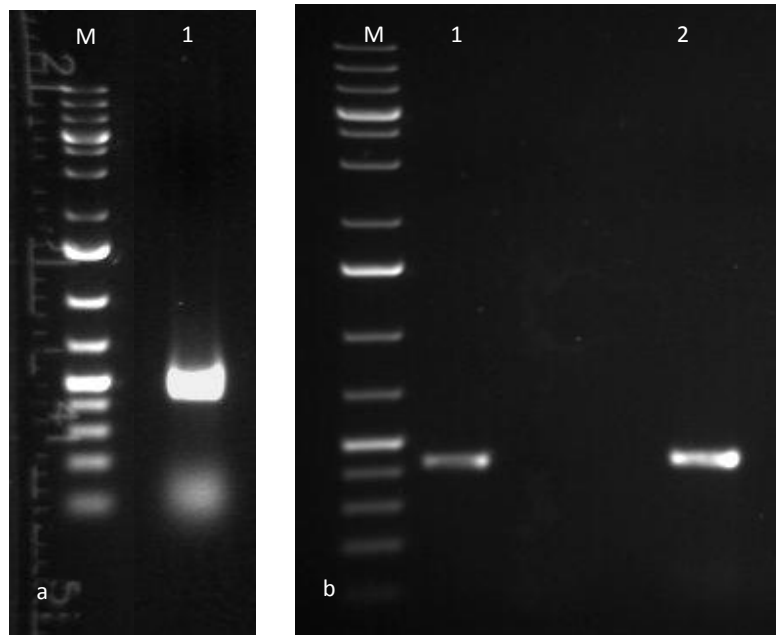


Fig. 4.19 a) First validation of the microdevice: the target region of *S. cerevisiae* 303 was successfully amplified, 8 μ l-PCR product loaded; M: 1 kb Ladder (Fermentas) b) Microchip-PCR (Lane 1) and PCR performed with Peltier thermal cycler Bio-Rad PTC-200 (Lane 2), 2 μ l-PCR product loaded.

4.2.6 2nd validation test: PCR with gDNA from different *S. cerevisiae* strains

Once verified that the rDNA gene of *S. cerevisiae* 303 was successfully amplified, microchip-PCR was tested also with the other wine yeast strains (*S. cerevisiae* 500 and 501). PCR was run in parallel on Peltier thermal cycler PTC-200 and simultaneously on three microchips, each one connected to an electronic board. Then, 2 μ l-PCR products were run on 1.2% TAE-agarose-EtBr gel and their relative quantities were assessed by comparing the obtained gel bands with that of the ladder (GeneRulerTM 1kb DNA Ladder Plus, Fermentas Life Sciences) under UV light lamp, through the ChemiDoc XRS Imaging System (Bio-Rad) and Image Lab software (Bio-Rad).

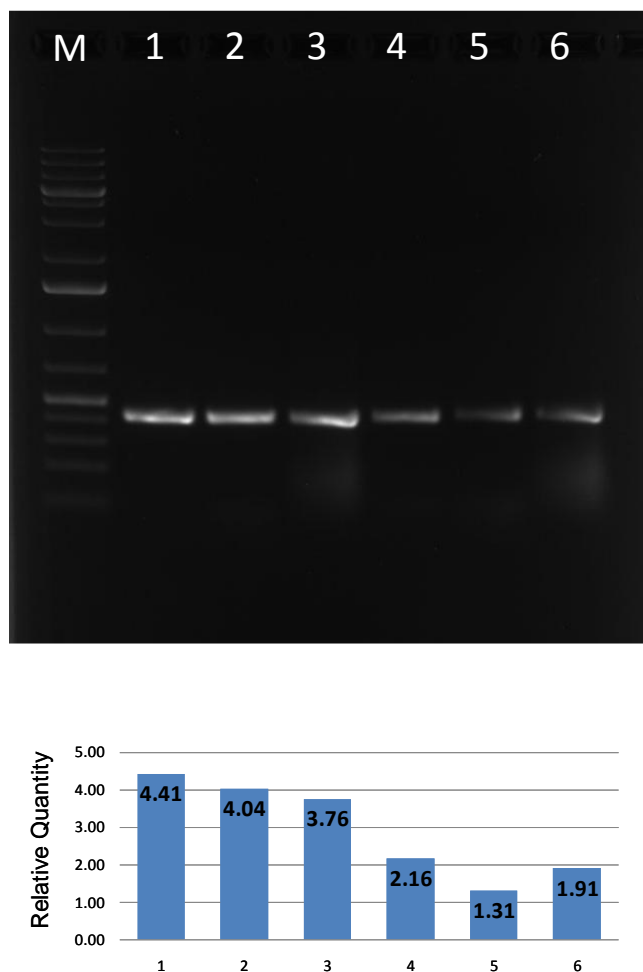


Fig 4.20. PCR amplifications of 420bp-DNA fragments of different *S. cerevisiae* (303, 500, 501) strains with Peltier Thermal Cycler PTC-200 (Lane: 1-2-3) and microdevice (Lane: 4-5-6); Lane M: 1kb Ladder (Fermentas). The values are relative to the 500bp band of the 1kb ladder, loaded on the first lane.

As can be seen from the electrophoretic pattern of figure 4.20, PCR reaction was positively performed with all wine strains. In both microchip and PTC-200 PCR machine, the highest relative quantity was obtained for *S. cerevisiae* 303, and for this reason it was chosen as DNA template for the following validation experiments.

4.2.7 3rd validation test: comparison of PCR efficiency and reproducibility with gDNA

To evaluate the efficiency and repeatability of the microchip-PCR, DNA amplification was performed in triplicate both within the microchamber and with the commercial Peltier thermal cycler (PTC-200, Bio-Rad) and the relative quantity was obtained through the ChemiDoc XRS Imaging System (Bio-Rad) and Image Lab software (Bio-Rad). A unique

mastermix was prepared in order to limit as much as possible variations in chemicals concentration that could influence the overall performance of the reaction.

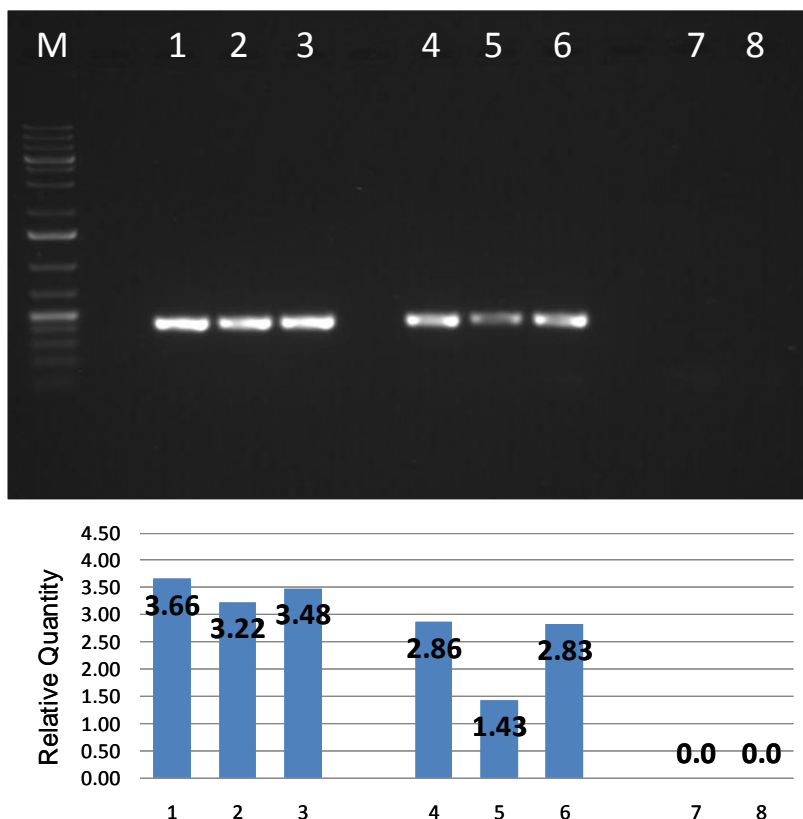


Fig. 4.21. Electrophoretic pattern and relative quantity assessment of PCR product from *S. cerevisiae* 303 performed with the commercial PTC200 thermal cycler (Lane 1-3) and with the microdevice (4-6). In Lanes 7 and 8 are loaded the negative controls (i.e. master mix with no DNA template) of PTC200-PCR and microdevice-PCR, respectively.

The relative quantity showed some variability among independent PCR reactions for both the commercial system and the microdevice (fig. 4.21). We observed a reduced reproducibility and efficiency in microdevice-PCR with respect to PTC200-PCR.

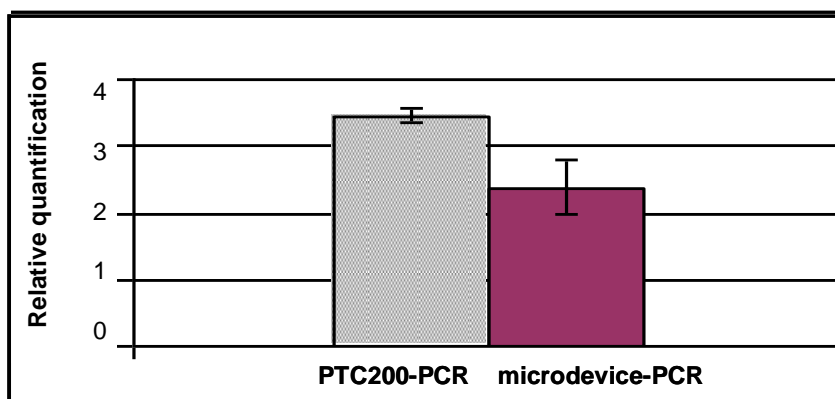


Fig. 4.22 Average of the relative quantities for PTC200-PCR and microchip-PCR

These effects were mainly due to chip-to-chip variability (~2%) and to the different thermal profiles of the two PCR systems. The negative controls (master mix without DNA template) were also loaded on EtBr-stained agarose gel in order to exclude the presence of false positive amplifications due to the presence of contaminants in the microchamber. As expected, no aspecific nucleic acids were detected (fig. 4.21, lane 8).

4.2.8 4th validation test: comparison of PCR efficiency and reproducibility with gDNA concentrations

PCR reproducibility and efficiency were further defined using diluted gDNA sample (1:10, 1:100, 1:1000) from *S. cerevisiae* 303 strain. Therefore, triplicate PTC200-PCR and microchip-PCR were carried out with 10-fold serial dilution ranging from 177ng (1:10) to 1,77ng (1:1000) of purified genomic DNA.

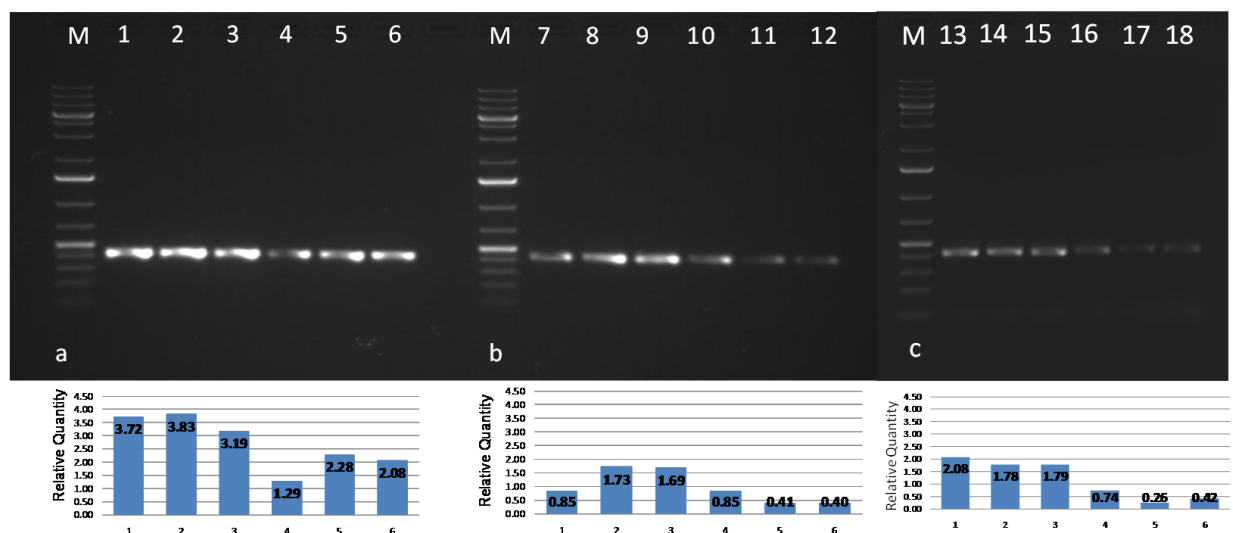


Fig. 4.23. DNA amplification of 10-fold serial dilution of yeast purified genomic DNA (a: 177ng, b: 17.7ng, c: 1,77ng) performed with commercial Peltier thermal cycler (Lanes: 1-3; 7-9; 13-15) and microdevice (Lanes: 4-6; 10-12; 16-18)

As shown in figure 4.23, microchip-PCR was successful also with the most diluted template sample. In particular, for DNA concentration ranging from 1777ng (fig. 4.21) to 177ng the amplified product of the microdevice-PCR is higher than 50% compared to the commercial-PCR. At lower template concentrations, the performance of the microdevice-PCR decrease to less than 25% compared to the commercial-PCR (fig. 4.24).

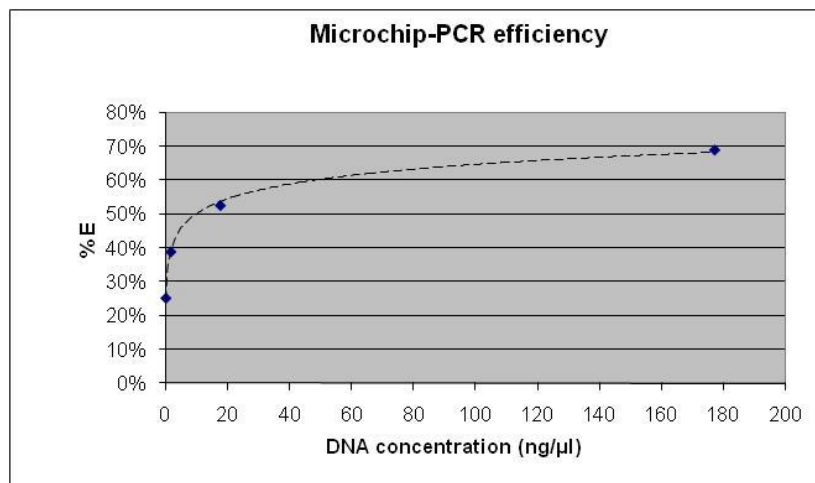


Fig.4.24. Amplification efficiency of microdevice-PCR with respect to the commercial-PCR in function of different gDNA concentration.

4.2.9 5th validation test: Colony-PCR

As reported in section 4.2.1, DNA extraction and purification is a laborious process that should be avoided for the perspective of fast and especially portable analytical systems (e.g. LOC- lab on chip, POCT - point of care testing). Therefore, the possibility to amplify DNA directly from cells is considered an important step towards more integrated, rapid and easy to use technologies. For this reason, the microdevice was characterized also with PCR performed directly from yeast cells (colony-PCR).

1-2 colonies were resuspended in 50 μ l distilled water and incubated for 5 min at 95°C in the commercial Peltier Thermal Cycler (PTC-200). The boiled suspension was centrifuged for 2 min at 5000 rpm and the supernatant was used as template for the PCR reaction. Moreover, the performance of the microdevice was also tested with a 10-fold dilution in sterile water of the described sample. As can be seen by observing the electrophoretic pattern of figure 4.25, an amplification product was observed with both commercial- and microdevice-PCR. Unfortunately, the PCR efficiency is extremely reduced (10%) using the microdevice in comparison to the PTC-200.

With the diluted sample no DNA was amplified within the microchamber while a weak band is visible for the PCR performed by the PTC-200 thermal cycler. It is worth noting that even the conventional system is in trouble with difficult samples since DNA is not purified and many contaminants can counteract or disturb the mechanism of action of the enzyme or by introducing changes in the chemical equilibrium of the reaction mix.

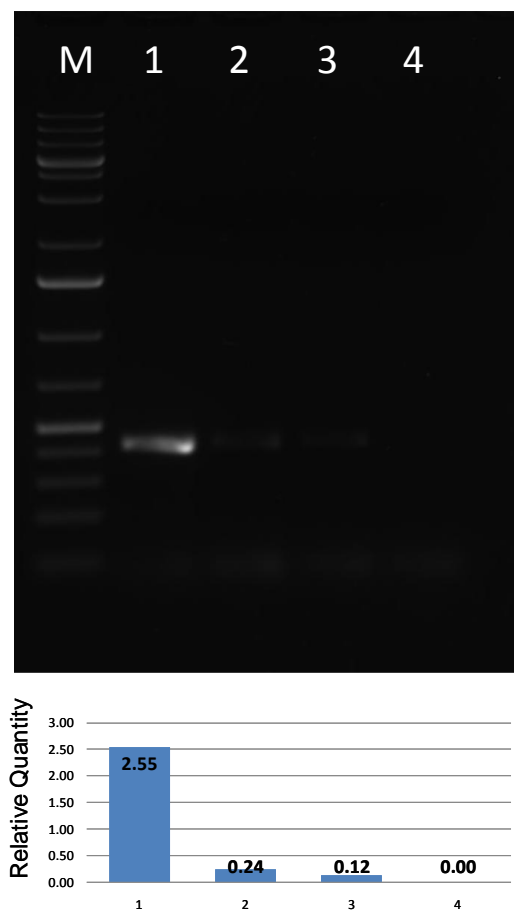


Fig. 4.25. Colony PCR starting from boiled yeast cells (Lane 1: PTC200-PCR; Lane 2: microdevice-PCR) and from 1:10 dilution of the boiled yeast cells (Lane 3: PTC200-PCR; Lane 4: microdevice-PCR).

4.3 Discussions

In this work, the development and validation of a microdevice-PCR for wine yeast analysis is described. Its architecture consists of a chamber-type-stationary chip with a hybrid structure: a silicon chip for the heating system and temperature sensors, and a PDMS microchamber for the containment of the reaction mix. The low fabrication costs of the polymeric chamber allows its usage as a disposable unit, thus avoiding sample-to-sample or run-to-run cross contaminations associated with cleaning and reusing PCR microchambers. To permit one-way use of the upper element, the double (PDMS-Silicon) structure is not glued and the contact between the two parts is assured by mechanical clamping, which in turn, ensures proper sealing of the inlet and outlet ports and prevents PCR mix from evaporation during thermal cycles. Moreover, the plastic ceiling compresses the polymeric chamber in such a way to limit gas bubble generation when the temperature approaches to 100°C during the dissociation of the DNA double strands. The unlikely occurrence of bub-

bles can be online controlled by optical inspection thanks to the transparency of both the PDMS chamber and the external cap. The whole master mix (10 μ l) is confined within the polymeric structure which contemporaneously prevents a direct contact of the solution with the metal tracks (i.e. avoids corrosion of platinum by chlorine) and also the aspecific absorption of reaction components on SiO₂-surface.

The microdevice was thermally characterized both on silicon and in presence of the PDMS chamber. The low thermal conductivity of the polymer negatively affects the thermal profile and the reaction speed; thus, temperature settings of the PCR program were adjusted according to a temperature feedback control supplied by a thermocouple inserted within the polymeric chamber. No difficulties were encountered in retrieving samples from the outlet of the chamber and no detectable evaporation phenomena were observed. On-chip PCR was successfully performed on three purified genomic DNA templates, extracted from *S. cerevisiae* wine strains. Then, 10-fold serial dilutions of purified DNA were loaded onto the microdevice, demonstrating the possibility to amplify DNA even at low concentrations. The relative efficiency of the microchip-PCR was higher than 50% for DNA concentration starting from 1777 ng to 177 ng gDNA, while it decreased to 40% and 25% for 17,7 ng and 1,77 ng, respectively. The microsystem was also capable to amplify DNA from boiled yeast cultures, avoiding the laborious process of DNA extraction and purification. This represented an important achievement for future on-site integrated lab-on-a-chip applications with very little or no pre-PCR manipulations.

Interestingly, in contrast to data reported in literature, nor static nor dynamic passivations were required to carry out on-chip PCR. PDMS showed a good biocompatibility and the evaporation was prevented with a plastic cover, without the necessity to introduce additives to increase the boiling point of the solution. Neither silanization of the internal walls nor external coating (e.g. with parylene) on the polymer surface were necessary for the success of PCR.

The reduced efficiency of the microdevice-PCR with respect to the conventional benchtop instrumentation was due to the presence of the insulating PDMS layer and higher ramping times. Optimization of these aspects was achieved by etching the silicon membrane below Pt heater and by increasing PDMS thermal conductivity through the addition of different concentrations (1, 5, 10 w/w %) of carbon nano-powder (see Appendix B).

However, the cooling rate remains the weakest point to be improved and the possibility to introduce a small cooling fan is under evaluation. The chip-to-chip variability is another

point that must be overcome through a better control of the mask resolution and the fabrication process.

Although some work is still needed to reduce assay times and improve PCR efficiency, this microsystem has successfully provided a miniaturized platform for DNA amplification of yeast strains. Future work will deal with the development of online detection module in order to obtain a truly portable and integrated DNA analyzer, as discussed in chapter 5.

Chapter 5

5 Conclusions and Future Outlook

In the framework of miniaturized systems for yeast's studies, two microsystems – *a cell-based biosensor and a PCR microdevice* – were investigated for the *cellular and molecular* analyses of wine strains.

With regard to the first device, a multiparametric system was investigated for wine yeast quality assessment. ISFET and impedimetric sensors were characterized in order to measure in real time pH and cell settling of yeasts under batch culture conditions.

The evaluation of yeast performance and robustness was focused on ethanol tolerance, as it is one of the main stress factors acting in winemaking process, and thus, one of the major causes of stuck fermentations.

Firstly, a positive trend correlation between yeast growth and extracellular acidification was demonstrated at several ethanol concentrations. Then, online pH measurements of different *Saccharomyces cerevisiae* wine strains were carried out by growing cells in function of critical alcohol concentrations. Interestingly, pH measurements were in good agreement with the experimental results obtained by conventional agar plates.

Additionally, preliminary resistivity measurements demonstrated the possibility to follow in real-time progressive settling of the cell suspension and be sensitive to both different particles sizes and cell concentrations at the inoculum level.

Although the validation of the two integrated sensors is still in an explorative phase, the encouraging preliminary results demonstrated the possibility to acquire online interesting physiological parameters without labelling and damaging cells and with a strong reduction of time (from 48-72 hours with agar plates to just 5 hours with the microdevice). The culture can be monitored before, during and after the exposure of chemical stress factors and cells can be recovered at any time for further experiments without enzymatic treatment (e.g. with trypsin) as typically required when adherent cells are employed.

Future improvements will mainly be addressed to the realization of integrated reference electrodes and to experimental measurements under tightly controlled and stable temperature, using the integrated temperature sensor as internal reference. Moreover, other impe-

dimetric sensors configurations and geometries will be evaluated in order to maximize the useful information that can be “caught” during sedimentation of yeasts.

In principle, impedance sensor showed great versatility and could be exploited for the *investigation of flocculation phenomena*, when yeast cells adhere to each other forming small aggregates or so called “flocs”. Many researchers proposed that yeast flocculation is strain-specific and is induced by nutrients starvation and other stress conditions. This process is considered extremely interesting for wineries, breweries and more in general for industrial applications but its control is very complicated and challengeable.

Futhermore, next experimental sessions with ISFET sensors could deal with the *screening of both commercial and wild yeasts strains* and with the *investigation of yeast tolerance to other fermentative stress factors* such as medium fatty acids, sulphites and acetic acid or nutrients depletion (e.g. with low level of thiamine). Finally, *yeast performance could be tested in liquid medium with a chemical composition similar to must*, come very close to the real winemaking conditions.

Other future perspectives regard the realization of an *array of CBBs* in order to realize a smart platform for the high throughput screening of cells, increasing the test points and reducing the experimental variable conditions (e.g. temperature effects, cell status, etc.).

Moreover, the possibility to *integrate other sensors* such as oxygen sensors could be very interesting to measure the transition from aerobic to anaerobic conditions. Enzymatic sensors could be also investigated for the online monitoring of specific cellular products in order to detect *multiple chemical and biotechnological parameters* within the same technological platform. Finally, an *underlying microfluidics* could be developed for *chemical gradient generations* (e.g. to deliver automatically different ethanol concentrations and avoid manual steps), making the platform potentially suitable for fast, quantitative and automated oenological characterization for the quality improvements of the winemaking process.

Concerning the second system, a PCR microdevice was biologically validated by successfully amplifying genomic DNA fragments extracted and purified from the same *Saccharomyces cerevisiae* wine strains tested with the multiparametric sensor. Serial diluted samples were positively amplified (even with 1,77 ng of gDNA) and the relative efficiency of the microdevice-PCR was compared to that obtained with the commercial thermal cycler. Finally, the outcome of PCR was successfully assessed also from boiled yeast cultures, indicating the possibility to overcome the laborious process of DNA extraction and purifica-

tion. This represented an important achievement for potential lab-on-chip applications with very little or no pre-PCR sample manipulations.

Future improvements will deal with the optimization of heating and cooling systems in order to achieve better amplification performance and faster PCR process.

The *detection module* is currently an open issue and optical or more likely electrochemical methods will be investigated towards the realization of a truly integrated system. At the same time, proper *microfluidics* (i.e. micropumps and microvalves) will be introduced for the liquid handling from the amplification to the detection module.

Other future plans could regard the simultaneous amplification of many DNA targets of interest (i.e. *multiplex PCR*), that could be performed by using different yeast species within the same PCR master mix.

Enzymatic digestion of amplified DNA could be another interesting sample-processing step to implement on the final platform. This would allow deeper analysis for yeast ecology studies such as typing of wine yeast strains and more in general yeast quality control (e.g. commercial and wild strains discrimination and fraud detection).

Ambitious future works could be addressed to *PCR performed on droplets of wine* in such a way to evaluate the integration of the microdevice-PCR into *industrial and automated quality control systems*. Thus, the microdevice-PCR could follow strain dynamics during fermentation such as for example to check the dominance of inoculated commercial strains over indigenous microorganisms present on the surface of the grape berries.

Although the two microsystems were developed separately, it cannot be excluded in future that they could be further investigated in such a way to couple them and obtain an *unique integrated platform for both cellular and molecular analyses*.

Finally, even though they were both characterized for yeast analysis, in principle they could work also with *other microorganisms* such as pathological bacteria in order to extend these systems also to important medical applications.

Acknowledgments

This work has been developed at the Bruno Kessler Foundation (FBK) in Trento - Italy, within the BioMEMS Research Unit, headed by Dr. Leandro Lorenzelli.

The first activity (“Electrochemical sensors for wine yeast analysis”) was partially funded by the project: “WMIS: Water Monitoring Integrated System”, under the L.P. n° 6/99 of the Provincia Autonoma di Trento. The second activity (“PCR microdevice for wine yeast analysis”) was partially funded by the European project: “POCEMON” (Point-Of-Care MONitoring and Diagnostics for Autoimmune Diseases, FP7-ICT-2007-216088).

The two devices presented in this work have been designed, fabricated, packaged and characterized by the BioMEMS group, in particular by Andrea Adami, Cristian Collini, Severino Pedrotti, Lara Odorizzi for the multiparametric sensors and by Cristian Collini and Elisa Morganti for the PCR microdevice.

Other collaborators have contributed to these activities and in particular Andrea Tindiani for the characterization of ISFETs sensors and the realization of the polymeric microchambers; Stefano Schmidt and Daniele Cortellazzi for the development of the PCR electronic board.

The analyzed yeasts have been kindly supplied by BioAnalisi Trentina s.r.l. (Rovereto, Trento) while the bias board for CBBs has been realized by Optoi Microelectronics s.r.l. (Gardolo, Trento).

The biological characterization of the electrochemical sensors has been carried out by using the laboratory facilities of FBK while the validation of the PCR microdevice has been performed in collaboration with Annalisa Ballarini and Professor Olivier Jousson from the Microbial Genomics Lab, Centre for Integrative Biology (CIBIO) – University of Trento.

Bibliography

- Abbas C.A., Yeasts in Food and Beverages, Book chapter, Production of Antioxidants, Aromas, Colours, Flavours, and Vitamins by Yeasts , 2006, Springer.
- Aguilera F., Peinado R. A., Millan C., Ortega J. M., Mauricio J.C., Relationship between ethanol tolerance, H⁺-ATPase activity and the lipid composition of the plasma membrane in different wine yeast strains, International Journal of Food Microbiology, 110 (2006), 34-42.
- Alexandre H. and Charpentier C., Biochemical aspects of stuck and sluggish fermentation in grape must, Journal of Industrial Microbiology and Biotechnology, (1998), 20, 20-27.
- Alexandre H., Rousseaux I., Charpentier C., Ethanol adaptation mechanisms in *Saccharomyces cerevisiae*, Biotechnol. Appl. Biochem., 20 (1994), 173-1783.
- Alexandre H., Rousseaux I., Charpentier C., Relationship between ethanol tolerance, lipid composition and plasma membrane fluidity in *Saccharomyces cerevisiae* and *Kloecklera apiculata*, FEMS Microbiol. Lett., 124 (1994), 17-22.
- Anderson R.C., Su X., Bogdan G.J., Fenton J. A miniature integrated device for automated multistep genetic assays. Nucleic Acids Research, (2000), Vol. 28, 12, [e60, i-vi].
- Aries V., Kirsop B.H., Sterols biosynthesis by strains of *Saccharomyces cerevisiae* in presence ad absence of dissolved oxygen, J. Inst. Brew., 84 (1978), 118-122.
- Arndt S., Seebach J., Psathaki K.P., Galla H.-J., Wegener J., Bioelectrical impedance assay to monitor changes in cell shape during apoptosis, Biosens. Bioelectron., 19 (2004), 583-594.

- Artigas J., Jimenez C., Dominguez C., Minguez S., Gonzalo A., Alonso J., Development of a multiparametric analyser based on ISFET sensors applied to process control in the wine industry, *Sens. Actuators B* 89 (2003), 199-204.
- Asami K. & Yonezawa T., Dielectric analysis of yeast cell growth, *Biochimica et Biophysica Acta*, 1245 (1995), 99-105.
- Ball C., Jin H., Sherlock G., Weng S., Matese J.C., Andrada R., Binkley G., Dolinski K., Dwight S.S., Harris M.A., Issel-Tarver L., Schroeder M., Botstein D., Cherry J.M., *Saccharomyces Genome Database provides tools to survey gene expression and functional analysis data*, *Nucleic Acids Res.* 29 (2001), 80-81.
- Bard A. J., Faulkner L.R., *Electrochemical methods, fundamentals and applications*, New York Willey, (1980).
- Bartowsky E., Bellon. J., Borneman A., Chambers P., Cordente A., Costello P., Curtin C., Forgan A., Henschke P., Kutyna D., McCarthy J., Macintyre O., Schmidt S., Tran T., Swiegers H., Ugliano M., Varela C., Willmott R., Pretorius S., Not all wine yeast are equal, *Microbiology Australia*, 8 (2), (2007), 55-58.
- Bataillon M., Rico A., Sablayrolles J.M., Salmon J.M., Barre P., Early Thiamin Assimilation by yeasts under enological conditions: impact on alcoholic fermentation kinetics, *J. of Fermentation and Bioengineering*, 82 (1996), 145-150.
- Baumann W. H., Lehmann M., Schwinde A., Eheret R., Brischwein M., Wolf B., Microelectronic sensor system for microphysiological application on living cells, *Sensors and Actuators B* 55, 1999, 77-89.
- Bell T., Ecology of microbial populations, In the *Princeton guide to ecology*, 2009, Princeton University Press
- Bergveld P., Development of an ion-sensitive solid-state device for neurophysiological measurements, *IEEE Trans. Biomed. Eng.* BME-17 (1970), 70-71.

- Bergveld P., Development, operation and application of the ion-sensitive field-effect transistor as a tool for electrophysiology, *IEEE Trans. Biomed. Eng. BME* 19 (1972), 342-351.
- Bergveld P., ISFETs for physiological measurements. Implantable sensors for closed-loop prosthetic systems, in: W.H. Ko (Ed.), Futura Publishing Company, Mount Kisco, New York, (1985), 89–114.
- Bergveld, P. Thirty years of ISFETOLOGY, What happened in the past 30 years and what may happen in the next 30 years, *Sensors and Actuators B*, 88 (2003), 1-20.
- Bergveld P., ISFET, Theory and Practice, *IEEE Sensor Conf. Toronto*, 2003
- Bettaieb F., Ponsonnet L., Lejeune P., Ouada H.B. ; Martelet C., Bakhrouf A., Jaffrezic-Renault N., Othmane A., Immobilization of *E. coli* bacteria in three-dimensional matrices for ISFET biosensor design, *Bioelectrochemistry*, 71 (2007), 118-125.
- Boekhout T., Robert V. (Eds), *Yeast in Food. Beneficial and Dentrimental Aspects*, Behr's Verlag, 2003.
- Bond U., Blomerg A., Principles and applications of genomics and proteomics in the analysis of industrial yeast strains, In *Yeast in Food and Beverages* (eds Querol A, Fleet G.H.), Springer (2006), 173-213.
- Bousse L., Bergveld P., Rooij N.F., Operation of chemically sensitive field effect sensors as a function of the insulator electrolyte interface, *IEEE*, 30 (1983), 1263 – 1270.
- Bousse L., Monstarshed, S., van der Schoot, B., de Rooij, N.F., Gimmel, P., Göpel, W., Zeta potential measurements of Ta₂O₅ and SiO₂ thin films., *J. Colloid Interface Sci.*, 147 (1991), 22-32.

- Bousse L., Parce W., Applying silicon micromachining to cellular metabolism, *IEEE Engineering in Medicine and Biology*, (1994), 396-401.
- Bratov A., Abramova N., Ipatov A., Recent trends in potentiometric sensor arrays- A review, *Analytica Chimica Acta*, 678 (2010), 149-159.
- Brischwein M., Motrescu E.R., Cabala E., Otto A.M., Grothe H., Wolf B., Functional cellular assays with multiparametric silicon sensor chips, *Lab on a chip*, 3 (2003), 234-240.
- Cabral M.G., Viegas C.A., S.A. I. Correia, Mechanism underlying the acquisition of resistance to octanoic-acid-induced death following exposure of *Saccharomyces cerevisiae* to mild stress imposed by octanoic acid or ethanol, *Arch. Microbiol.*, 175 (2001), 301-307.
- Cady P., Progress in impedance measurements in microbiology, In Sharpe A.N. and Clark D.S. (ed.), *Mechanizing microbiology*, Springfield, 1978.
- Cady N.C., Stelick S., Kunnavakkam M.V., Batt C.A., Real-time PCR detection of *Listeria monocytogenes* using an integrated microfluidics platform, *Sens. Actuators B Chem.*, 107 (2005), 332–341.
- Cameron-Clarke A., Hulse G.A., Clifton L., Cantrell I.C., The use of adenylate kinase measurement to determine causes of lysis in lager yeast, *J. Am. Soc. Brew. Chem.*, 61 (2003), 152-156.
- Campbell C.E., Laane M.M., Haugarvoll E., Giaever I., Monitoring viral-induced cell death using electric cell-substrate impedance sensing, *Biosens. Bioelectron.*, 23 (2007), 536-542.
- Casey G.P. and Ingledew W.M., Ethanol tolerance in yeasts, *Critical Rev. in Microbiology*, (1986), 13, 19-280.

- Castellarnau M., Zine N., Bausells J., Madrid C., Juarez A., Samitier J., Errachid A., ISFET-based biosensor to monitor sugar metabolism in bacteria, *Materials Science and Engineering C*, 28 (2008), 680-685.
- Castrillo J. I., Ugalde U. O., A general model of yeast energy metabolism on aerobic chemostat culture. *Yeast*, 10 (1994), 185-197.
- Castrillo J. I., De Miguel I., Ugalde U. O., Proton Production and Consumption Pathways in Yeast Metabolism. A Chemostat Culture Analysis, *Yeast*, 11 (1995), 1353-1365.
- Ceriotti L., Kob A., Drechsler S., Ponti J., Thedinga E., Colpo P., Ehret R., Rossi F., Online monitoring of BALB/3T3 metabolism and adhesion with multiparametric chip-based system, *Analytical Biochemistry*, 371 (2007) (a), 92-104.
- Ceriotti L., Ponti J., Broggi F., Kob A., Drechsler S., Thedinga E., Colpo P., Sabbioni E., Ehret R., Rossi F., Real-time assessment of cytotoxicity by impedance measurement on a 96-well plate, *Sens. Actuat. B*, 123 (2007) (b), 769-778.
- Ceriotti L., Ponti J., Colpo P., Sabbioni E., Rossi F., Assessment of cytotoxicity by impedance spectroscopy, *Biosens. Bioelectron.*, 22 (2007) (c), 3057-3063.
- Chen P.C., Accelerating micro-scale PCR (Polymerase Chain Reaction) for modular Lab-on-a-chip system, dissertation, (2006).
- Sa-Correia I., Synergistic effects of ethanol, octanoic and decanoic acids on the kinetics and activation parameters of thermal death in *Saccharomyces bayanus*, *Biotechnol. and Bioengineering*, 28 (1986), 761-763.
- Christensen T. B., Pedersen C.M., Grondahl K.G., Jensen T.G., Sekulovic A., Bang D.D. and Wolf A., PCR biocompatibility of lab-on-a-chip and MEMS materials. *J. Micromech. Microeng.*, (2007), 17, 1527-1532.

- Christensen T. B., Bang D. D., Wolff A. Multiplex polymerase chain reaction (PCR) on a SU-8 chip. *Microelectronic Engineering*, (2008), 85, 1278-1281.
- Cho Y.K., Kim J., Lee Y., Kim Y.A., Namkoong K., Lim H., Oh K.W., Kim S., Han J., Park C., Pak Y.E., Ki C.S., Choi J.R., Myeong H.K., Ko C., Clinical evaluation of microscale chip-based PCR system for rapid detection of hepatitis B virus, *Biosens. Bioelectron.*, 21, (2006), 2161-2169.
- Consolandi C., Severgnini M., Frosini A., Caramenti G., De Fazio M., Ferrara F., Zocco A., Fischetti A., Palmieri M. De Bellis G., Polymerase chain reaction of 2-kb cyanobacterial gene and human anti- α -chymotrypsin gene from genomic DNA on In-Check single-use microfabricated silicon chip, *Anal. Biochem.*, 353 (2006), 191-197.
- Crews N., Wittwer C., Gale B., Continuous-flow thermal gradient PCR, *Biomed. Microdevices*, 10 (2008), 187–195.
- Crueger W, Crueger A., *Biotechnology: a textbook of industrial microbiology*. Brock TD, editor. Sunderland: Sinauer Associates Inc., (1990), 64-73.
- D'Amore T., Panchal C.J., Russel I., Stewart G.G., A study of Ethanol tolerance in yeast, *Critical Reviews in Biotechnology*, 9 (1990), 287-304.
- de Melo J.V., Soldatkin A.P., Martelet C., Jaffrezic-Renault N., Cosnier S., Use of competitive inhibition for driving sensitivity and dynamic range of urea ENFETs, *Biosensors and Bioelectronics* 18 (2003), 345-351.
- Dzyadevich S.V., Korpan Y.I., Arkhipova V.N., Alesina M.Y., Martelet C., El'Skaya A.V., Soldatkin, A.P., Application of enzyme field-effect transistors for determination of glucose concentrations in blood serum, *Biosensors and Bioelectronics*, 14 (1999), 183-187.
- Easley C.J., Karlinsey J.M., Bienvenue J.M., Legendre L.A., Roper M.G., Feldman S.H., Hughes M.A., Hewlett E.L., Merkel T.J., Ferrance J.P., Landers J.P., A fully

- integrated microfluidic genetic analysis system with sample-in-answer-out capability. *Proc. Nat. Acad. Sci. USA*, (2006), 103, 19272-19277.
- Eden R. & Eden G., *Impedance Microbiology*, Research Studies Press Ltd., John Wiley & Sons Inc., New York, 1984
 - Elliott S., Fagin K. D., Narhi L. O., Miller J. A., Jones M. , Koski R., Peters M., Hsieh P., Sachdev R., Rosenfeld R. D., Rohde M. F., Arakawa T., Yeast-derived recombinant human insulin-like growth factor I: Production, purification, and structural characterization, *Journal of Protein Chemistry*, (1990), 9 (1), 95-104.
 - Erill I., Campoy S., Barbè J., Aguilò J. Biochemical analysis and optimization of inhibition and absorption phenomena in glass-silicon PCR-chips. *Sensor and Actuators B*, (2003), 96, 685-692.
 - Fang T.H., Ramalingam N., Xian-Duib D., Ngin T.S., Xianting Z., Kuan A.T.L., huat E.Y.P., Hai-Qing G., Real-time PCR microfluidic devices with concurrent electrochemical detection, *Biosens. Bioelectronics*, 24 (2009), 2131-2136.
 - Felbel J., Bieber I., Pipper J., Kohler J.M., Investigations on the compatibility of chemically oxidized silicon (SiO_x)-surfaces for applications towards chip-based polymerase chain reaction, *Chem. Eng. J.*, 101 (1-3), (2004), 333-338.
 - Firstenberg-Eden R., Eden G., *Impedance Microbiology*, (1984), Wiley, Letchworth.
 - Fleet G.H., *Wine Microbiology and Biotechnology*, (2002), Taylor & Francis.
 - Fleet G.H., Yeast interaction and wine flavour, *Int. J. Food Microbiol.*, 86 (2003), 11-22.
 - Fleet G.H., Yeast in foods and beverages: impact on product quality and safety, *Current Opinion in Biotechnology*, 18 (2007), 170-175.

- Freese E., Sheu C.W., Galliers E., Function of lipophilic acids as antimicrobial food additives, *Nature*, 241 (1973), 321-325.
- Frey O., Bonneick S., Hierlemann A., Lichtenberg J. Autonomous microfluidics multi-channel chip for real-time PCR with integrated liquid handling. *Biomed. Microdevices*, (2007), 9, 711-718
- Fung C.D., Cheung W. P., A generalized theory of an Electrolyte-Insulator-semiconductor Field Effect Transistor, *IEEE transactions on electron devices*, 1 (1986), 8-18.
- Gabriel P., Dienstbier M., Matoulkova D., Kosar K., Sigler K., Optimised Acidification Power Test of Yeast Vitality and its Use in Brewing Practice, *J. Inst. Brew.*, 114, (2008), 270–276.
- Garrison M.W., Baker D.E., Therapeutic advances in the prevention of hepatitis B: yeast-derived recombinant hepatitis B vaccines, *DICP, The Annals of Pharmacotherapy*, (1991), 25 (6), 617-627.
- Gavin A.-C., Bosche M., Krause R., Grandi P., Marzioch M., Bauer A.,Schultz J., Rick J.M., Michon A-M, Cruciat C-M, Remor M, Hofert C, Schelder M, Brajenovic M, Ruffner H, Merino A, Klein K, Hudak M, Dickson D, Rudi T, Gnau V, Bauch A, Bastuck S, Huhse B, Leutwein C, Heurtier M-A, Copley RR, Edelmann A, Querfurth E, Rybin V, Drewes G, Raida M, Bouwmeester T, Bork P, Seraphin B, Kuster B, Neubauer G, Superti-Furga G Functional organization of the yeast proteome by systematic analysis of protein complexes, *Nature* 415 (2002), 141–147
- Gerlach F., Seitz D., Herrmann S., Mayr H., Ziegler G., Vonau W., Konzeption für ein kompatibles Sensorarray-System mit Schnellankopplungsmechanismus für eine Online-Messung in der Zellkulturtechnik (Concept for a compatible sensor array with a fast coupling mechanism for on-line measurements in cell cultures), *Dresdner Beiträge zur Sensorik*, 29 (2007), 245-248.

- Giaever I., Keese C.R., An electrical impedance method to continuously monitor morphology and motion of cells in culture, *Nature*, 366 (1993), 591-592.
- Giordano B. C., Ferrance J., Swedberg S., Huhmer A. F. R. and Landers J. P. Polymerase Chain Reaction in Polymeric Microchips: DNA Amplification in Less Than 240 Seconds. *Analytical Biochemistry*, (2001), 291, 124-132.
- Gnan S., Luedecke L.O., Impedance measurements in raw milk as an alternative to the standard plate count, *J. Food Prot.*, 45 (1982), 4-7.
- Goepel W., Hesse J., Zemel J.N.. *Sensors - A comprehensive survey*. VCH, 1991.
- Goffeau A, Barrell BG, Bussey H, Davis RW, Dujon B, Feldmann H, Galibert F, Hoheisel JD, Jacq C, Johnston M, Louis EJ, Mewes HW, Murakami Y, Philippsen P, Tettelin H, Oliver SG, Life with 6,000 genes, *Science* 274 (1996), 563–567.
- Gomez R., Bashir A., Bhunia A. K., *Microscale Electronic Detection of Bacterial Metabolism, Sensors and Actuators B*, 86 (2002), 198-208.
- Gong H., Ramalingam N., Chen L., Che J., Wang Q., Wang Y., Yang X., Yap P.H.E., Neo C.H., Microfluidic handling of PCR solution and DNA amplification on a reaction chamber array biochip, *Biomed. Microdevices*, 8 (2006), 167-176.
- Grattarola M., Martinoia S., Meloni M., Tedesco M., Parodi M. T., On-line extracellular pH measurements in culture as tool for cell metabolism monitoring, *S.T.P. Pharma Sc.*, 1 (1993), 31-34.
- Guillamon J.M., Sabate J., Barrio E., Cano J., Querol A., Rapid identification of wine yeast species based on RFLP analysis of the ribosomal internal transcribed spacer (ITS) region, *Arch. Microbiol.*, 169 (1998), 387-392.
- Guo M., Chen J., Yun X., Chen K., Nie L., Yao S., Monitoring of cell growth and assessment of cytotoxicity using electrochemical impedance spectroscopy, *Biochim. Biophys. Acta*, 1760 (2006), 432-439.

- Guth U., Gerlach F., Decker M., Oelßner W., Vonau W., Solid-state reference electrodes for potentiometric sensors, *J. Solid State Electrochem.* 13 (2009), 27-39.
- Guttenberg Z., Muller H., Habermuller H., Geisbauer A., Pipper J., Felbel J., Kielpinski M., Scriba J., Wixforth A., Planar chip device for PCR and hybridization with surface acoustic pump. *Lab on Chip*, (2005), 5, 308-317.
- Harame D. L., Bousse L. J., Shott J.D., Meindl J.D., Ion-sensing devices with silicon nitride and borosilicate glass insulator, *IEEE Trans. Electron Devices* 8 (1987), 1700-1707.
- Harris C. M., Kell D.B., The radio-frequency dielectric properties of yeast cells measured with a rapid, automated, frequency domain dielectric spectrometer, *J. Bioelectrochem. Bioeng.*, 11 (1983), 15-28.
- Hartwell L. H., Periodic density fluctuation during the yeast cell cycle and the selection of synchronous cultures, *J. of Bacteriology*, 104 (1970), 1280-1285.
- Hashimoto M., Barany F. and Soper S.A. Polymerase chain reaction/ligase detection of low-abundant DNA point mutations. *Biosens. Bioelectron.*, (2006), 21, 1915-1923
- Heard G.M., Fleet G.H., Growth of natural yeast flora during the fermentation of inoculated wines, *Appl. Environ. Microbiol.*, 50 (1985), 727-728.
- Henschke P.A., Wine Yeast, In *Yeast Sugar Metabolism*, Technomic Publishing Co. (1997), 527-560.
- Hobson N.S., Tothill I., Turner A.P.F., Microbial detection, *Biosensors and Bioelectronics*, 11(5), (1996), 455-477.

- House D., Chon C.H., Creech C.B., Skaar E.P., Dongquing L., Miniature on-chip detection of unpurified methicillin-resistant *Staphylococcus aureus* (MRSA) DNA using real-time PCR, *Journal of Biotechnology*, 146 (2010), 93-99.
- Hu X.H., Wang M.H., Tan T., Li J.R., Yang ., Leach L., Zhang R.M., Luo Z.W., Genetic Dissection of Ethanol Tolerance in the Budding Yeast *Saccharomyces cerevisiae*, *Genetics*, 175 (2007), 1479-1487.
- Huth J., Werner S., Müller H., The proton extrusion of growing yeast cultures as an on-line parameter in fermentation processes. *J. Basic Microbiol.*, 30 (1990), 561-567.
- Imai T., Nakajima I., Ohno T., Development of a new method for evaluation of yeast vitality by measuring internal pH, *J. Am. Soc. Brew. Chem.* 52 (1994), 5-8.
- Imfeld K., Neukom S., Maccione A., Bornat Y., Martinoia S., Farine P.A., Koudelka-Hep M., Berdondini L., Large-scale, high-resolution data acquisition system for extracellular recording of electrophysiological activity, *IEEE Trans Biomed. Eng.*, 55 (2008), 2064-2073.
- Ingledew W.M., Kunkee R., Factors influencing sluggish fermentations on grape juice, *Am. J. Enol. Vitic.*, 36 (1985), 65-76
- Ingram L.O. and T.M. Buttke, Effects of alcohol on microorganisms, *Adv. Microbiol. Physiol.*, (1984), 25, 253-300.
- Iserentant D., Geenens W., Verachtert H., Titrated acidification power: a simple and sensitive method to measure yeast vitality and its relation to other vitality measurements. *J. Am. Soc. Brew. Chem.*, 54 (1996), 110–114.
- Ishida S., Lee J., Thiele D. J., Herskowitz I., Uptake of the anticancer drug cisplatin mediated by the copper transporter Ctr1 in yeast and mammals, *PNAS*, 99 (2002), 14298-14302.

- Ishizaki A., Tripetchkul S., Tonokawa M., Shi Z. P., Shimizu K., pH-mediated control methods for continuous ethanol fermentation using *Zymomonas mobilis*. *J. Ferment. Bioeng.* 77(1994), 541–547.
- Ismail A.A., Ali A.M.M., Selection of high ethanol yielding *Saccharomyces*. II. Genetics of ethanol tolerance. *Folia Microbiologica*, 16 (1971), 350-354.
- Iversen J. J. L., Thomsen J. K., Cox R. P., On-line growth measurements in bioreactors by titrating metabolic proton exchange. *Appl. Microbiol. Biotechnol.*, 42 (1994), 256–262.
- Ivorra C., Perez-Ortin J.E., del Olmo M.L., An inverse correlation between stress resistance and stuck fermentations in wine yeasts. A molecular study. *Biotechnol. Bioengineer.*, (1999), 64 (6): 698-708.
- Jamasb S., Collins S., Smith R. L., A physical model for drift in pH ISFETs, *Sensors and Actuators B* 49 (1998), 146–155.
- Jimenez C., Bratov A., Abramova N., Baldi A., *Encyclopedia of Sensors*, American Scientific Publishers, Pennsylvania, USA, (2006), 151-196.
- Johnson C.C., Moss S.D., Janata J.A., Selective chemical sensitive FET transducers, USA Patent 4, 020, 830 (1977).
- Johnston M., Genome sequencing: The complete code for a eukaryotic cell, *Current Biology* 6 (1996), 500–503.
- Kara B.V. Simpson W.M., Hammond R.M., Prediction of the fermentation performance of brewing yeast with the acidification power test, *J. Inst. Brew.*, 94 (1988), 153-158.
- Kassir Y., Simchen G., Monitoring Meiosis and Sporulation in *Saccharomyces cerevisiae*, In *Guide to yeast genetics and molecular and cell biology*, (2004), Gulf Professional Publishing.

- Ke C., Berney A., Mathewson A., Sheehan M.M., Rapid amplification for the detection of *Mycobacterium tuberculosis* using a non-contact heating method in a silicon microreactor based thermal cycler, *Sensors and Actuators B*, 102 (2004), 308-314.
- Ke C., Keller A.M., Berney A., Sheehan M., Mathewson A., Single step cell lysis/PCR detection of *Escherichia Coli* in an independently controllable silicon microreactor, *Sens. Actuators B*, 120 (2007), 538-544.
- Khanna V. K., Advances in chemical sensors, biosensors and microsystems based on ion-sensitive field-effect transistor, *Indian Journ. of Pure & Appl. Physics*, 45 (2007), 345-353.
- Kilian S.G., Du Preez J. C., Gericke M., The effects of ethanol on growth rate and passive proton diffusion in yeast, *Appl. Microbiol. Biotechnol.*, 32 (1989), 90-94
- Kim J.A., Lee J.Y., Seong S., Cha S.H., Lee S.H., Kim J.J., Park T.H., Fabrication and characterization of a PDMS-glass hybrid continuous-flow PCR chip, *Biochem.Eng. J.*, 29 (2006), 91-97.
- Kim H., Dixit S., Green C.J., Faris G.W., Nanodroplet real-time PCR system with laser assisted heating, *Opt. Express*, 17 (2009), 218-227.
- Kim Y.-H., Park J.-S., Jung H.I., An impedimetric biosensor for real-time monitoring of bacterial growth in a microbial fermentor, *Sensor and Actuators B*, 138 (2009), 270-277.
- Koh C.G., Tan W., Zhao M.Q., Ricco A.J., Fan Z.H., Integrating polymerase chain reaction, valving, and electrophoresis in a plastic device for bacterial detection, *Anal. Chem.* 75 (17), (2003) 4591–4598.
- Kopp MU, de Mello AJ, Manz A., Chemical amplification: continuous-flow PCR on a chip, *Science*, (1998), vol. 280, 1046-1048.

- Kotyk A., Proton extrusion in yeast, *Methods in enzymology*, 174, (1989), Academic Press, New York, 592–603
- Kotyk A., Dependence of the kinetics of secondary active transports in yeast on H⁺-ATPase acidification, *J. Membr. Biol.* 138 (1994), 29-35.
- Krishnan M., Ugaz V.M., Burns MA., PCR in a Rayleigh-Benard convection cell, *Science*, (2002), 298:793.
- Krommenhoek E.E., Gardeniers J.G.E., Bomer J.G., Van den Berg A., Li X., Ottens M., van der Wielen L.A.M., van Dedem G.W.K., Van Leeuwen M., van Gulik W.M., Heijnen J.J., Monitoring of yeast cell concentration using a micromachined impedance sensor, *Sensor and Actuators B*, 115 (2006), 384-389.
- Krommenhoek E.E., van Leeuwen M., Gardeniers H., van Gulik W. M, van den Berg A., Li X., Ottens M., van der Wielen L.A.M., Heijnen J.J., Lab-scale fermentation tests of microchip with integrated electrochemical sensors for pH, temperature, dissolved oxygen and viable biomass concentration, *Biotechnology and Bioengineering*, 99 (2008), 884-892.
- Kubota S, Takeo I, Kume K, *et al.* Effect of ethanol on cell growth of budding yeast: Genes that are important for cell growth in the presence of ethanol, *Biosci. Biotechnol. Biochem.*, 72 (2004), 968-72.
- Kumar G.R., Goyashiki R., Ramakrishnan V., Karpel J. E., Bisson L.F., Genes required for Ethanol Tolerance and Utilization in *Saccharomyces cerevisiae*, *Am. J. Enol. Vitiv.*, (2008), 59 (4), 401-411.
- Lafon-Lafourcade S., Geneix C., Ribereau-Gayon P., Inhibition of alcoholic fermentation of grape must by fatty acid produced by yeast and their elimination by yeast ghosts, *Appl. Environ. Microbiol.*, 47 (1984), 1246-1249.

- Lambrechts M. G., Pretorius I.S., Yeasts and its importance to wine aroma- a review. *S. Afr. J. Enol. Vitic.*, 21 (2000), 97-129.
- Leao C., Van Uden N., Effects of ethanol and other alkanols on the glucose transport system of *Saccharomyces cerevisiae*, *Biotechnol. Lett.* 4 (1982), 721-724.
- Leao C., Van Uden N., Effects of ethanol and other alkanols on passive proton influx in the yeast *Saccharomyces cerevisiae*, *Biochim. Biophys. Acta* 774 (1984), 43-48.
- Lee T. M. H., Carles M.C. and Hsing I. M. Microfabricated PCR-electrochemical device for simultaneous DNA amplification and detection. *Lab on Chip*, (2003), 3, 100-105.
- Lee J.G., Cheong K.H., Huh N., Kim S., Choi J.W., Ko C., Microchip-based one step DNA extraction and real-time PCR in one chamber for rapid pathogen identification, *Lab on Chip*, 6 (2006), 886-895.
- Lee D., Chen P.J., Lee G.B., The evolution of real-time PCR machines to real-time PCR chips, *Biosensors and Bioelectronics*, 25 (2010), 1820-1824.
- Legendre L.A., Bienvenue J.M., Roper M.G., Ferrance J.P., Landers J.P., A simple, valveless microfluidic sample preparation device for extraction and amplification of DNA from nanoliter-volume samples, *Anal. Chem*, 78 (2006), 1444-1451.
- Lehmann M., Baumann W., Brischwein M., Ehret R. Kraus M., Schwinde A., Bitzenhofer M., Freund I., Wolf B., Non-invasive measurement of cell membrane associated proton gradients by ion-sensitive field effect transistor arrays for microphysiological and bioelectrical applications, *Biosensors and Bioelectronics*, 15 (2000), 117-124.
- Lehmann M., Baumann W., Brischwein M., Gahle H. J., Freund I., Ehret R., Drechsler S., Palzer, Kleintges M. H., Sieben U., Wolf B., Simultaneous measure-

ment of cellular respiration and acidification with a single CMOS ISFET, (2001), *Biosensors & Bioelectronics*, 195-203

- Lehmann M., Baumann W., New insights into the nanometer-scaled cell-surface interspace by cell-sensor measurements, *Exp. Cell. Res.*, 305 (2005), 374-382.
- Liu H. R., Yang J., Lenigk R., Bonanno J., Grodzinski P. Self-Contained, Fully Integrated Biochip for Sample Preparation, Polymerase Chain Reaction Amplification, and DNA Microarray Detection. *Anal. Chem.*, (2004), 76, 1824-1831.
- Lorenzelli L., Margesin B., Martinoia S., Tedesco M. T. Valle M., Bioelectrochemical signal monitoring of in-vitro cultured cells by means of an automated microsystem based on solid state sensor-array, *Biosensors and Bioelectronics*, 18 (2003), 621-626.
- Luo X. L., Xu J.J., Zhao W., Chen H.Y., A novel glucose ENFET based on the special reactivity of MnO₂ nanoparticles, *Biosensors and Bioelectronics* 19 (2004), 1295-1300.
- Malfeito-Ferreira M., Guerra J.P.M., Loureiro V., Proton extrusion as indicator of the adaptive state of yeast starters for the continuous production of sparkling wines, *Am. J. Enol. Viticult.* 41 (1990), 219–222.
- Marcus J.S., Anderson W.F., Quake S.R., Parallel picoliter RT-PCR assays using microfluidics, *Anal. Chem*, 78 (2006), 956-958.
- Matsubara Y, Kerman K., Kobayashi M., Yamanura S., Morita Y., Tamiya E., Microchamber array based DNA quantification and specific sequence detection from a single copy via PCR in nanoliters volumes, *Biosensors and Bioelectronics*, 20 (2005), 1482-1490.

- Markx G.H., Davey C. L., The dielectric properties of biological cells at radiofrequencies: Applications in biotechnology, *Enzyme and Microbial technology*, 25 (1999), 161-171.
- Martinoia S., Lorenzelli L., Massobrio G., Conci P., Lui A., Temperature effects on the ISFET behaviour: simulations and measurements, *Sensors and Actuators B* 50 (1998), 60-68.
- Martinoia S., Lorenzelli L., Massobrio G., Margesin B., Lui A., A CAD system for developing chemical sensor-based microsystems with an ISFET-CMOS compatible technology, *Sensor Mater.*, 1999, 11 (5), 279-295.
- Martinoia S., Rosso N., Grattarola M., Lorenzelli L., Margesin B., Zen M., Development of ISFET array-based microsystems for bioelectrochemical measurements of cell populations, *Biosensors and Bioelectronics*, 16 (2001), 1043-1050.
- Martinoia S., Massobrio G., Modeling and simulation of silicon neuron-to-ISFET junction, *Biosensors and Bioelectronics*, 19 (2004), 1487-1496.
- Martinoia S., Massobrio G., Lorenzelli L., Modeling ISFET microsensor and ISFET-based microsystems: a review, *Sensors and Actuators B*, 105 (2005), 14–27.
- Mas S., Ossard F., Ghommidh C., On-line determination of flocculating *Saccharomyces cerevisiae* concentration and growth rate using a capacitance probe, *Biotechnology Letters*, 23 (2001), 1125-1129.
- Massobrio G., Martinoia S., Grattarola M., Use of SPICE for modeling silicon-based chemical sensors, *Sensors and Materials*, 6 (2) (1994), 101-123.
- Masson P., Autran J.L., Munteanu D., DYANMOS: a numerical MOSFET model including quantum-mechanical and near-interface trap transient effects. *Solid-State Electronics* 46, (2002) 1051-1059.

- Mateo J.J., Jimenez M., Huerta T., Pastor A., Contribution of different yeasts isolated from musts of Monastrell grapes to the aroma of wine, *Int J. Food Microbiol.*, 14 (1991), 153-160.
- Medawar W., Strehaiano P., Delia M.-L., Yeast growth: lag phase modelling in alcoholic media, *Food Microbiology*, 20 (2003), 527-532.
- Mestres P., Morguet A., The Bionas technology for anticancer drug screening, *Expert Opinion on Drug Discovery*, 4 (7) (2009), 785-797.
- Mewes H.W., Albermann K., Bahr M., Frishman D., Gleissner A., Hani J., Heumann K., Kleine K., Maieri A., Oliver S.G., Pfeiffer F., Zollner A., Overview of the yeast genome, *Nature* 387 (1997), 7-8.
- Mannazzu I., Angelozzi D., Belviso S., Budroni M, Farris G.A., Goffrini P., Lodi T., Marzona M., Bardi L., Behaviour of *Saccharomyces cerevisiae* wine strains during adaptation to unfavourable conditions of fermentation on synthetic medium: Cell lipid composition, membrane integrity, viability and fermentative activity, *International Journal of Food Microbiology*, 121 (2008), 84-91.
- Mewes H.W., Frishman D., Guldener U., Mannhaupt G., Mayer K., Mokrejs M., Morgenstern B., Munsterkötter M., Rudd S., Weil B., MIPS: a database for genomes and protein sequences, *Nucleic Acids Res.*, 30 (2002), 31-34.
- Mishima K., Mimura A., Takahara Y., On-line monitoring of cell concentrations during yeast cultivation by dielectric measurements, *J. Ferment. Bioeng.*, 72 (1991), 296-299.
- Monteiro G.A., Supply P., Goffeau A., S.A. Correia I., The in vivo activation of *Saccharomyces cerevisiae* plasma membrane H⁺-ATPase by ethanol depends on the expression of *PMA1* gene, but not of the *PMA2* gene, *Yeast*, 10 (1994), 1439-1446.

- Mohri S., Shimizu J., Goda N., Miyasaka T., Fujita A., Nakamura M., Kajiya F., Measurements of CO₂, lactic acid and sodium bicarbonate secreted by cultured cells using a flow-through type pH/CO₂ sensor system based on ISFET, *Sensors and Actuators B*, 115 (2006), 519-525.
- Mohri S., Yamada A., Goda N., Nakamura M., Naruse K., Kajiya F., Application of a flow-through type pH/CO₂ sensor system based on ISFET for evaluation of the glucose dependency of the metabolic pathways in cultured cells, *Sens. Actuators B*, 134 (2008), 447-450.
- Morguet A., Putz N., G.Gomez de las Heras S., Mestres P., Correlation between cell substrate impedance and attachment and spreading of cells growing on artificial surfaces: Scanning electron microscopy studies, *Microsc. Microanal.*, 13, (2007), 246-247.
- Mullis K. B., Faloona F., Scharf S., Saiki R., Horn G., Erlich H. Specific enzymatic amplification of DNA in vitro: the polymerase chain reaction. *Cold Spring Harbor Symp. Quant. Biol.*, (1986), 51, 263-273.
- Münchow G., Dadic D., Doffing F., Hardt S., Drese K.S. Automated chip-based device for simple and fast nucleic acid amplification. *Expert Rev. Mol. Diagn.*, (2005), 5, 613–620.
- Neaves P., Waddell M.J., Prentice G.A., A medium for the detection of Lancefield group D cocci in skimmed milk powder by measurement of conductivity changes, *J. Appl. Bacteriol.*, 65 (1988), 437- 448.
- Neuzil P., Pipper J., Hsieh T.M., Disposable real-time microPCR device: lab-on-a-chip at a low cost, *Mol. BioSyst.*, 2 (2006), 292-298.
- Noble P., Dziuba M., Jed Harrison D., Albritton W.A., Factors influencing capacitance-based monitoring of microbial growth, *Journal of Microbiological Methods*, 37 (1999), 51-64.

- Northrup MA, Ching MT, White RM, Watson RT. DNA amplification in a micro fabricated reaction chamber. Proceeding of the Transducers '93, (1993), 924-926.
- Nwachukwu I.N., Ibekwe V.I., Nwabueze R.N., Anyanwu B.N., Characterisation of palm wine yeast isolates for industrial utilisation, African Journal of Biotechnology, 19 (2006), 1725-1728.
- Oelßner W., Zosel j., Guth U., Pechstein T., Babel W., Connery J.G., Demuth C., Gansey M. G., Verbug J. B., Encapsulation of ISFET sensor chips, Sensors and Actuators, 105 (2005), 104-117.
- Offenhäuser A, Sprössler C., Matsuszawa M., Knoll W., Field-Effect transistor array for monitoring electrical activity from mammalian neurons in culture, Biosensors and Bioelectronics, 12 (1997), 819-826.
- Offenhäuser A., Knoll W., Cell-transistor hybrid systems and their potential applications, Trends Biotech 19 (2001), 62-65.
- Ohta K., Supanwong K., Hayashida S., Environmental effects of ethanol tolerance of *Zymomonas mobilis*, J. Bacteriol., 59 (1981), 453-456.
- Ough C.F., Davenport M., Joseph K., Effects of certain vitamins on growth and fermentation rate of several commercial active dry wine yeasts, Am. J. Enol. Vitic., 40 (1989), 208-213.
- Opekarová M., Sigler K., Acidification power: indicator of metabolic activity and autolytic changes in *Saccharomyces cerevisiae*, Folia Microbiol, 27 (1982), 395–403.
- Owicky J.C., Parce J.W., Biosensors based on the energy metabolism of living cell: the physical chemistry and cell biology of extracellular acidification, Biosensors and Bioelectronics, 7 (1992), 255-272.

- Ottensen E.A., Hong J.W., Quake S.R., Leadbetter J.R., Microfluidic digital PCR enables multigene analysis of individual environmental bacteria, *Science*, (2006), 314, 1464-1467.
- Panaro N.J., Lou X.J., Fortina P., Kricka L.J., Wilding P., Micropillar array chip for integrated white blood cell isolation and PCR, *Biomol. Eng.*, 21 (2005), 157-162.
- Park K., Choi S., Lee M., Sohn B., Choi S., ISFET glucose sensor system with fast recovery characteristics by employing electrolysis, *Sensors and Actuators B*, 83 (2002), 90-7.
- Parsons AB, Lopez A, Givoni IE *et al.*, Exploring the mode-of-action of bioactive compounds by chemical-genetic profiling in yeast, *Cell*, 126, (2006), 611-25.
- Pascual C., Alonso A., Garcia I., Romay C., Kotyk A., Effect of ethanol on glucose transport, key glycolytic enzymes and proton extrusion in *Saccharomyces cerevisiae*, *Biotechnol. Bioeng.*, 32 (1988), 374-378.
- Patil S., Patil B., Gokhale D., Novel supplements enhance ethanol production in cane molasses fermentation by recycling Yeast cells, *Biotechnol. Lett.*, 11 (1989), 213-216.
- Patino H., Edelen C., Miller J., Alternative measures of yeast vitality: use of cumulative acidification power and conductance, *J. Am. Soc. Brew. Chem.*, 51 (1993), 128-132.
- Piper P. W., The heat-shock and ethanol stress responses of yeast exhibit extensive similarity and functional overlap, *FEMS Microb. Lett.*, 134 (1995), 121-127.
- Poghossian A., Schöning M.J., Schroth P., Simonis A., Luth H., An ISFET-based penicillin sensor with high sensitivity, low detection limit and long lifetime, *Sensor and Actuators B* 76 (2001), 519-526.

- Poghossian A., Ingebrandt S., Offenhäuser A., Schöning M.J., Field-effect devices for detecting cellular signals, *Seminars in Cell & Developmental Biology*, 20 (2009), 41-48.
- Pohanka M., Skladal P., Electrochemical biosensors – principles and applications, *Journal of Applied Biomedicine*, 6 (2008), 57-64.
- Prakash A.R., Adamia S., Sieben V., Pilarski P., Backhouse C.J. Small volume PCR in PDMS biochips with integrated fluid control and vapour barrier. *Sensors and Actuators B*, (2006), 113, 398-409.
- Pretorius I.S., Bauer F., Meeting the consumer challenge through genetically customized wine-yeast strains, *TRENDS in Biotechnology* 20 (2002), 426-432.
- Qain D.E., Studies on the physiology – impact on fermentation performance and product quality, *J. Inst.Brew.*, 95 (1988), 315–323.
- Querol A., Barrio E., Huerta T., Ramon D., Molecular Monitoring of Wine Fermentations Conducted by Active Dry Yeast Strains, *Applied and Environmental Microbiology*, 58 (1992), 2948-2953.
- Querol A., Fleet G.H. (Eds), *Yeasts in Food and Beverages*, Springer, 2006
- Ress C., Pedrotti S., Lorenzelli L., Passerotti S., Malavolta M., Candioli E., Characterization of a new device for yeast cell growth monitoring, In *Proceedings of the 13th Italian Conference on Sensors and Microsystems*, World Scientific Publishing, (2009), 233-237.
- Riis S.B., Pedersen H.M., Sorensen N.K., M Jokobsen, Flow cytometry and acidification power test as rapid techniques for determination of the activity of starter cultures of *Lactobacillus delbruckii ssp. Bulgaricus*, *Food microbiology*, 12 (1995), 245-250.

- Ro DK, Paradise EM, Ouellet M, Fisher KJ, Newman KL, Ndungu JM, Ho KA, Eachus RA, Ham TS, Kirby J, Chang MC, Withers ST, Shiba Y, Sarpong R, Keasling JD, Production of the antimalarial drug precursor artemisinic acid in engineered yeast, *Nature*, 440 (2006), 940-943.
- Romano P., Fiore C., Paraggio M., Caruso M., Capece A. Function of yeast species and strains in wine flavour, *Int. J. Food Microbiol.*, 86 (2003), 169-180.
- Roos W., Luckner M., Relation between proton extrusion and fluxes of ammonium ions and organic acids in *Penicillium cyclopium*, *J. Gen. Microbiol.*, 130 (1984), 1007-1014.
- Rosa M.F., Sa-Correia I., In vivo activation by ethanol of plasma membrane ATPase of *Saccharomyces cerevisiae*, *Applied and Environmental Microbiology*, (1991) 57, 830-835.
- Rosa M.F., Sa-Correia I., Ethanol tolerance and activity of plasma membrane ATPase in *Kluyveromyces marxianus* and *Saccharomyces cerevisiae*, *Enzyme and Microb. Technology*, 14 (1992), 23-27.
- Rose A.H., Recent research on industrially important strains of *S. cerevisiae*, *Biology and Activity of Yeasts*, Edited by F.A. Skinner, S.M. Passmore & R.R. Davenport. London: Academic Press, (1980), 103-121.
- SA-Correia I., Synergistic effects of ethanol, octanoic, decanoic acids on the kinetics and the activation parameters of thermal death in *Saccharomyces bayanus*, *Biotechnol. Bioeng.* 28 (1986), 761-763.
- Salmon J. M., Vincent O., Mauricio J.C., Bely M., Barre P., Sugar transport inhibition and apparent loss of activity in *Saccharomyces cerevisiae* as a major limiting factor of enological fermentation, *American Journal of Enology and Viticulture*, 44 (1993), 56-64.

- Senillou A., Jaffrezic-Renault N., Martelet C., Cosnier S., A miniaturized urea sensor based on the integration of both ammonium based urea ENFET and a reference FET in a single chip, *Talanta*, 50 (1990), 219-26.
- Schäpper D., M. N. H. Z. Alam, N. Szita, A. E. Lantz, K. V. Gernaey, Application of microbioreactors in fermentation process development: a review, *Anal. Bioanal. Chem.*, 395 (2009), 679–695.
- Schmidt S.A., Tran T., Chambers P.J., Herderich M.J., Pretorius I.S., Developing indicators of wine yeast performance: an overview of the impact of ethanol stress, *Australian & New Zealand Wine Industry Journal*, 21 (2006), 24-30.
- Schneegaß I., Brautigam R., Kohler J.M., Miniaturized flow-through PCR with different template types in a silicon chip thermocycler, *Lab on a chip*, (2001), 1, 42-49.
- Schöning M., Schultze J.W., Poghossian A., Measuring seven parameters by two ISFET moduls in a microcell set-up, *Int. Journal of Comp. Engineering Science*, 4 (2003), 257-260.
- Schöning M., “Playing around” with Field-Effect Sensors on the Basis of EIS Structures, LAPS and ISFETs, *Sensors* 5 (2005), 126-138
- Schöning M., Poghossian A., BioFEDs (Field-Effect Devices): State-of-the-Art and New Directions, *Electroanalysis* 18 (2006), 1893-1900.
- Serrano R., Structure and function of proton translocating ATPase in plasma membrane of plants and fungi, *Biochimica et Biophysica Acta*, (1988) 947, 1-28.
- Sherry A.E., Patterson M.F., Kilpatrick D., Madden R.H., Evaluation of the use of conductimetry for the rapid and precise measurement of *Salmonella spp.* growth rates, *Journal of Microbiological Methods*, 67 (2006), 86-92.

- Shiono S., Hanazato Y., Nakako M., Advances in Enzymatically Coupled Field Effect Transistor, *Bioanalytical Applications of Enzymes* 36 (1992), 151-179
- Schmidhuber M., Becker B., Wiest J., Wolf B., Development of a multiparametric handheld biosensor for use in mobile applications, *IEEE* (2009), 94-101.
- Schutz M, Gafner J., Analysis of yeast strain population during spontaneous and induced alcoholic fermentations, *J. Appl. Bacteriol.*, 75 (1993), 551-558.
- Sigler K., Knotkova A., Kotyk A., Factors governing substrate-induced generation and extrusion of protons in the yeast *Saccharomyces cerevisiae*, *Biochim. Biophys. Acta*, 643 (1981a), 572-582.
- Sigler K., Kotyk A., Knotkova A., Opekarova M., Processes involved in the creation of buffering capacity and in substrate-induced proton extrusion in the yeast *Saccharomyces cerevisiae*, *Biochim. Biophys. Acta*, 643 (1981b), 583-592.
- Sigler K., Hofer M., Mechanism of acid extrusion in yeast, *Biochim. Biophys. Acta*, 1071 (1991), 375-391.
- Sigler K., Mikyska A., Kosar K., Gabriel P., Dienstbier M., Factors affecting the outcome of the acidification power test of yeast quality: critical reappraisal, *Folia Microbiol.*, 51 (2006), 525-534.
- Silley P. and Forsythe S., Impedance microbiology – a rapid change for microbiologists, *Journal of Applied Bacteriology*, 80 (1996), 233-243.
- Simon J.A., Bedalov A., Yeast as a model system for anticancer drug discovery, *Nat. Rev. Cancer*, 4 (2004), 481-492.
- Snyder M. and Kumar A., Yeast genomics: past, present, and future promise, *Funct. Integr. Genomics*, 2 (2002), 135-137.

- Soldatkin A.P., Montoriol J., Sant W., Martelet C., Jaffrezic-Renault N., A novel urea sensitive biosensor with extended dynamic range based on recombinant urease and ISFETs, *Biosensors and Bioelectronics* 19 (2003), 131-135.
- Soley A., Lecina M., Gamez X., Cairò J.J., Riu P., Rossel X., Bragos R., Godia F., On-line monitoring of yeast cell growth by impedance spectroscopy, *Journal of Biotechnology*, 118 (2005), 398-405.
- Solly K., Wang X, Xu X., Strulovici B., Zheng W., Application of real-time cell electronic sensing (RT-CES) technology to cell-based assays, *Assay Drug Dev. Technol.*, 2 (2004), 363-372.
- Srinivasan K., Mahadevan R., Characterization of proton production and consumption associated with microbial metabolism, *BMC Biotechnology*, 10 (2010), 1-10.
- Stevens S., Hofemyer J. H.S., Effects of ethanol, octanoic and decanoic acids on fermentation and the passive influx of protons through the plasma membrane of *Saccharomyces cerevisiae*, *Appl. Microbiol. Biotechnol.*, 38 (1993), 656-663.
- Stewart G.N., The changes produced by the growth of bacteria in the molecular concentration and electrical conductivity of culture media, *J. Exp. Med.*, 4 (1898), 235- 243.
- Swiegers J., Bartowsky E., Henschke P, Pretorius I, Yeast and bacterial modulation of wine aroma and flavour, *Aust. J. Grape Wine Res.*, 11 (2005), 127-138.
- Tanghe A., Prior B., Thevelein J.M., Yeast responses to stress, In *Biodiversity and Ecophysiology of Yeasts*, Springer (2006), 175-195.
- Thedinga E., Kob A., Holst H., Keuer A., Drechsler S., Niendorf R., Baumann W., Freund I., Lehmann M., Ehret R., Online monitoring of cell metabolism for studying pharmacodynamic effects, *Toxicology and Applied Pharmacology*, 220 (2007), 33-44.

- Thomas D.S., Rose A.H., Inhibitory effect of ethanol on growth and solute accumulation by *Saccharomyces cerevisiae* as affected by plasma-membrane lipid composition, *Arch. Microbiol.*, 122 (1979), 19-55.
- Tomaszewski D., Yang C.M., Jaroszewicz B., Zaborowski M., Grabiec P., Pijanowska D.G., Electrical characterization of ISFETs, *Journal of telecommunications and information technology*, 3 (2007), 55-60.
- Trung N., Saito M., Takabayashi H., Viet P.H., Tamiya E., Takamura Y., Multi-chamber PCR chip with simple liquid introduction utilizing the gas permeability of polydimethylsiloxane, *Sensors and Actuators B*, 149 (2010), 284-290.
- Ur A.M.D., Brown D.F.J., Impedance monitoring of bacterial activity, *J. Med. Microbiol.*, 8 (1975), 19-28.
- van Leewen M., Krommenhoek E.E., Heijnen J.J., Gardeniers H., van der Wielen L.A.M., van Gulik W.M., Aerobic batch cultivation in micro bioreactor with integrated electrochemical sensor array, *Biotechnol. Prog.*, 26 (1), (2010), 293-300.
- Vassanelli S., Fromherz P., Transistor-records of excitable neurons from rat brain, *Appl. Phys A*, 66 (1998), 459-463.
- Velten T, Ruf H, Barrow D, Aspragathos N, Lazarou P, Jung E, Malek C, Richter M, Kruckow J, Wackerle M. Packaging of Bio-MEMS: Strategies, Technologies, and Applications. *IEEE Trans. Adv. Packag.*, 28 (2005), 533–546.
- Vincenzini M., Romano P., Farris G.A, *Microbiologia del vino*, CEA, pp.435-450, 2005.
- Viegas C.A., Rosa M.F., S.A.-Correia I., Novais J. M., Inhibition of yeast growth by octanoic and decanoic acids produced during ethanol fermentation, *Appl. Environ. Microbiol.*, 55 (1989), 21-28.

- Viegas C.A., S.A.-Correia I., Activation of plasma membrane ATPase of *Saccharomyces cerevisiae* by octanoic acid, *Journal of General Microbiology* 137 (1991), 645-651.
- Viegas C.A., Almeida P.F., Cavaco M., S.A.-Correia I., The H⁺-ATPase in the plasma membrane of *Saccharomyces cerevisiae* is activated during growth latency in octanoic acid-supplemented medium accompanying the decrease in intracellular pH and cell viability, *Appl. Environm Microb.*, 64 (1998), 779-783.
- Vicente A., Castrillo J. I., Teixeira J. A., Ugalde U., On-Line Estimation of Biomass Through pH Control Analysis in Aerobic Yeast Fermentation Systems, *Biotechnol. and Bioeng.*, 58 (1998), 445-450.
- Vonau W., Guth U., pH Monitoring: a review, *J. Solid State Electrochem.*, 10 (2006), 746-752.
- Vonau W., Herrmann S., German Patent DE 10 2007 050 477
- Wang J., Cai R., Xu J., Liu Z., Study of the effect of thiamine on the metabolism of yeast by intrinsic fluorescence, *Luminescence*, 20 (2005), 216-219.
- Wang J., Chen Z., Corstjens P.L.A.M., Mauk M.G., Bau H.H., A disposable microfluidic cassette for DNA amplification and detection, *Lab on Chip*, 6 (2006), 46-53.
- Wegener J., Keese C.R., Giaever I., Electric cell-substrate impedance sensing (ECIS) as a noninvasive means to monitor the kinetics of cell spreading to artificial surfaces, *Exp. Cell. Res.* 259 (2000), 158-166.
- Wellhoener U., Geiger E., Definition of the physiological condition of a brewer's yeast by means of enzyme activity measurements during propagation and fermentation, *Proc. 29th Congr. Eur. Brewery Convention*, (2003), 598-608.
- White T. J., Bruns T., Lee S., Taylor J. W., Amplification and direct sequencing of fungal ribosomal RNA genes for phylogenetics. In: *PCR Protocols: A Guide to*

- Methods and Applications, eds. Innis, M. A., Gelfand D. H., Sninsky J. J., White T. J.. Academic Press, Inc., New York (1990), 315-322.
- Wiest J., Schmidhuber M., Ressler J., Scholz A., Brischwein M., Wolf B., Cell based assays for diagnostic and therapy on multiparametric biosensor chips with an intelligent mobile lab, IFMBE Proc. 2005, 10, 132-135
 - Xiao C. Luong J.H.T., On-line monitoring of cell growth and cytotoxicity using electric cell-substrate impedance sensing (ECIS), Biotechnol. Prog., 19 (2003), 1000-1105.
 - Xiao C. Luong J.H.T., Assessment of cytotoxicity by emerging impedance spectroscopy, Toxicol. Appl. Pharmacol., 206 (2005), 102-112.
 - Yan W.P., Du L.Q., Wang J., Ma L.Z., Zhu J.B., Simulation and experimental study of PCR chip based on silicon, Sens. Actuators B, 108 (2005), 695-699.
 - Yao L., Liu B., Chen T., Liu S., Zuo T., Micro Flow-through PCR in a PMMA Chip Fabricated by KrF Excimer Laser, Biomedical Microdevices, 7 (2005), 253–257.
 - Yates D.E., Levine S., Healy T.W., Site-binding model of the electrical double layer at the oxide/water interface, J. Chem. Soc., Faraday Trans. I, 70, (1974), 1807-18.
 - Yeon J.H., Park J.K., Cytotoxicity test based on electrochemical impedance measurements of HepG2 cultured in microfabricated cell chip, Anal. Biochem., 341 (2005), 308-315.
 - Yoshinobu T., Schöning M. J., Otto R., Furuichi K., Mourzina Yu., Ermolenko Yu., Iwasaki H., Portable light-addressable potentiometric sensor (LAPS) for multisensor applications, Sensors and Actuators B, 95 (2003), 352-356.

- Yuqing M., Jianguo G., Jianrong C., Ion sensitive field effect transducer-based biosensors, *Biotechnology Advances* 21 (2003), 527-534.
- Zhang Z., Boccazzi P., Choi H.G., Perozziello G., Sinskey A.J., Jensen K.F., Microchemostat-microbial continuous culture in a polymer-based, instrumented microbioreactor, *Lab on a Chip*, 6 (2006), 906-913.
- Zhang C., Xu J., Ma W., Zheng W., PCR microfluidic devices for DNA amplification, *Biotechnology Advances*, 24 (2006), 243–284.
- Zhang C., Xing D., Miniaturized PCR chips for nucleic acid amplification and analysis: latest advances and future trends, *Nucleic Acids Research*, 35, (2007), 4223-4237.
- Zuzuarregui A., del Olmo M.L., Analyses of stress resistance under laboratory conditions constitute a suitable criterion for wine yeast selection, *Antonie van Leeuwenhoek*, 85 (2004), 271–280.

Appendix A: General principles of Ion-Sensitive Field Effect Transistors (ISFETs)

The working principle of an ISFET is generally explained by comparing it with its electronic analogue, the MOSFET (Metal Oxide Semiconductor Field-Effect Transistor).

ISFET can be considered as a MOSFET, in which the gate metalization is replaced by an external reference electrode exposed to the aqueous solution, which in turn is in contact with the dielectric gate that composes the sensitive part of the sensor (fig. 1A).

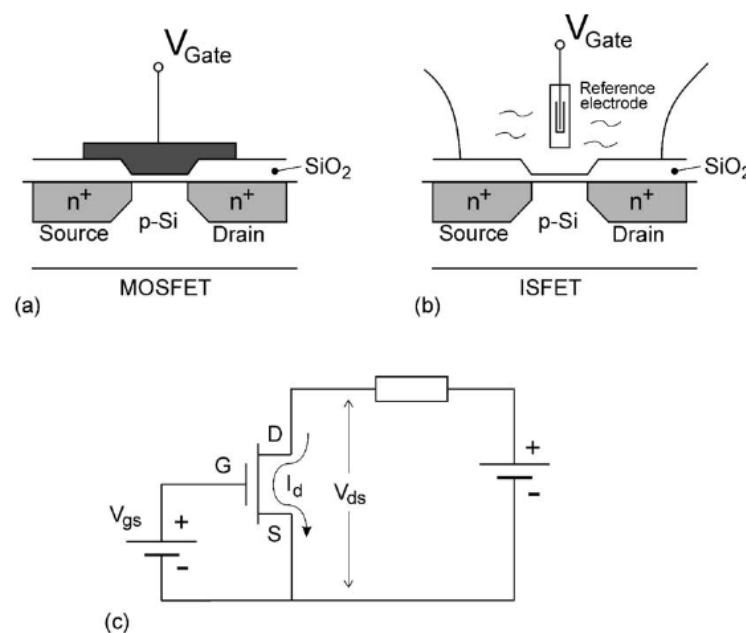


Fig. 1A. Schematic representation of a) MOSFET, b) ISFET and c) common electronic diagram. Both devices have the same electrical equivalent circuit [Bergveld, 2003]

If we consider n-channel MOSFET, we have a p-type substrate in which there are two n⁺ regions: source and drain.

The region between source and drain is influenced by the gate electrode. If we apply a high positive voltage, the silicon surface can be inverted and the conductivity between drain and source can be modulated by changing the gate voltage. The reference electrode of an ISFET has the same function of the gate electrode of a MOSFET, it polarizes the dielectric interface (Fig. 2A).

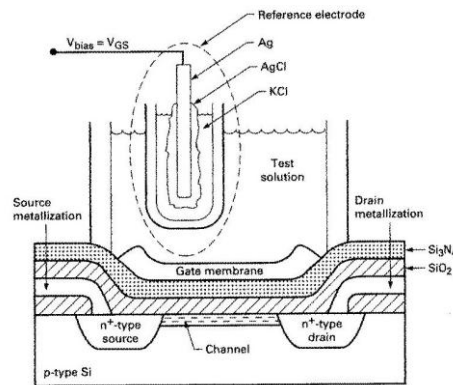


Fig. 2A ISFET structure

In the linear region (i.e. $V_{DS} < V_{GS} - V_{Th}$) (fig 3A), the general equation for the drain current of a MOSFET is given by:

$$I_{DS} = \beta (V_{GS} - V_{Th} - \frac{1}{2} V_{DS}) V_{DS} \quad (1)$$

where I_{DS} is the drain-source current, V_{DS} is the drain-source voltage, V_{GS} the gate voltage and V_{Th} the threshold voltage. β is the current gain and it is a design constant because it depends on the geometrical features of the sensor:

$$\beta = \mu C_{ox} W/L \quad (2)$$

where μ is the electron mobility in the channel (assuming n-channel transistor), C_{ox} is the gate insulator capacitance per unit area, and W/L is the geometrical factor, given by the ratio between width and length of the channel.

The equation 1 is valid for both ISFET and MOSFET for the triode (linear) mode; as regarding the saturation region, the equation that models I_{DS} is different but it is not reported in this section because it is not relevant for the understanding of the operational principle of the Ion-Sensitive FETs.

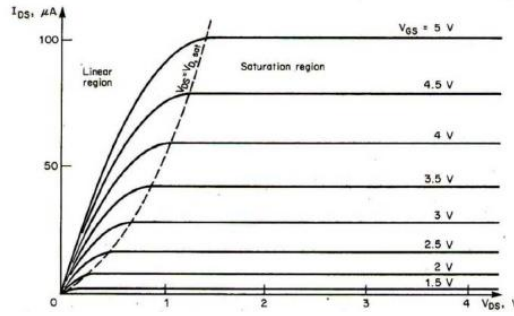


Fig. 3A MOSFET drain current vs. drain-to-source voltage; the boundary between linear and saturation regions is indicated by a dashed parabola.

The threshold voltage V_{Th} is given by:

$$V_{Th} = (\Phi_M - \Phi_{Si}) / q - (Q_{ss} + Q_{ox} + Q_B) / C_{ox} + 2\Phi_F \quad (3)$$

where Φ_M and Φ_{Si} are the working function of the metal gate and of silicon respectively, Q_{ss} is the surface state density at the silicon interface, Q_{ox} the fixed oxide charge and Q_B is the depletion charge in the silicon. The last term Φ_F is the Fermi-potential.

From the equation (3) it can be seen that V_{Th} of a MOSFET is determined by the material properties that are expressed by the working function Φ and charge accumulation.

Additionally, in the case of an ISFET, V_{th} contains two other terms, which reflect the constant potential of the reference electrode (E_{ref}), and the interfacial potential $\Psi + X^{sol}$ at the solution/oxide interface [Bergveld, 2003]. Therefore, if we take into account these contributions, the threshold voltage equation becomes

$$V_{Th} = E_{ref} - \psi + X_{sol} - \frac{\Phi_{Si}}{q} - \frac{Q_{ss} + Q_{ox} + Q_B}{C_{ox}} + 2\Phi_F \quad (4)$$

E_{ref} includes Φ_M whereas X^{sol} is the surface dipole potential. All terms are constant, except Ψ , which results from a chemical reaction, usually governed by the dissociation of oxide surface groups. This term makes the ISFET sensitive to the electrolyte pH, as can be simplified

$$\Psi = f(\text{pH})$$

As Bergveld explained very well, ISFET is electronically identical to a MOSFET and can be seen as an electronic device with one additional feature: the possibility to chemically modify the threshold voltage via the interfacial potential at the electrolyte/oxide interface.

Hence, the working mechanism of ISFET is based on the generation by the dielectric layer of an interfacial potential at the electrolyte/oxide interface that depends on the H_3O^+ ion concentration present in the solution. The change of the surface charge modifies V_{Th} and therefore I_{DS} current. Since the most common polarization process works with constant V_{DS} and I_{DS} , the sensor response to pH changes is translated by changes in V_{GS} .

In this condition, working with low V_{DS} values with respect to $V_{\text{GS}} - V_{\text{Th}}$, I_{DS} modeled in equation 1 becomes:

$$I_{\text{DS}} = \beta V_{\text{DS}} (V_{\text{GS}} - V_{\text{Th}}) \quad (5)$$

where

$$V_{\text{GS}} = I_{\text{DS}} / \beta V_{\text{DS}} + V_{\text{Th}} \quad (6)$$

Now, by replacing V_{Th} with the equation 5, V_{GS} is given by

$$V_{\text{GS}} = \frac{1}{\beta} \frac{I_{\text{DS}}}{V_{\text{DS}}} + (E_{\text{ref}} - \Psi) - \left(\frac{\Phi_{\text{Si}}}{q} - \frac{Q_{\text{SS}} + Q_{\text{OX}} + Q_{\text{B}}}{C_{\text{OX}}} - X^{\text{sol}} \right) + 2\Phi_{\text{F}} \quad (7)$$

and by considering the constant terms, the equation 7 can be easily simplified as

$$V_{\text{GS}} = \Psi(\text{pH}) + \text{const.} \quad (8)$$

This equation (8) demonstrates that changes of pH solution correspond to linear changes of V_{GS} .

As can be observed in picture (4A), changes in pH can be detected as $I_{\text{DS}} - V_{\text{GS}}$ translation.

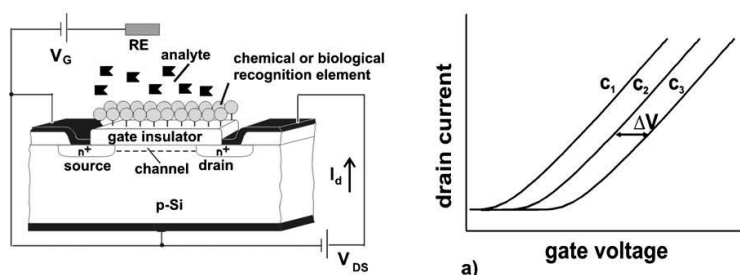


Fig. 4A. Structure and typical response of an ISFET [Schoning and Poghossian, 2006]

- **Theoretical hints on the oxide-electrolyte interface**

The mechanism responsible for the oxide surface charge can be described by the site-binding model, which describes the equilibrium between the so-called amphoteric SiOH surface sites and H_3O^+ ions that are present in the bulk solution [Yates et al., 1974]

From this interaction, there is a surface charge distribution due to the entrapped ions to the reactive sites of the dielectric substrate and this generates the Inner Helmholtz Plane (IHP). The charge that is now present on the surface of the sensor attracts new opposite charges, causing the generation of another layer, the Outer Helmholtz Plane (OHP) [Bard and Faulkner, 1980].

Therefore, an electrical double layer (fig. 4A) is built up at the solid/liquid interface and it is associated with the surface potential Ψ (pH).

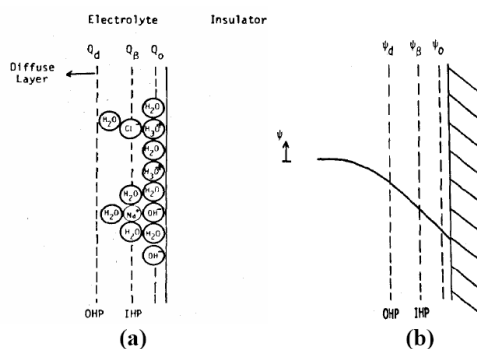


Fig. 5A a) Charge distribution and b) potential profile at the dielectric-electrolyte interface [Fung et al., 1986]

The surface of any metal oxide always contains hydroxyl groups, and if we consider the gate made of a silicon dioxide insulating layer, SiOH groups. These groups may donate or accept protons from the solution, leaving a negatively or positively charged surface group respectively, as illustrated in fig. 6A

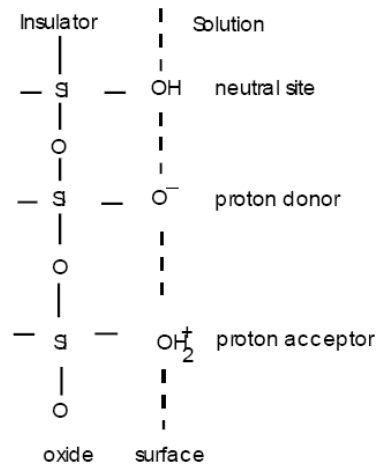
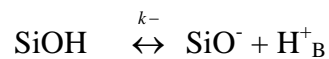
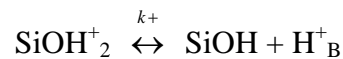


Fig. 6A. Schematic representation of the site-binding model [Bergveld, 2003]

According to the site dissociation model, SiOH groups can be protonated/deprotonated as



with H_B^+ representing the protons in the bulk of the solution.

The two constants for the chemical equilibrium at the interface (not for the bulk reaction) are [Bousse et al., 1983]:

$$k_+ = \frac{[\text{SiOH}][\text{H}^+]_s}{[\text{SiOH}_2^+]}$$

$$k_- = \frac{[SiO^-][H^+]_s}{[SiOH]} \quad (9)$$

where $[H^+]_s$ is the proton concentration at the solid/electrolyte interface, that is related to the $[H^+]_B$ by the Boltzmann equation:

$$[H^+]_s = [H^+]_B \exp(-q\Psi/KT) \quad (10)$$

then, by considering the pH definition ($pH = -\log[H^+]_B$) and the eqns (9) it is possible to obtain the dependence of the surface potential Ψ with the pH of the solution:

$$2.303 (pH_{pzc} - pH) = (q\Psi/KT) + \sinh^{-1}(q\Psi/\beta KT) \quad (11)$$

where pH_{pzc} is the value of the pH for which the oxide surface is electrically neutral (it depends on the insulating material, e.g. SiO_2 $pH_{pzc} = 2$, Al_2O_3 $pH_{pzc} = 6.8$, Si_3N_4 $pH_{pzc} = 8.5$, Ta_2O_5 $pH_{pzc} = 3$ [Bousse et al., 1991; Massobrio et al., 1994; Martinoia et al., 2005]) and β determines the final sensitivity

$$\beta = \frac{2q^2 N_s \sqrt{k_+ + k_-}}{KTC_d} \quad (12)$$

As it can be noticed from the equation 12, β depends on the equilibrium constants K_+ and K_- and on two other terms, N_s and C_d , that are the number of surface site per unit aerea ($N_s = SiOH^+_2 + SiOH + SiO^-$) and the double layer capacitance per unit aerea, respectively.

For relative large values of β ($\beta > q\Psi/KT$), the resulting equation for the surface potential Ψ is

$$\Psi(pH) = 2.303 \frac{KT}{q} \frac{\beta}{\beta + 1} (pH_{pzc} - pH) \quad (13)$$

Hence, the relation between the surface potential Ψ and pH can be highlighted by the general expression for the pH sensitivity of an ISFET:

$$\Delta\Psi/\Delta\text{pH}_B = - 2.303 \alpha \text{KT}/q \quad (14)$$

$$\text{with } \alpha = \frac{1}{\frac{2.303KTC_{dif}}{q^2 \beta_{int}} + 1} \quad (15)$$

The term α is a dimensionless sensitivity parameter that varies between 0 and 1, depending on the intrinsic buffer capacity of the oxide surface (β_{int}) – that can be seen as the ability of the dielectric surface to deliver or take up protons – and the differential double-layer capacitance C_{dif} .

If $\alpha = 1$, the ISFET has the so-called Nernstian sensitivity of 59.2 mV/pH (at 298 K), that is the maximum achievable sensitivity. For oxides with $\alpha < 1$, a sub-Nernstian response can be expected.

In particular, β_{int} of SiO_2 does not reach high values and the pH sensitivity for this specific dielectric layer is about 20-40 mV/pH, depending also on the electrolyte concentration via C_{dif} . The sensor response is lower than Nernstian value and it has not a linear behaviour [Goepel et al, 1991].

Therefore, other inorganic layers have been investigated as gate materials such as Si_3N_4 , Al_2O_3 and Ta_2O_5 with higher values of β_{int} . In particular, Ta_2O_5 has the largest surface buffer capacity (fig. 7A[a]) if compared with the other dielectric layers and β_{int} is so high that the value of the double layer capacity has no influence (fig. 7[b]), showing a pH sensitivity up to 58 mV/pH over a pH range from 1 to 12.

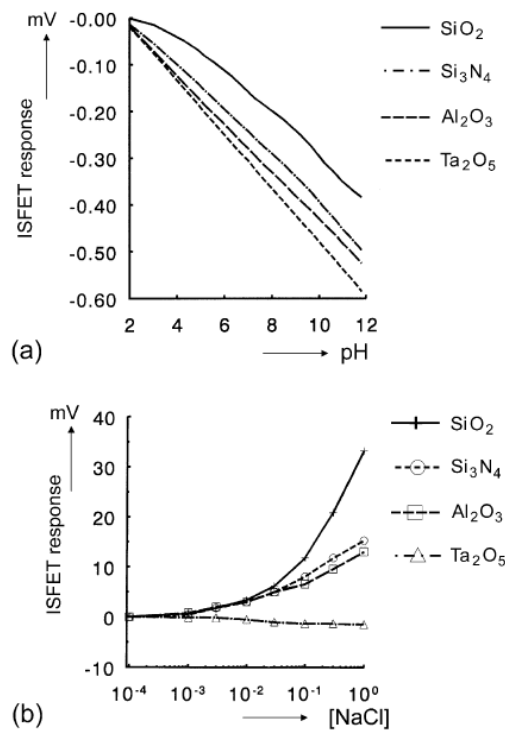


Fig. 7A. ISFET responses of four typical inorganic gate materials (SiO_2 , Si_3N_4 , Al_2O_3 and Ta_2O_5) (a) to different pH values and (b) to different electrolyte concentrations at constant pH [Bergveld, 2003]

The selectivity and actual chemical sensitivity of the ISFET are completely controlled by the properties of the electrolyte/insulator interface. Thus, the choice of the proper gate insulator plays a key role since it determines the fundamental parameters of the device.

If we consider a multilayer made of $\text{Si}_3\text{N}_4/\text{SiO}_2$, it is possible to achieve a sensitivity of $45\div 50$ mV/pH [Matsuo and Esashi, 1991]. However, this sensitivity decreases over time due to the slow oxidation of Si_3N_4 when it is immersed in aqueous solutions.

To overcome this problem, the thin layer of oxide is removed by a short HF treatment. This allows to achieve an higher sensitivity, that can be more than 55 mV/pH.

- Drift

One of the major problems of ISFET is the transient behaviour, generally referred to as drift that is characterized by a threshold voltage shift. This phenomenon limits its application for long-term monitoring measurements. To date, the exact cause of ISFET drift is not completely clear.

There are different interpretations and equations that try to model some typical aspects of drift, but there is not a general theory able to describe and deeply explain all the physical/chemical mechanisms that are involved.

Here are reported the two most well known models that refers on n-channel FETs with Si_3N_4 deposited on SiO_2 as gate insulator.

According to Jamasb *et al.*, ISFET drift mainly depends on the hydratation of the oxide surface. When immersed to a liquid solution, the top layer of the gate oxide gets hydrated. This chemical modification of the surface of the oxide layer changes its dielectric constant and therefore the overall gate capacitance. The thickness of the modified surface changes over time, by causing a drift of the electrical characteristics of the ion sensor. As the hydratation process goes on, the number of free sites for the ion conduction decreases [Jamasb et al., 1998]. The mathematical model proposed by Jamasb *et al.* considers an exponential decrease of the ion diffusion up to the achievement of a constant value, which corresponds to a zero drift. Thus, the equation matches the experimental conditions only up to 10-20 hours and then it goes far from the long-term measurements.

Another possible model is reported by Harame *et al.*, that takes into account buried sites of NH underneath the dielectric surface. It is assumed that these groups react with hydrogen ions in the electrolyte, as the surface groups do according to the site-binding model. The reactivity of these internal sites may produce the ISFET drift by causing a response delay of the potentiometric sensor [Harame et al., 1987].

The models proposed by Jamasb and Harame are just two possible interpretations to justify the phenomenon. Many others works in literature reported other factors that might influence the drift behaviour, such as the presence of traps and charges inside the dielectric layer [Masson et al., 2002] or possible contaminations of the gate insulator by the interaction with the external environment.

However, the drift can be seen as a sum of different factors and working and/or technological conditions. The presence of impurities in the gate insulator or of buried reactive sites depends on the microfabrication process, in particular on the chosen deposition technique. For example, if we deposite Si_3N_4 with LPCVD we can reduce the concentration of hydrogen ions in the bulk of the dielectric layer.

Therefore, some possible tricks during the fabrication of the device (from the choice of the dielectric layer to the deposition techniques), may limit this phenomenon for long-time measurements.

The usual way of coping with the effect of drift in chemical sensors is to carry out calibrations at regular intervals. The long-term drift rate of ISFETs is very constant and reproducible under constant temperature and around constant pH. Therefore, this rate can be determined prior to any long-term measurement and the measurement itself can be compensated for the transient response of the device on-line.

- Temperature effects on the ISFET behaviour

The temperature may have several effects on the ISFET response by acting in different ways: it might influence the behavior of the semiconductor, modify the surface potential at the liquid/solid interface and change the reactivity of the gate surface sites.

In the fig.8A is represented the dependence of the ISFET behaviour from the temperature and it can be noticed that by working at the isothermal point the temperature influence can be minimized. Thus, the ion sensor is generally polarized at this point in order to limit the effect of the temperature on the measurement [Martinoia et al., 1998].

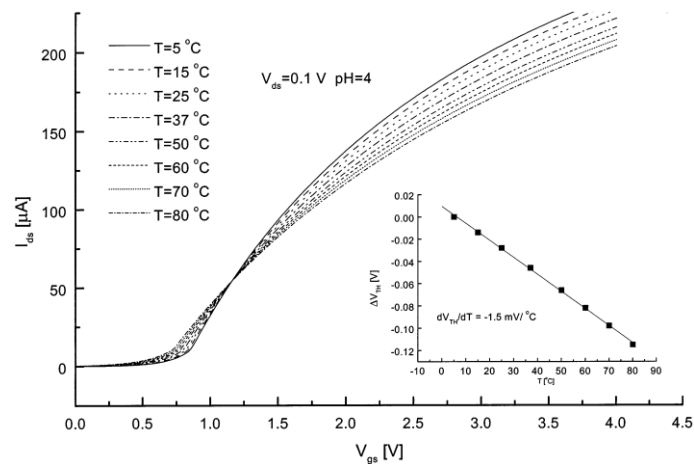


Fig. 8A. Simulated input curves ($I_{ds} - V_{gs}$) of the Si_3N_4 -gate ISFET over a wide range of temperatures ($T= 5\text{--}80^\circ\text{C}$). The inset shows the linear regression of the threshold voltage variations obtained from the input curves [Martinoia et al., 1998].

Appendix B: Thermal improvements of the PCR microdevice

To improve the thermal profile of on-chip PCR, both the silicon and PDMS chamber were modified. As regarding the bottom part, a 90 μ m-silicon membrane was realized to get faster heating and cooling rates (fig. 1B).



Fig. 1B. Cross section of the TMAH wet etched silicon membrane

The design of the device was supported by analytical and finite elements simulations in such a way to evaluate the thermal requirements. A coupled thermal electric simulation was performed using commercial software (Ansys[®]). Two different elements were used for modelling: the thermo-electric element SOLID69 for the heater and the thermal element SOLID70 for the other components. The simulated structure was a stack of different materials: the PCB on the bottom, the silicon bulk with 90 μ m thick membrane, the platinum heater and the PDMS chamber filled with the PCR mix (Table 2B).

TABLE 2B. Material properties

Material	Resistivity Ω /square	Thermal conductivity (W/mK)	Heat capacitance (J/KgK)
Platinum	0.96	71.6	192
PDMS	-	0.15	1460
Silicon	-	150	700
PCB	-	0.2	2000

A voltage of 22V (2.9W) was applied to the heater and a boundary condition of convection was applied to the external walls. Simulations showed that in this condition good temperature uniformity was achieved in the PCR chamber. The silicon surface reached the 95 $^{\circ}$ C from 65 $^{\circ}$ C with a rate of 10 $^{\circ}$ C/s and cools down from 95 $^{\circ}$ C to 65 $^{\circ}$ C with a rate of 1.7 $^{\circ}$ C/s.

As negative aspect, simulation showed that with 400 μ m of PDMS membrane the temperature in the chamber after 30s simulation is 8 $^{\circ}$ C lower than the temperature on the surface of the silicon due to the low thermal conductivity of the PDMS. Therefore, the etching of the bulk silicon is not sufficient and the conductivity of the chamber needs to be improved.

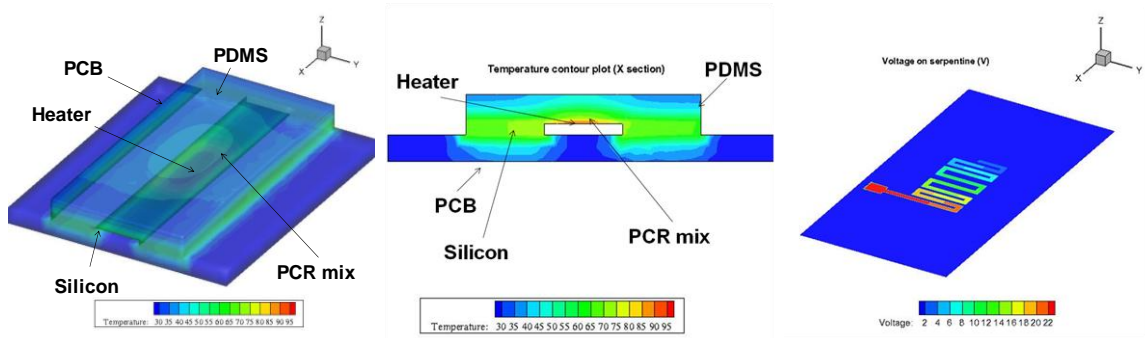


FIG. 3.B: (Left and middle) Simulated temperature distribution in the PCR device; (right) simulated voltage distribution on the heater (performed by Elisa Morganti)

By TMAH wet etching, two 90 μ m silicon membranes were realized. The difference between the two kinds of membrane is that the long membrane was etched throughout the whole length of the chip thus creating a channel below the heater; instead, the short membrane is etched just below the heater forming a tub. As shown in Figure 4B, with the long membrane the cooling time is about 15s (2 $^{\circ}$ C/s) and the heating time from 72 $^{\circ}$ C to 95 $^{\circ}$ C is 1.5s (11.5 $^{\circ}$ C/s). The short membrane shows the highest heating rate (from 1.9 $^{\circ}$ C/s of the bulk silicon to 11.5 $^{\circ}$ C/s of the silicon membrane) while for the cooling process no great variations are detected from the short and long membranes.

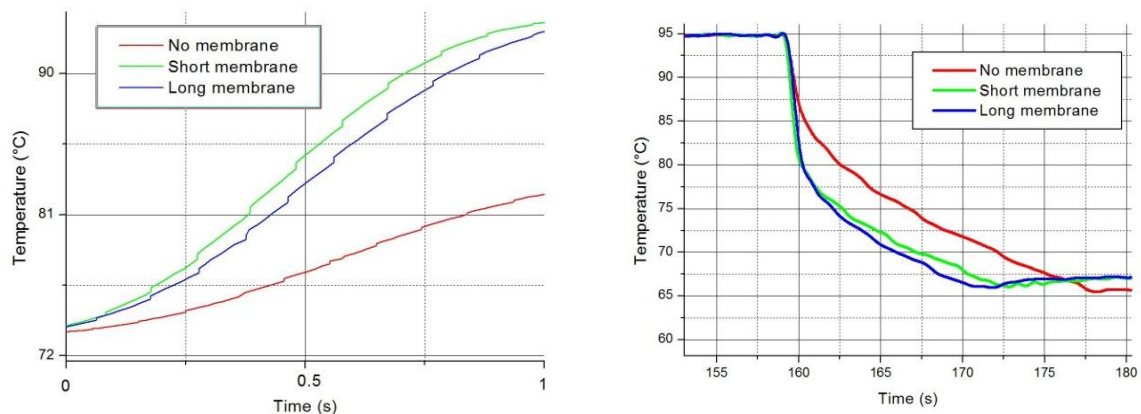


FIGURE 4B: Heating (left) and cooling (right) of the silicon surface with different silicon membrane configurations: no membrane (red), short membrane (green), long membrane (blue).

Beside the improvements on the silicon chip, the polymeric chamber was modified in order to increment its thermal conductivity. In particular, carbon nano-powder was mixed with PDMS curing agent before adding the pre-polymer in a ratio 20:1. Three different concentrations of carbon powder versus curing agent were used: 1, 5, and 10 (w/w %). The measurements reported in figure 5B show that in the case of 10% carbon, the temperature is much closer to the set point, thus increasing the temperature control accuracy.

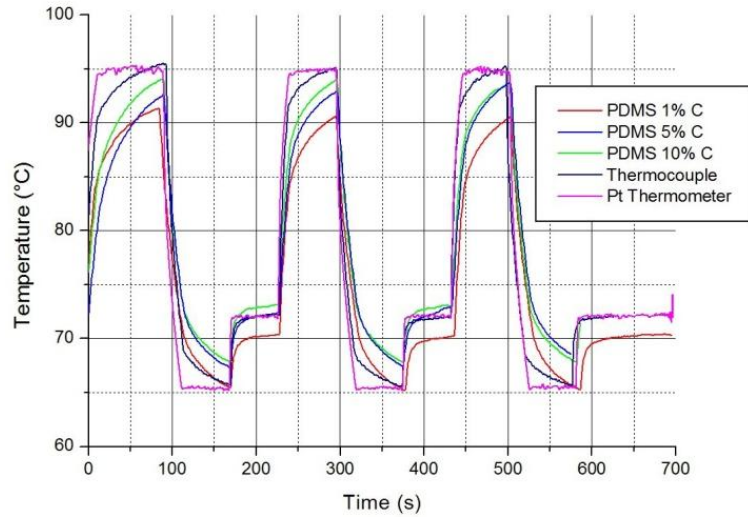


FIGURE 5B: Comparison among the temperatures measured on the top of the PDMS membrane using different concentrations of the carbon nano-powder in the PDMS curing agent.

As can be deduced by observing fig 4B and 5B, the cooling rate still represents the weak point of the device. However, the coupling of short silicon membrane and the PDMS carbon nano-powder will improve the overall thermal profiles and lead to a better temperature control that, in turn, can be translated as real opportunities to get higher PCR efficiency.

Appendix C: List of related publications

- C. Ressa, S. Pedrotti, L. Lorenzelli, S. Passerotti, M. Malavolta and E. Candioli, "Characterization of a new device for yeast cell growth monitoring". In *Proceedings of the 13th Italian Conference on Sensors and Microsystems*. World Scientific Publishing pp. 233—237 (2009).
- E. Morganti, C. Collini, C. Ressa, A. Adami and L. Lorenzelli, Design and Fabrication of a Micro PCR Module for POC Applications. In *The Online Journal of Scientific Posters*. Technology Networks (2009).
[ISSN: 1754-1417. <http://www.eposters.net/index.aspx?id=2494>.]
- C. Ressa, A. Adami, L. Lorenzelli, C. Collini, A. Tindiani, A. Maglione and G. Soncini, Development and characterization of a multiparametric microsensor for yeast cell growth monitoring, *Procedia Chemistry*, vol. 1, no. 1, pp. 1059-1062, Elsevier, 2009

Conferences

- E. Morganti, C. Collini, C. Ressa, A. Adami, L. Lorenzelli, Technological approaches for improving the thermal behavior in an integrated micro polymerase chain reaction (μ PCR) module, **SSI 2011**, 22-23 March, Dresden, Germany.
- C. Ressa, A. Tindiani, A. Adami, L. Odorizzi, C. Collini, S. Pedrotti, L. Lorenzelli, A Multiparametric Microsensor Platform For Yeast Growth Monitoring, **MEMS IN ITALY 2010**, 28 June-1 July 2010, Otranto, Italy.
- E. Morganti, C. Collini, C. Ressa, A. Tindiani, L. Lorenzelli, A micro polymerase chain reaction (μ PCR) module for integrated and portable DNA analyses systems, **MEMS IN ITALY 2010**, 28 June -1 July 2010, Otranto, Italy.

- C. Ress, A. Tindiani, A. Adami, C. Collini, S. Pedrotti, L. Odorizzi, L. Lorenzelli - Wine yeast quality assessment with integrated multiparametric microsensors - **Bio-sensors 2010**, 26- 28 May 2010, Glasgow, UK
- C. Ress, A. Tindiani, A. Adami, C. Collini, S. Pedrotti, L. Odorizzi, L. Lorenzelli, A multiparametric electrochemical microsensor for wine yeast quality assessment. **Smart Systems Integration 2010**, 23-24 March 2010, Como, Italy
- C. Ress, A. Adami, L. Lorenzelli, C. Collini, A. Tindiani, A. Maglione and G. Soncini, Development and characterization of a multiparametric microsensor for yeast cell growth monitoring - **Euroensors 2009** – 6-9 September 2009, Lausanne, Switzerland.
- E. Morganti, C. Collini, C. Ress, A. Adami and L. Lorenzelli, Design and Fabrication of a Micro PCR Module for POC Applications. **Lab-on-a-Chip European Congress**, 18-19 May 2009, Stockholm, Sweden.
- C. Ress, S. Pedrotti, L. Lorenzelli, S. Passerotti, M. Malavolta, E. Candioli, Characterization of a new device for yeast cell growth monitoring - **AISEM 2008**, 13th National Conference on Sensors and Microsystems, 19-21 February 2008, Roma.

Appendix D: Other relevant publications

Other research activities were carried for the development of MEMS-based devices. In particular, they were mainly focused on *biocompatibility studies of microfabricated materials*, *characterization of MEAs (Micro Electrode Arrays) for cell electroporation*, and *investigations of optimal polymeric materials for microfluidics platform devoted to anti-osteoporosis drug screening*. Papers and conferences in these topics are reported here as “Other relevant publications” because these activities are not described in this thesis.

- C. Ressa, L. Odorizzi, C. Collini, L. Lorenzelli, S. Forti, C. Pederzoli, L. Lunelli, L. Vanzetti, N. Coppede', T. Toccoli, G. Tarabella, S. Iannotta, Comparative bioaffinity studies for *in-vitro* cell assays on MEMS-based devices, *Sensors and Microsystems: AISEM 2009 Proceedings*, Lecture Notes in Electrical Engineering 54: 83-87, 2010, Springer.
- L. Odorizzi, C. Ressa, R. Cunaccia, C. Collini, E. Morganti and L. Lorenzelli, A fully integrated system for single-site electroporation and addressed cell drug delivery, *Sensors and Microsystems: AISEM 2009 Proceedings*, Lecture Notes in Electrical Engineering 54: 319–322, 2010, Springer.
- L. Odorizzi, C. Ressa, C. Collini, E. Morganti, L. Lorenzelli, N. Coppede', A.B. Alabi, S. Iannotta, L. Vidalino, P. Macchi, An Enhanced Platform for Cell Electroporation: Controlled Delivery and Electrodes Functionalization, *Euroensors 2010 Proceedings*. Procedia Engineering 5: 45-48 (2010)
- C. Collini, E. Morganti, R. Cunaccia, L. Odorizzi, C. Ressa, and L. Lorenzelli, A. De Toni, G. Marinaro, M. Borgo, M. Maschietto, Fabrication and characterization of a fully integrated microdevice for in-vitro single cell assays. In The Online Journal of Scientific Posters.

Conferences

- F. Nason, E. Morganti , C. Collini , C. Ressa , G. Pennati, F. Boschetti, G. Lombardi, A. Colombini, G. Banfi, L. Lorenzelli , G. Dubini - Design of microfluidic devices for drug screening on in-vitro cells to optimize osteoporosis therapies –**MNE 2010**, 19-22 September 2010, Genoa, Italy.
- L. Odorizzi, C. Ressa, C. Collini, E. Morganti, L. Lorenzelli, N. Coppedè, A.B. Alabi, S. Iannotta, L. Vidalino, P. Macchi - An Enhanced Platform for Cell Electroporation: Controlled Delivery and Electrodes Functionalization – **Euroensors 2010**, 5-8 September 2010, Linz, Austria.
- F. Nason , E. Morganti , A. Tindiani , C. Collini , C. Ressa , G. Pennati, F. Boschetti, G. Lombardi , A. Colombini, G. Banfi, L. Lorenzelli, G. Dubini - Design Of Microfluidic Devices For Drug Screening On In-Vitro Cells To Optimize Osteoporosis Therapies - **GNB 2010**, 8-10 July, Torino, Italy.
- C. Collini, E. Morganti, L. Odorizzi, C. Ressa, L. Lorenzelli, N. Coppedè, A.B. Alabi, S. Iannotta, L. Vidalino, P. Macchi - Functionalized Microelectrodes Arrays With Integrated Microfluidic Channels For Single-Site Multiple Transfections - **GNB 2010**, 8-10 July, Torino, Italy.
- L. Odorizzi, C. Ressa, C. Collini, E. Morganti, R. Cunaccia, L. Lorenzelli, - A New Mea For Single-Site Multiple Transfections: Surface Functionalization And Microfluidics Integration, **MEMS IN ITALY 2010**, 28 June-1 July 2010, Otranto, Italy.
- A. Ferrario, M. Scaramuzza, A. De Toni, L. Odorizzi, C. Ressa, C. Collini, E. Morganti, L. Lorenzelli - Advanced electrical characterization of an innovative micro-electronic/microfluidic device. **Biosensors 2010**, 26- 28 May 2010, Glasgow, UK
- C. Ressa, A. Tindiani , E. Morganti , C. Collini , L. Lorenzelli , A. Colombini , G. Lombardi, G. Banfi, F. Nason, G. Pennati, F. Boschetti, G. Dubini - A microfluidic platform for anti-osteoporosis drug screening: biocompatibility study of polymeric

materials, **Congresso Nazionale Biomateriali 2010**, 24-26 May 2010, Camogli, Italy.

- L. Odorizzi, C. Ressa, C. Collini, E. Morganti, L. Lorenzelli, N. Coppedè, A.B. Alabi, S. Iannotta, L. Vidalino, P. Macchi, - An integrated platform for single-site cell electroporation, **Congresso Nazionale Biomateriali 2010**, 24-26 May 2010, Camogli, Italy.
- C. Ressa, L. Odorizzi, C. Collini, L. Lorenzelli, S. Forti, C. Pederzoli, L. Lunelli, L. Vanzetti, N. Coppede', T. Toccoli, G. Tarabella, S. Iannotta - Comparative bioaffinity studies for *in-vitro* cell assays on MEMS-based devices - **AISEM 2009**, 14th National Conference on Sensors and Microsystems, 24-26 February 2009, Pavia.
- L. Odorizzi, C. Ressa, R. Cunaccia, C. Collini, E. Morganti, L. Lorenzelli - A fully integrated system for single-site electroporation and addressed cell drug delivery - **AISEM 2009**, 14th National Conference on Sensors and Microsystems, 24-26 February 2009, Pavia.